

UC Berkeley

UC Berkeley Electronic Theses and Dissertations

Title

Optimal Intercity Transportation Services with Heterogeneous Demand and Variable Fuel Price

Permalink

<https://escholarship.org/uc/item/5nx0n2x7>

Author

Ryerson, Megan Smirti

Publication Date

2010

Peer reviewed|Thesis/dissertation

**Optimal Intercity Transportation Services
with Heterogeneous Demand and Variable Fuel Price**

by

Megan Smirti Ryerson

A dissertation submitted in partial satisfaction of the

requirements for the degree of

Doctor of Philosophy

in

Engineering – Civil and Environmental Engineering

in the

Graduate Division

of the

University of California, Berkeley

Committee in charge:

Professor Mark Hansen, Chair

Professor Samer Madanat

Professor Robert Leachman

Fall 2010

Abstract

Optimal Intercity Transportation Services
with Heterogeneous Demand and Variable Fuel Price

by

Megan Smirti Ryerson

Doctor of Philosophy in Engineering – Civil and Environmental Engineering

University of California, Berkeley

Professor Mark Hansen, Chair

In this thesis we examine how fuel price variation affects the optimal mix of services in intercity transportation. Towards this end, we make two main contributions. The first is the development of an analytic total logistics cost model of intercity transportation, which is sensitive to fuel price and incorporates multiple classes of vehicles serving passengers with differentiated values of time. The second is an empirical investigation of the cost relationship between fuel price and operating cost for intercity transportation vehicles. The analytic total logistics cost models are combined with the empirical models to gain insights into the impact of fuel price on optimal service mixes in representative corridors.

We consider a scheduled intercity transportation corridor on which different classes of intercity transportation vehicles serve passengers with differentiated values of time. In determining optimal service mix, we consider a central planner choosing the vehicles and service frequencies that provide the minimum total logistics cost for an intercity transportation corridor. The total logistics cost is the sum of the two main intercity transportation cost components: vehicle operator cost and passenger cost. In considering operating and passenger costs together, we balance cost efficiency and level of service of alternative vehicles with different cost structures and service attributes.

In developing the total logistics cost model, we seek both analytic insights and numerical examples. To keep the model analytically tractable while at the same time incorporating multiple objectives, including fuel cost, operating cost, schedule delay, and line-haul time, we incorporate the continuum approximation method from logistics. In employing the continuum approximation, discrete variables are considered continuous, leading to analytic functions from which we can evaluate qualitatively the relationships among fuel price, service level, and comparative vehicle cost. An investigation of the analytic model suggests that, while a fuel price increase would increase costs for any corridor, the rate of cost increase for a corridor served by a mix of vehicle technologies diminishes more rapidly with fuel price. We also find that an increase in fuel price causes vehicles to become more differentiated with respect to the value of time of the passengers they serve. In other words, under high fuel prices the total logistics cost can be minimized by effectively segregating passengers on different types of vehicles according to their values of time.

We complement the analytic findings with an empirical investigation of the cost relationship between fuel price and operating cost for different classes of intercity transportation vehicles. We perform this analysis for a subset of intercity transportation vehicles for which data is readily available: jet and turboprop aircraft. In developing a translog operating cost model for jet aircraft, we estimate a flexible functional form that provides a detailed representation of the empirical relationship between fuel cost and operating cost, allowing for substitution, scale, aircraft age, and other effects – including interactions – to be captured. The function reveals that as fuel price increases, airlines will take steps to use fuel more efficiently by leveraging other inputs; however, the potential for this supplier input substitution for fuel is rather modest. This finding reinforces the formulation of the analytic total logistics cost model, in which the only actions available to a central planner to reduce costs are changing technologies and service frequencies. It also proves that empirical models with simpler functional forms are able to accurately predict operating costs, despite the lack of variable interactions. Using linear empirical operating cost models, we estimate operating cost and total logistics costs for intercity transportation corridors served by single vehicle fleets of three different aircraft classes. We find that a specific turboprop aircraft model, with a relatively low fuel consumption rate, provides intercity transportation service with the minimum operating cost compared with a jet with smaller seating capacity over all fuel prices considered and medium-capacity jets for some fuel prices. However, this is no longer the case when total logistics cost is considered, due to the lower quality of passenger service turboprops provide. At a given intercity transportation corridor distance, the fuel price for which the total logistics cost per passenger is equal across turboprops and low-capacity jets is in the fuel price range experienced from 2004 and expected through 2020. For this fuel price range, the total logistics cost per passenger for the medium-capacity jet is generally lower than the turboprop and always lower the low-capacity jet. This suggests that a mix of services between intercity transportation vehicles could minimize cost for this range of fuel price.

To investigate the possibility of mixing services to reduce costs further, we combine the analytic total logistics cost model with the empirical models. In addition to a jet and turboprop aircraft model, we build a high speed rail cost model and consider high speed rail as an additional intercity transportation technology. We find the minimum cost vehicle combination to be sensitive to fuel price in a small transition zone within which the cost ordering of vehicle combinations changes significantly, whereas outside this zone the orderings are stable. As the transition area is in the range of fuel prices forecasted between the years 2010-2035, the results indicate fuel price changes between 2010 and 2035 may dramatically alter the most cost-effective ways to provide intercity passenger transport. We find that high speed rail is a part of a mixed vehicle service that can reduce total logistics cost, suggesting that an integrated air and rail strategy could be an effective tool to manage costs and fuel consumption for an intercity transportation system.

to
Anders

Contents

List of Tables	vi
List of Figures.....	vii
Acknowledgements	x
1. Introduction	1
1.1 Problem Statement.....	1
1.2 Environmental Concern	4
1.2.1 Greenhouse Gas Emissions	4
1.2.2 Fuel	5
1.3 Short Haul Intercity Transportation System Trends	6
1.3.1 Growth Trends	6
1.3.2 New and Redesigned Aircraft Types.....	7
1.3.3 High Speed Rail.....	9
1.3.4 Mode Split	11
1.3.5 Value of Time.....	12
1.4 Central Planner Response to a Fuel Price Increase	14
2. The Potential of Turboprops for Reducing Aviation Fuel Consumption	17
2.1 Model Formulation	18
2.2 Aircraft Operating Cost Model.....	20
2.2.1 Carrier Component Costs	20
2.2.2 Parametric Operating Cost Comparison.....	22
2.3 Passenger Cost Model.....	24

2.3.1	Parametric Operating and Passenger Cost Analysis.....	25
2.3.2	Value of Frequency	26
2.4	Market Penetration Analysis.....	28
2.5	Conclusions.....	30
3.	The Impact of Fuel Price on Jet Aircraft Operating Costs	31
3.1	Translog Operating Cost Model	32
3.2	Data for Operating Cost Model	33
3.3	Operating Cost Model Estimation	35
3.3.1	Regularity Conditions.....	36
3.3.2	Interpretation of TM Results	40
3.3.3	Translog Operating Cost Prediction	41
3.4	Leontief and Translog Operating Cost Model Comparison	44
3.5	Linear Operating Cost Model	47
3.6	Conclusions.....	49
4.	System Optimal Mathematical Models of Intercity Transportation.....	50
4.1	Total Logistics Cost Function Assumptions and Structure	51
4.2	Total Logistics Cost Models for Passenger Scenario One.....	52
4.2.1	Single Vehicle Fleets	57
4.2.2	Mixed Vehicle Fleets.....	58
4.3	Total Logistics Cost Models for Passenger Scenario Two	69
4.4	Total Logistics Cost Models for Passenger Scenario Three	81
4.5	Conclusions.....	91
5.	Numerical Case Study.....	93

5.1	Additional Model Development	93
5.1.1	Turboprop Operating Cost.....	94
5.1.2	Jet and Turboprop Ownership Cost.....	94
5.1.3	High Speed Rail Cost	95
5.1.4	Travel Time	99
5.1.5	Additional Inputs	100
5.2	Numerical Examples.....	101
5.2.1	Sensitivity of Total Logistics Cost to Fuel Price.....	101
5.2.2	Sensitivity of Total Logistics Cost to Distance	103
5.2.3	Sensitivity of Total Logistics Cost to Passenger Demand and Value of Time.....	104
5.3	High Speed Rail Infrastructure Costs	106
5.4	Conclusions.....	108
6.	Conclusions	110
6.1	Contributions	110
6.2	Future Work.....	112
	Bibliography	114
	Appendix 1: Jet Aircraft Operating Cost Model Estimates.....	123
A1.1	Aircraft Models and Airlines in Operating Cost Analysis	123
A1.2	Jet Aircraft Translog Operating Cost Model Results.....	124
A1.3	Jet Aircraft Pilot Cost per Block Hour Model Results.....	127
A1.4	Jet Aircraft Fuel Consumption Linear Model	128
A1.5	Jet Aircraft Operating Cost (without Fuel) Linear Model	129

Appendix 2: Total Logistics Cost Model, Case 2-2	130
A2.1 Full Total Logistics Cost Function, Case 2-2	130
A2.1 Truncated Total Logistics Cost Function, Case 2-2.....	130
Appendix 3: Linear Operating Cost Model Results	131
A3.1 Turboprop Aircraft Fuel Consumption Linear Model	131
A3.2 Turboprop Aircraft Operating Cost (without Fuel) Linear Model.....	132
A3.3 Jet Aircraft Ownership Linear Model	133
A3.4 Turboprop Aircraft Ownership Linear Model	134
Appendix 4: Travel Time Model Results	135
A4.1 Jet Aircraft.....	135
A4.2 Turboprop Aircraft	135
A4.3 High Speed Rail	135

List of Tables

Table 2.1	Details of representative aircraft.....	20
Table 2.2	Operating cost equations, total and per passenger.....	22
Table 2.3	Operating and passenger cost equations, total and per passenger.	25
Table 3.1	Variables of the operating cost model.	34
Table 3.2	Summary statistics of variables in the operating cost model.....	35
Table 3.3	Linear homogeneity regularity conditions calculation.	38
Table 3.4	Negative second derivatives (%) with respect to factor prices.....	39
Table 3.5	Select operating cost model empirical results.	41
Table 3.6	Leontief Technology model operating cost coefficients.	44
Table 5.1	California High Speed Rail segments.....	96
Table 5.2	Trainset operating statistics for CA HSR, 2020-2035.....	96
Table 5.3	Operating cost categories for High Speed Rail.	98
Table 5.4	Operating cost for European High Speed Rail systems.....	98
Table 5.5	Literature summary on traveler inputs.....	101
Table 5.6	Infrastructure and related costs for CA HSR.....	107
Table 5.7	Global infrastructure costs for HSR projects.....	108

List of Figures

Figure 1.1	Labor and fuel as a percent of operating cost, 2003-2009.....	5
Figure 1.2	U.S. jet fuel price (dollars per gallon).	6
Figure 1.3	Cumulative distribution function of aircraft model seat capacities owned/leased by US carriers, 2006.	8
Figure 1.4	Aircraft trends for short haul travel and U.S. jet fuel price paid by airlines (dollars per gallon).	9
Figure 1.5	Designated High Speed Rail corridors in the United States.	10
Figure 1.6	Rail market share (compared with air) against rail travel time for select European intercity transportation corridors.	11
Figure 1.7	Mode share and distance for certain California corridor city pair markets.	12
Figure 1.8	Mode share and distance for certain Northeast corridor city pair markets..	12
Figure 1.9	Distribution of total system passenger one-way fares per mile.	13
Figure 1.10	Inputs and output of single and mixed vehicle production processes.	14
Figure 1.11	Illustration of input substitution and induced technological change.	15
Figure 2.1	Percent difference operating cost per passenger contour curve for regional jet and turboprop comparison and narrow body and turboprop comparison.....	24
Figure 2.2	Percent difference in total cost per passenger contour curve for regional jet and turboprop and narrow body and turboprop comparison.	26
Figure 2.3	Zero percent difference total cost including schedule delay per passenger contour curve for regional jet and turboprop, and narrow body and turboprop comparison.	28

Figure 2.4	Potential fraction of passengers served by a turboprop with the lowest total cost per passenger compared with a regional jet and a narrow body.	29
Figure 2.5	Potential fraction of passengers served on a turboprop for the lowest comparative total cost per passenger.	30
Figure 3.1	Seat capacity corresponding to the minimum operating cost per seat mile for a range of fuel prices and distances.	42
Figure 3.2	Seat capacity corresponding to the minimum operating cost per seat mile for a range of fuel prices and distances, labor price considered endogenous.	43
Figure 3.3	Predicted operating cost per departure, Leontief Technology vs. translog operating cost model.	46
Figure 3.4	Seat-miles per gallon of fuel vs. seats.	48
Figure 4.1	Generalized cost (time) and related quantities for the single vehicle case, passenger scenario 1.	55
Figure 4.2	Generalized cost (time) and related quantities for the mixed vehicle case, passenger scenario 1.	56
Figure 4.3	Generalized cost (time) and related quantities under the violated passenger assignment assumption, Case 1-1 and 1-2.	61
Figure 4.4	Generalized cost (time) and related quantities under the violated passenger assignment assumption, Case 1-3.	63
Figure 4.5	Generalized cost (time) and related quantities under the violated passenger assignment assumption, Case 1-5.	67
Figure 4.6	Passenger scenario 1 solution algorithm.	68

Figure 4.7	Generalized cost (time) and related quantities for the single vehicle case, passenger scenario 2.....	70
Figure 4.8	Generalized cost (time) and related quantities for the mixed vehicle case for passenger scenario 2.....	72
Figure 4.9	CDF and indifference value of time, mixed vehicle case.....	73
Figure 4.10	CDF and indifference value of time, Case 2-2.....	78
Figure 4.11	Passenger scenario 2 solution algorithm.....	81
Figure 4.12	Headway and cycle representation in passenger scenario 3.....	82
Figure 4.13	Generalized cost (time), time regions, and related quantities for passenger scenario 3. 83	
Figure 4.14	Indifference value of time, Case 3-1.....	88
Figure 4.15	Indifference value of time, Case 3-2.....	89
Figure 4.16	Passenger scenario 3 solution algorithm.....	90
Figure 5.1	Total logistics cost vs. fuel price.....	102
Figure 5.2	Frequency vs. fuel price.....	103
Figure 5.3	Total logistics cost vs. distance.....	104
Figure 5.4	Total logistics cost vs. total passenger flow.....	105
Figure 5.5	Total logistics cost vs. percent of business passengers.....	105
Figure 5.6	Total logistics cost vs. business passenger value of time.....	106
Figure 5.7	Total logistics cost vs. fuel price with infrastructure cost curve.....	109
Figure 6.1	Intercity transportation environmental impact assessment framework.....	112

Acknowledgements

My doctoral work at the University of California, Berkeley was a professional and personal journey to become a transportation researcher and an educator. As the years went by and I learned more and more, I saw the truth in the words, “It never gets easier, you just go faster.”¹ I am grateful to those who dedicated their time and expertise to help me go faster, some of whom are acknowledged here.

My dissertation research was skillfully advised by Professor Mark Hansen, for whom my gratitude cannot be adequately expressed on this page. During my time at Berkeley, Mark struck the perfect balance of mentor and educator. He fostered my interest in aviation by exposing me to a range of research topics. He helped shape the issues addressed in my dissertation, challenged me to consider the problem from multiple perspectives, and empowered me to achieve solutions on my own. Mark’s judicious approach to complex transportation questions and his inclusive, unbiased, and jovial manner made an indelible mark on my approach to research. Mark is the professor I work to impress, the mentor from whom I seek advice and guidance, and the friend with whom I share the funny stories of the day. Working out the results presented in the pages of this thesis on the chalkboard, talking about my next steps over soup, and joking around walking to BART together were the best moments of my graduate career.

I am grateful for the guidance and education I received from all Berkeley faculty members. As a research mentor and committee member, Professor Samer Madanat encouraged me to be precise in my explanations and use the most rigorous research methods. As a teaching mentor, Samer helped me become a more effective educator and taught me to balance my time among students in a large class. While I was his student researcher for just one semester, Professor Martin Wachs taught me to be critical of research results and transportation policies while remaining objective. I deeply value his steadfast commitment to my progress in the field and his devoted involvement in my career.

Professor Carlos Daganzo challenged me to come to Berkeley, sparked my interest in logistics, and provided research comments that helped shape a specific model presented in this dissertation. Professor Joan Walker is a mentor and my role-model of a successful young faculty member. I learned about effective teaching as a student in Professor Michael Cassidy’s well paced, communicated, and organized traffic operations courses. The guidance of Professors Robert Leachman, Adib Kanafani, and Betty Deakin were especially helpful as I sought to define a broader representation of intercity transportation including rail.

I am fortunate to be a member of the Berkeley transportation community and the research group NEXTOR, where I continue to derive great benefit from discussions with

¹ Professional cyclist Greg LeMond.

colleagues including David Lovell, Seth Young, Chieh-Yu Hsiao, Yu Zhang, Yoonjin Yoon, Amy Kim, Jing Xiong, Tasos Nikoleris, Gurkaran Buxi, and Elliot Martin. In preparing this dissertation, Gautam Gupta challenged me like an advisor and joked with me as a friend. Bo Zou is my model of dedication and reason, a confidant and the true embodiment of Confucius' statement "Never contract friendship with a man that is not better than thyself." Despite the 2500-miles separating our schools, I am grateful to have Andrew Churchill as a colleague and friend with whom I shared the highs and lows of graduate student life. Mikhail Chester is my go-to expert on the greater environmental issues related to intercity transportation. Cecily Way pushed me to be a faster runner and a critical thinker over the thousands of miles we covered together as graduate students on our hybrid road runs/transportation debates.

I am grateful for a group of close colleagues who helped guide my dissertation and consistently challenge me to articulate the practical implications of my work. Patty Clark provided the airport perspective for my dissertation research that led to the definition of the research question. Patty remains an advisor and a kindred spirit in many ways. Matthew Coogan constantly challenges me to apply my models to the issues of today. Matt is the example of an adept research manager, and being a member of his team is a welcome component of my work. Joe Post at the Federal Aviation Administration helped provide a reasoned view on the future of aviation. I would additionally like to thank Jürgen Müller, the researchers at the Eurocontrol Experimental Center, and the aviation researchers at the DLR in Cologne, Germany for sparking my interest in the impact of environmental policies on aviation during my visit in the summer of 2007.

In the pursuit of research not constrained by the scope of a single transportation institution, I assembled a portfolio of funders. I am deeply thankful for the financial support of the University of California Transportation Center, the U.S. Department of Transportation Eisenhower Transportation Fellowship Program, and NASA Ames.

I feel lucky to have parents who encouraged me to pursue any field I desired and helped cultivate my love of science and math from a young age. If all girls had parents like Katherine and Stephen Smirti, gender imbalance in engineering would not exist. Their unwavering support motivates me to be a better person and researcher and give back to the field by mentoring future female engineers. Additionally, as born and bred New Yorkers, they are their own brand of transportation experts. Mom and Dad, even though I can't really do anything about it, call me anytime with requests to have your flight depart on time.

My deepest appreciation and gratitude goes to my husband Anders, who can spot the difference between a B767 and an A330 and knows the best spot for a date is one with a good view of the airport. He had patience when this research came first and celebrated every big and small result presented in these pages. He has been the pillar of strength on which I leaned through every challenge I faced at Berkeley. I dedicate my dissertation to Anders for his unending support and love that enables me to reach goals unachievable without him.

1.

Introduction

1.1 Problem Statement

The challenges of climate change policy related to aviation – a global pollutant and a mode with local, regional, and international components – have motivated considerable research. On both the macro and micro scale, research agendas in aviation and climate change are driven by the domains of sponsoring organizations. Policy relevant research serves a clear purpose in supporting the decision making of organizations and therefore focuses on actions within their purview. This can lead to suboptimal solutions; a component is optimized rather than the system, and the solution is at most second best. In this research, we take a systems-level point of view in investigating the effects of climate change policy on aviation.

Greenhouse gas emissions (GHG), the gases that cause climate change, pose new challenges in the context of aviation and the broader intercity transportation system. The impacts of greenhouse gas emissions are spatially and temporally distributed rather than concentrated. As global rather than local pollutants that are not experienced at the point of emission (compared with noise), the pressure to reduce their emission is diminished and the locus of responsibility for doing so is unclear. The spatial distribution of GHG emissions is matched by the spatial distribution of aviation, a mode with local (airports), regional, national, and international components. Aviation organizations are grappling with unclear roles to regulate and reduce the emission of a pollutant with impacts outside their jurisdiction along with the need to remain competitive.

While greenhouse gases are global pollutants, policy organizations are local in nature. Policies to curtail aviation-related GHG emissions are being considered at many levels, from local airport authorities to the International Civil Aviation Organization (ICAO). Existing research in intercity transportation reflects these policy-making institutions and their roles. As the European Commission is planning on the inclusion of aviation in their GHG emissions trading scheme (EU-ETS), researchers have investigated the macroeconomic and microeconomic impacts. Anger (2010) finds the macroeconomic impact to be small using the Energy–Environment–Economy Model. Microeconomic research finds the increase in airline costs is not significant enough to reduce demand, and that the cost increase can be passed along to customers without a change in operations (Albers et al., 2009; Scheelhaase and Grimme, 2007). Research on the actions of airport operators to reduce GHG emissions is similarly focused on actions that fall within the purview of airport operators, such as those described by Kim et al. (2009). However, as asserted by Reimer and Putnam (2007), in the absence of relaxing

constraints on the airport operator, their ability to reduce GHG emissions is minimal. Research into how the regulatory agency overseeing US aviation, the Federal Aviation Administration (FAA), could change descent profiles through Continuous Descent Approaches (CDA) to reduce GHG emissions has also yielded incremental but measurable results (Clarke et al., 2004). Finally, in an effort to inform transportation policy at a systems level, Chester (2008) performs an intermodal comparison of GHG pollutants from specific intercity transportation vehicles; Chester and Horvath (2010) build on this foundation with a parametric analysis over load factor.

This body of research reflects the scope of existing policymaking institutions. In the US, the airlines set operations, routes, and vehicle technology; the airports provide and manage infrastructure; and the FAA provides guidance and policy related to airline and airport operations. Aircraft operators play a large role in choosing and altering operational frequency and vehicle types while considering passenger demands and preferences, airport restrictions, and competition. Research has implicitly limited itself in considering competition, a constraint supported by research and practice. At congested airports, airlines will lose their slots, or allowances to perform a take-off and landing operation at an airport, if they are underutilized. Furthermore, Wei and Hansen (2005) found that airlines could positively influence their market share by increasing vehicle frequency instead of vehicle size. While examples of research investigating the potential of larger vehicle sizes and decreased operations to reduce delays at a congested airport exist (for example, Coogan et al., 2009), research tends to reflect the airline concern of competition. Contrasted with the role of the aircraft operators, the FAA and airport operators have essentially no direct control of vehicle operation activity, including whether an airline serves a particular airport, the frequency or time of day of service, or the aircraft type or size used to provide service. Airports have a long-standing right to set minimum landing fees to reduce airfield delay during periods of congestion, a right amended in 2008 by the FAA to give airports expanded ability to influence operations (Federal Aviation Administration, 2008). While airports are constrained to use landing fees to limit congestion, not environmental impacts, Ryerson and Hansen (2009) found that lifting this constraint would give airports the ability to influence aircraft size, technology, and fuel consumption.

In developing a methodology to capture the system optimal organization of intercity transportation under a climate change policy, we consider a central planner minimizing the total logistics cost, the sum of the two main intercity transportation cost components: vehicle (aircraft) operators and passengers. We define the goal of the central planner as finding the optimal (least cost) service mix – which vehicles and at what operational level – of an intercity transportation corridor. In summing and comparing costs for single and mixed vehicle scheduled services, this methodology determines the vehicle size, technology mix, and frequency to serve an intercity transportation corridor. The total logistics cost will include both vehicle operating costs and costs incurred by the passenger to capture the cost-reducing potential of alternative vehicles with different cost structures and service attributes.

In determining optimal service mix, a central planner could deploy new intercity modes – such as high speed rail – as well as new and redesigned aircraft at different operational levels. These vehicles have differentiated service qualities and inputs needed to produce passenger output. It could therefore be advantageous to serve an intercity corridor with a single vehicle technology, or alternately, a mix of vehicle technologies appealing to passenger subpopulations. This is particularly the case for short- and medium-haul intercity transportation, where diverse passenger travel purposes lead to highly differentiated passenger values of time. To capture the impact of aviation climate change policy, we formulate the models to be sensitive to fuel price. Fuel prices may change significantly in the future because of market conditions or environmental policies, as fuel consumption is directly correlated with the production of carbon dioxide (CO₂), the most abundant GHG.

In modeling the actions of a central planner in response to aviation climate policy, we develop both empirical models and analytic models. Empirical vehicle operating cost models provide direct insights into the relationship between operating cost and fuel price and guide development of the analytic models. To determine the vehicle technology combination that provides service at the lowest cost in response to an environmental policy, we develop analytic total logistics cost models of an intercity transportation corridor serving multiple passenger groups. This cost model captures input substitution within the production process of a vehicle combination. It also captures the effects of induced technological change, which is the movement to a more environmentally benign production process brought about by an environmental policy. The results of analytic models are combined with those of empirical models to determine the vehicle technology combination and level of key inputs that minimize cost for a corridor. In this research, we define passengers by their demand for travel and their value of time. We begin the analytic models with discrete passenger groups building to the consideration of passenger value of time to follow a continuous distribution. In formulating the model this way, with passengers following a continuous distribution and with fuel price as a parameter, we keep the definition of passengers and climate policy as general as possible.

In considering an intercity transportation corridor from a total logistics cost approach, we draw from the logistics literature. Smilowitz and Daganzo (2007) and Daganzo and Newell (1993) consider a central planner organizing freight services by minimizing the operating cost and the cost of holding packages as inventory. A similar approach is illustrated in urban transportation, such as the work of Meyer and Miller (1984) and Keeler et al. (1975). The total logistics cost approach is employed to a more limited extent in aviation. Viton (1986) minimizes a total logistics cost model of an aviation corridor by assigning discrete aircraft models to different corridors. Hansen (1991) uses a total logistics cost model to compare the cost of two aviation corridors served by different aircraft technology, serving varied origin-destination pairs in the same city pair. In the total logistics cost model developed in this research, we address the skepticism shared by Viton (1986) and Keeler et al. (1975) in using one value of time to represent all passengers due to multiple time classifications (travel time, schedule delay) and varying values of passenger time (high-valued business travelers, low-valued leisure travelers). In a logistics setting, Smilowitz et al. (2003) consider two vehicle technologies serving two

packages with specific values of time, and find that an integrated network compared with separate distribution yields cost savings. Finally, in this research, we keep fuel price a parameter and evaluate how optimal solution changes parametrically with this key variable, a practice demonstrated by Oster and McKey (1984) in their evaluation of aircraft operating cost over stage length.

In developing a system optimal model of a central planner solution parametrically over fuel price, we capture fundamental factors shaping the optimal mix of services on an intercity corridor – such environmental concern (1.2), traffic density, vehicle technology, and passenger preferences (1.3) – in a model that is analytically tractable.

1.2 Environmental Concern

1.2.1 Greenhouse Gas Emissions

It is well known that the operation of transport vehicles is a major component of anthropogenic climate change – the warming of the Earth’s temperatures due to human activities. The production, delivery, and combustion of transportation fuels increase levels of greenhouse gases in the atmosphere (Environmental Protection Agency, 2007). The transportation sector is responsible for 13 percent of global GHG emissions and 28 percent of United States domestic GHG emissions, making it the fifth and second largest contributor respectively (Pew Center on Global Climate Change, 2004). Recent estimates of global shares put aviation at two to three percent based on recent work accomplished by IPCC (Williams, 2007). Of the principal anthropogenic greenhouse gases (Carbon Dioxide (CO₂); Methane (CH₄); Nitrous Oxide (N₂O); and Fluorinated Gases), CO₂ is directly produced through the burning of fossil fuels (Environmental Protection Agency, 2010). In addition to the anthropogenic greenhouse gases there are other mechanisms through which aircraft operations affect climate, such as contrail formation (Waitz et al., 2004; Kim et al., 2007).

Regulating and reducing the impacts of greenhouse gas emissions is more challenging than doing so with other pollutants, as GHGs are spatially and temporally distributed rather than concentrated. Unlike noise emissions from an aircraft overflight, GHG emission impacts are long term rather than immediate. Unlike criteria pollutants, GHG emissions are felt worldwide through the warming of the earth, rather than localized. Greenhouse gas emissions also have varying warming potential in the atmosphere that can vary depending on the spatial distribution of the emission. These challenges motivated a common metric in GHG policy: the emission of the most abundant greenhouse gas – Carbon Dioxide (CO₂) that is directly correlated with the burning of fossil fuels (Environmental Protection Agency, 2010). State, federal, and international initiatives are looking to regulate the amount of CO₂ released into the atmosphere by a variety of sectors through a variety of policy levers. A constraint on CO₂ emissions is a resource constraint imposed on the production process and it is well known that such constraints can be represented through shadow prices on the associated resources; fuel price increases will most likely follow (Plaut, 1998). To this end, we consider CO₂ emissions policy as a change in fuel price. Such a perspective keeps the discussion general, a benefit because the mechanism through which CO₂ will be regulated is not

known in the United States. Moreover, uncertainty about the future of fuel costs makes the study of fuel price changes an additional compelling topic.

1.2.2 Fuel

Fuel and labor are the largest components of operating cost an airline faces. From 2000-2009, about 50% of airline operating expenses are comprised of fuel and labor. However, throughout this period, the relative shares of fuel and labor saw a large shift as fuel prices rose and labor costs remained relatively constant shown in Figure 1.1, highlighting the volatility of fuel prices (Air Transport Association, 2010).

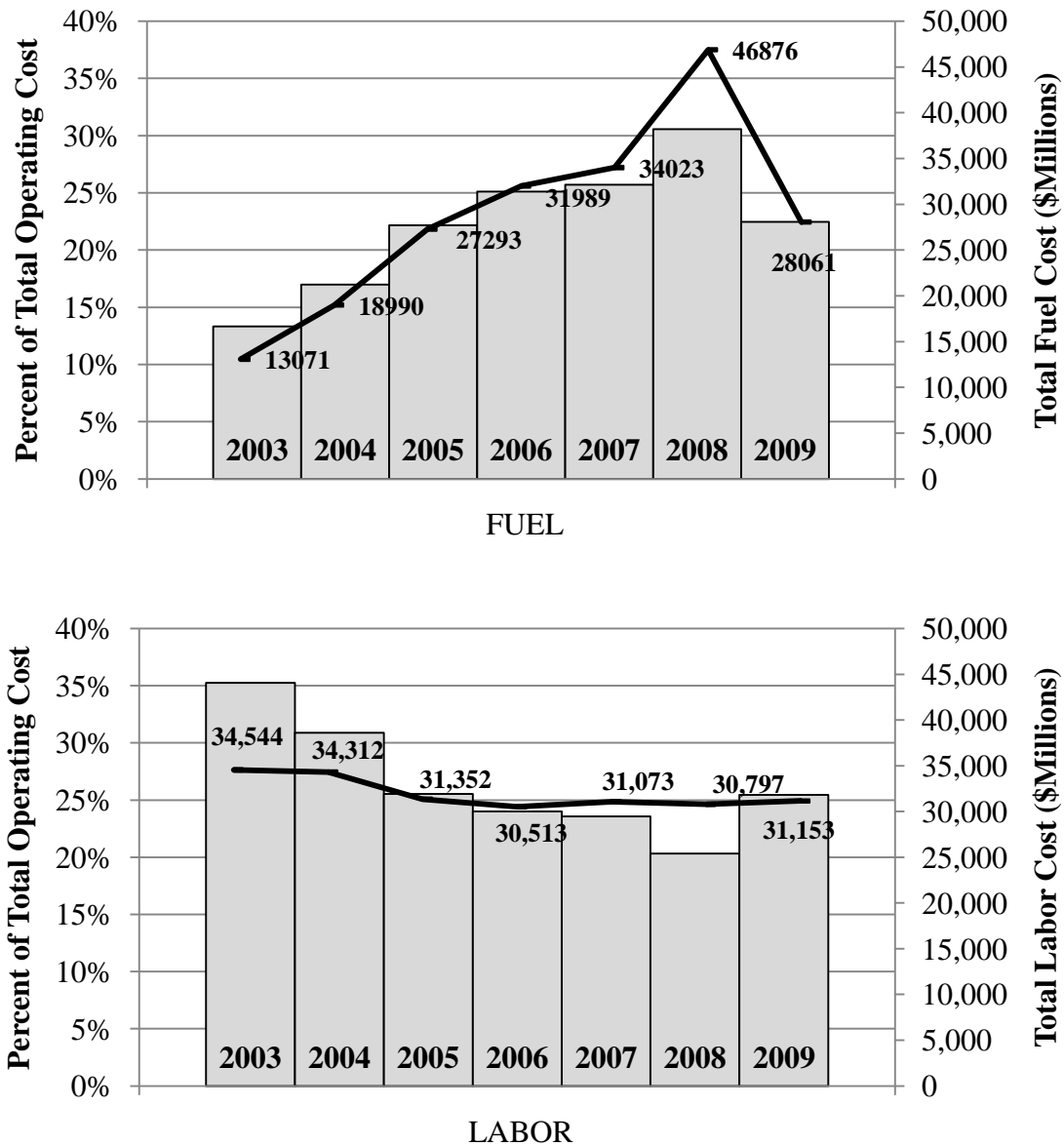


Figure 1.1 Labor and fuel as a percent of operating cost, 2003-2009.

Because of the fuel cost volatility and the large role fuel plays in total operating costs, airlines engage in fuel hedging contracts to secure a certain price for fuel. There are a variety of hedging instruments (described by Carter et al., 2004) through which airlines can secure a fuel rate over a period. The practice of hedging can shield an airline from the volatility of oil prices and in turn stabilize airline costs (Morrell and Swan, 2006). Hedging, however, carries its own uncertainty and limitations. Hedging involves contracting for fuel, and requires airlines to pay in advance to secure a fuel price – an impossibility for many US carriers struggling with cash flow. Furthermore, it is possible that an airline can incorrectly predict the trend in oil prices. For an illustration, consider Figure 1.2. The bold line shows the price that the U.S. passenger airlines paid for fuel in a given quarter, while the dotted line represents the refiner price. Before the large fuel price spike in 2008 airlines were generally paying less than the price at the refiner, however, after the spike airlines were paying more, mostly due to fuel contracts.

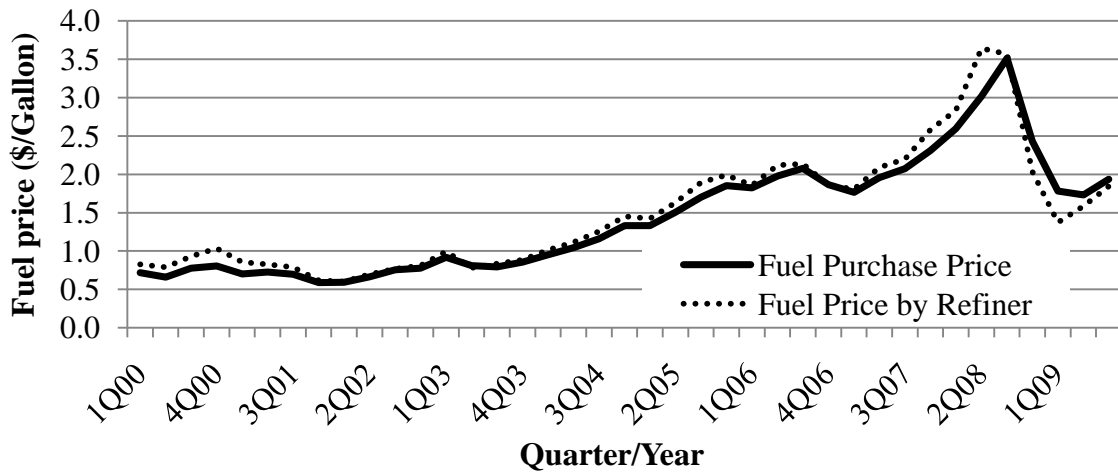


Figure 1.2 U.S. jet fuel price (dollars per gallon).

Also evident in Figure 1.2 is the fluctuation in the price of aviation jet fuel. Aviation fuel price increased more than threefold from 2004 to 2008 and then quickly fell back to pre-2004 levels. While airlines and manufacturers strive to continually improve their product through innovative technology and procedures, such actions resulted in modest efficiency growth compared with the peaks of fuel fluctuations (Air Transport Association, 2010).

1.3 Short Haul Intercity Transportation System Trends

There are trends that make short to medium-haul intercity transportation a fitting sector for which to develop environmental policy impact models. These is rapid growth throughout the system, modal diversity, and passengers with differentiated values of time.

1.3.1 Growth Trends

Air transport demand – passenger demand for service and airline demand for operations – has grown rapidly in recent decades. Despite a traffic decline precipitated by the recession in the second half of the first decade of the 21st century, FAA projections show traffic levels recovering by 2012 followed by a 30 percent growth by 2025 (Ball et al.,

2010). The FAA has plans to meet some of the demand increase through the development of additional runways; however, by their own estimates, this increase in infrastructure will not be sufficient to meet all the demand at many congested airports (Federal Aviation Administration, 2007). This growth will be somewhat accommodated by a new technology and operational infrastructure termed the Next Generation Air Transportation System (NextGen); similar plans exist for the European airspace system (Smirti and Hansen, 2007; Eurocontrol, 2007). Both are large-scale modernization initiatives with similar goals: to transform the current air transportation system for their respective regions to meet the growing demand for air transportation. Initiatives beyond NextGen exist yet tend to be more politically contentious. Coogan et al. (2009) discuss demand management initiatives, actions to reduce operations but maintain passenger and freight throughput with larger aircraft, such as congestion pricing and operational caps.

1.3.2 New and Redesigned Aircraft Types

New air transportation vehicles currently in research, development, and deployment stages offer extensive options for the transformation of intercity transportation. These new vehicles are segmented by their propulsion systems: aircraft with jet engines and aircraft with turboprop engines. These two vehicle classes present new opportunities to deploy vehicles to offer customizable service and meet environmental and operating cost objectives.

Aircraft with jet engines are prominent in number in the intercity transportation system and varied in the capacity offered. A trend for jet aircraft is the expanding range of vehicle capacity, such that in 2010, there are aircraft of all sizes between the range of 30 seats and 500 seats. Figure 1.3 shows a cumulative distribution function of single aircraft seat capacities owned or leased by US carriers in 2006 as reported to the US Department of Transportation. As can be seen, there is a large range in seat capacity (37 - 412) and available models span this range almost continuously. Furthermore, Figure 1.3 only includes aircraft operated by US carriers on domestic routes, and does not include notable aircraft such as the Airbus 340 which has between 261 and 380 seats depending on variant (Airbus, 2010). Boeing is currently developing two variants of the 787 aircraft series: the 787-8 Dreamliner will have a capacity of 210 - 250 seats and the 787-9 will have a capacity of 250 – 290 seats (Boeing Company, 2010). This will further reduce the one gap between aircraft sizes 276-360 shown in Figure 1.3.

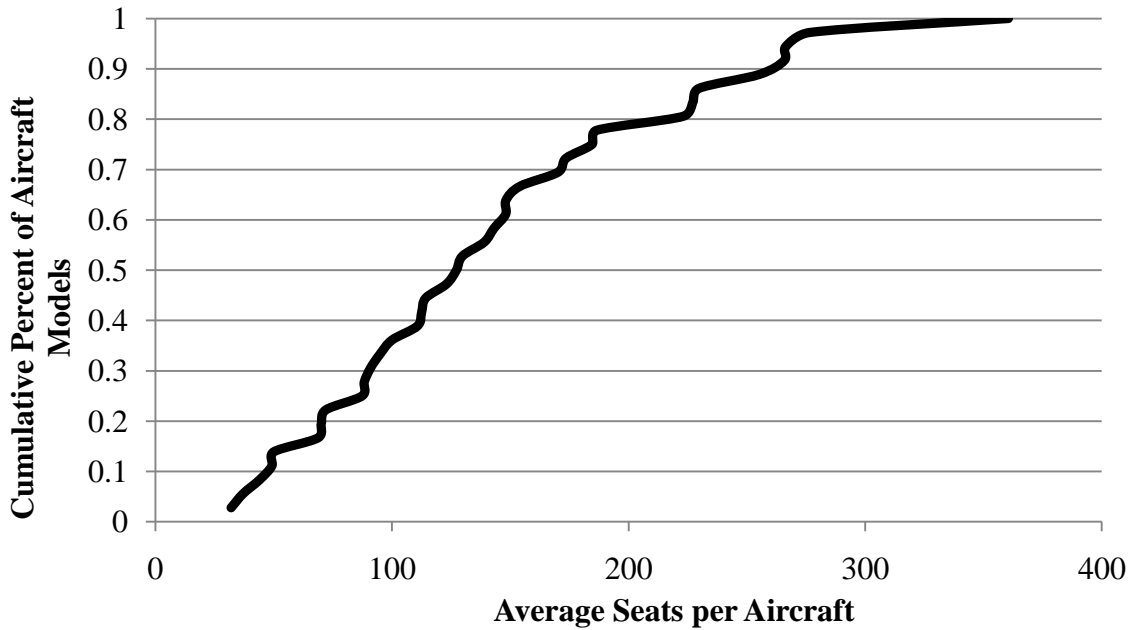


Figure 1.3 Cumulative distribution function of aircraft model seat capacities owned/leased by US carriers, 2006.

There is also an expanding of the seat capacity boundaries for aircraft jet engines. Vehicles with very limited capacity include subsonic business jets and very light jets (VLJs) used in commercial service. Both vehicles types have jet engines that enable high cruise speeds and also have long ranges of over 1000 miles. Their small size (three to eight seats for VLJs and eight to 19 seats for business jets) and relatively light weight make them suitable for landing at both public and private use airports (Espinoza et al., 2008; Bonnefoy and Hansman, 2007). These features allow for a customizable, potentially on-demand service, such as what was offered by DayJet (Espinoza et al., 2008). On the large end of the spectrum, Airbus delivered the first high capacity Airbus 380, which seats 525 in a three-class configuration but could potentially seat over 800 passengers in a one-class configuration (Airbus, 2007).

The second class of aircraft are updated turboprops offering low operating cost and a lower tier of passenger service. Prior to recent redesign efforts, turboprop aircraft were relatively loud, uncomfortable aircraft with a limited operational range. Because of this, turboprops fell out of favor with the introduction of regional jets (Johnston, 1995; Mozdzanowska and Hansman, 2004). Considering passenger preferences, abandoning the turboprop was not unwise: passenger disutility of turboprop travel, estimated by Adler et al. (2005), is estimated to be a non-trivial fraction of airfare. However, recent improvements to passenger level of service and operating range, coupled with the fuel price increases of 2008 have caused a surge of interest in new turboprop models. Two domestic carriers have adopted turboprops in their regional markets and international low cost carriers have emerged offering an all-turboprop fleet (for example, Canada's *Porter Airlines*). Many cite the ability of redesigned turboprops, with higher levels of passenger service than their predecessors, to balance operating cost and passenger service. As noted

by Aviation international News: “Nothing re-ignites interest in new turboprops faster than a good old-fashioned ‘fuel crisis’” (Huber, 2008).

Comparative aircraft costs depend on fuel price. This is particularly the case for aircraft serving short haul markets (under-1000 miles). Short haul markets may be competitively served by three main aircraft types: turboprops, noted for their low fuel consumption; regional jets, 30-90 seat jets noted for their passenger service qualities; and narrow body jets, 105-150 seat jets noted for their balance of operating costs and passenger service ability. Figure 1.4 shows the change in United States airline ownership and leasing levels (summed to represent vehicle presence in the market) of these three different aircraft types gathered from US Department of Transportation data overlaid on the jet fuel purchase price from 1996-2009. Recent years have witnessed a shift away from turboprops toward regional jets, while the narrow body aircraft share remained stable. While regional jets are less fuel efficient on a per seat-basis, turboprops offer a lower level of passenger service in the form of comfort, speed, and perceived safety. As seen in Figure 1.4, regional jets continue to be owned or leased in greater numbers even as fuel prices increase. One possible explanation is that despite high operating costs, the regional jet enables high frequencies and a high level of service that is valued by passengers. Another is that airlines expected the surge to be temporary. It may be that, since turboprops are more fuel efficient, increasing fuel prices could make this advantage outweigh the importance of passenger preference for a higher level of service and reverse the trend of regional jet adoption.

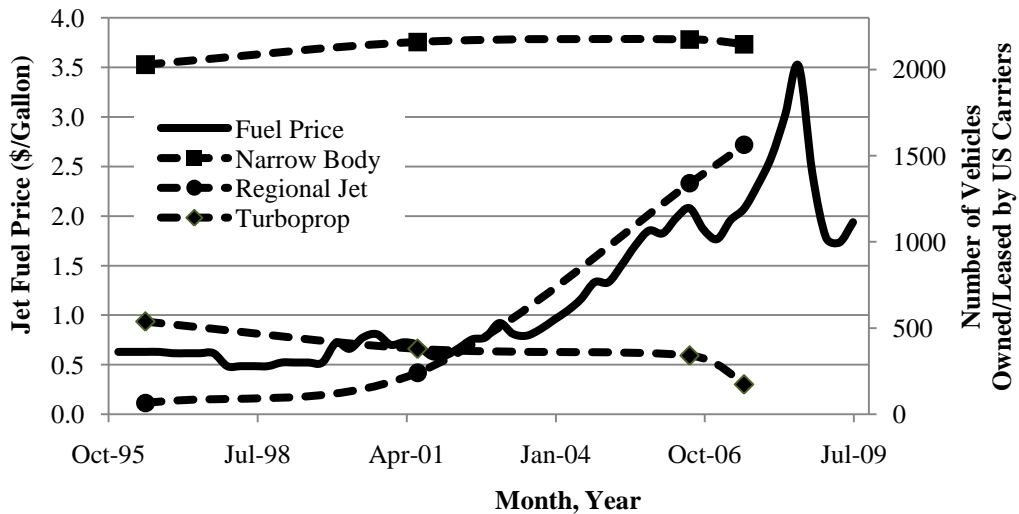


Figure 1.4 Aircraft trends for short haul travel and U.S. jet fuel price paid by airlines (dollars per gallon).

1.3.3 High Speed Rail

The development of a high speed rail (HSR) network in the United States presents a new opportunity to transform intercity transportation. In February 2009, the American Recovery and Reinvestment Act allocated \$8 billion for intercity rail projects. As reported by the Federal Rail Administration (2010), there are ten designated high-speed corridors to receive Federal funding shown in Figure 1.5 (Federal Railroad

Administration, 2010). California HSR is one such corridor that also has a state-wide mandate to develop HSR. On November 4, 2008, California voters approved Proposition 1A which authorized funding and made into law that “a clean, efficient high-speed train service linking Southern California, the Sacramento San Joaquin Valley, and the San Francisco Bay Area” will be built (California High Speed Rail Authority, 2009). The comparatively lower operational GHG emission travel mode of the HSR has potential to reduce GHG emissions and fuel consumption from the entire intercity travel system; however, the comparative emissions are highly dependent on vehicle load factor (Chester, 2008; Chester and Horvath, 2010).



Figure 1.5 Designated High Speed Rail corridors in the United States.

The definition of high speed rail varies across systems. The European Directive on Interoperability defines HSR as a train that achieves a maximum speed of 250km/h (155 mph); this provides an imprecise picture of HSR, however, as some trains achieve higher *average* speeds while others achieve higher *maximum* speeds (Steer Davis Gleeve, 2006). In the United States, the California HSR system is designed to travel at a 220 mph maximum speed and 170 mph average speed, covering San Francisco to Los Angeles in 2:40 time (California High Speed Rail Authority, 2009). Whatever the precise definition, there is a clear relationship between travel time and market share. As shown in Figure 1.6 (from Steer Davis Gleeve, 2006), the travel time on a HSR system is a strong determinant of rail market share when compared with air transport. For intercity transport travel times below 3-4 hours, the market share for rail is consistently higher than 50%. This highlights the strong potential for intermodal competition in short- to medium-haul intercity transportation corridors.

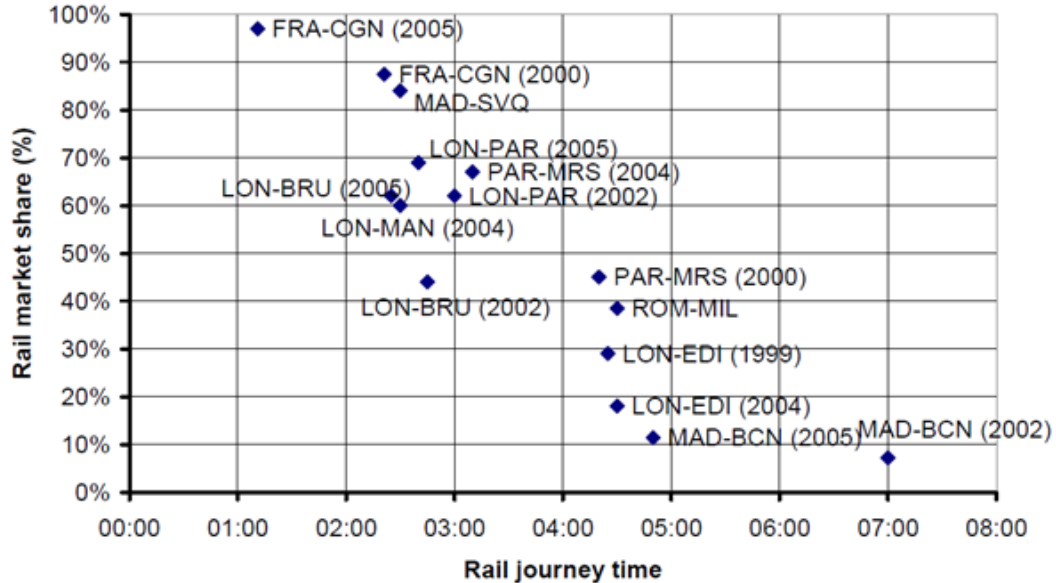


Figure 1.6 Rail market share (compared with air) against rail travel time for select European intercity transportation corridors.

1.3.4 Mode Split

Coogan et al. (2009) report on the intercity mode shares for the two mega-coastal corridors of the US: the California corridor and the Northeast corridor. Mode shares are challenging to estimate because of the diversity of organizations that capture this information. We can see that California, a region with robust short distance rail service but lacking high-quality long distance rail service, has an intercity mode share dominated by auto for short distance and auto and air for the medium-haul distances (Figure 1.7, with distances in miles by driving). In Figure 1.8 we see the rail and air mode shares on the North East Corridor, but only as a percentage of the total air and rail market share (auto excluded). We see rail playing a much larger role in the mode share, as the intercity rail travel times are very competitive with air transportation. We see the same trend in both corridors, which is that longer distances equal higher mode share for air.

In this research, we will consider high speed rail as the only alternative to air transportation. While auto plays a large role in intercity transportation, a recent HSR study provide a compelling argument for this scope definition. The Office of the Inspector General (OIG) investigated two improvement scenarios to the rail service travel times in the North East Corridor (Federal Railroad Administration, 2008). The first scenario was three-hour travel time between Boston and New York and 2.5 hour travel time between New York and Washington; the second scenario cut travel times by 0.5 hours on both segments. The study found that the loss in air ridership would be 10.6 and 20.3 percent under scenario one and two respectively, while the loss in auto ridership would be 0.3 and 0.6 percent. The negligible loss in auto ridership is explained by the service similarities between air and HSR compared with the flexibility an auto mode provides. OIG explains that those who choose auto do so for a reason – long airport/HSR

station access or egress times, or multiple destinations dispersed around a region – such that these passengers would be very unlikely to switch modes.

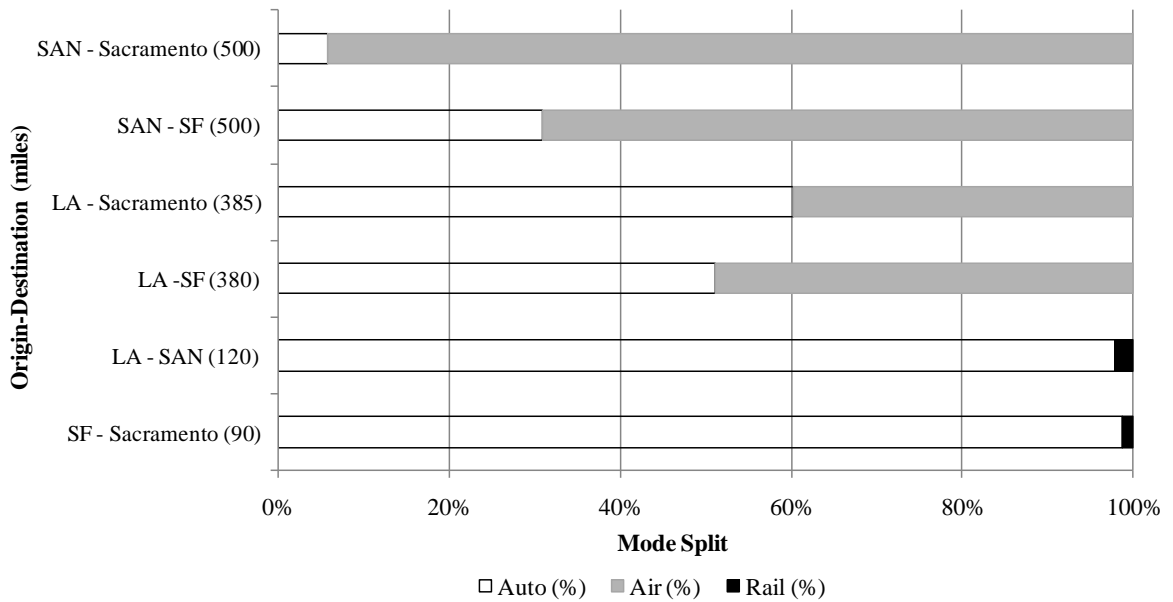


Figure 1.7 Mode share and distance for certain California corridor city pair markets.

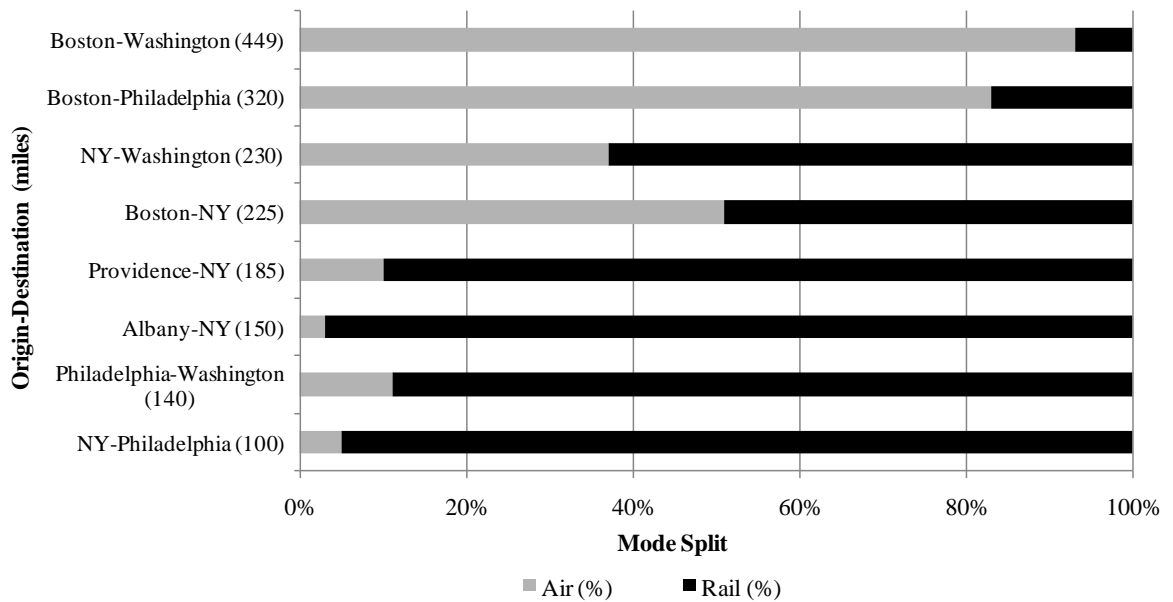


Figure 1.8 Mode share and distance for certain Northeast corridor city pair markets.

1.3.5 Value of Time

An individual passenger can experience multiple values of time throughout a day and across situations. In aviation this has been proven through empirical value of time investigations. Using a combination of revealed and stated preference surveys for air transportation users, Adler et al. (2005) use a mixed logit model to estimate the value of

flying time, schedule delay, and on-time performance assuming all non-fixed parameters are normally distributed. Another study pointing to the existence of passenger heterogeneity is Berry et al. (1996). By assuming that the preferences for prices and flight characteristics are correlated, they estimate different sets of coefficients for each group using a random utility model. They find an existence of two groups of passengers, one exhibiting more price elasticity.

These two studies represent two snapshots in time approximately 10 years apart. Considering data of actual air tickets purchased 10 years apart, we can show that while passenger value of time differentiation is present in both years, this differentiation has grown with time. It is very clear that the value of time is become more dispersed, as in there is growing income disparity, when one considers the change in airfares over time. Using the Airline Origin and Destination Survey (DB1B) from the Bureau of Transportation Statistics, a 10% sample of airline tickets purchased domestically, we can evaluate the change in airfares in a span of 15 years. We consider the cumulative percent of passengers who paid a given fare per mile for all segments between 350 and 500 miles in two years: 1993 (in 2008 dollars) and 2008 (both in the second quarter, shown in Figure 1.9). The distribution of passenger fares has a steeper slope in 1993, representing a more limited distribution of fares compared with 2008. In 1993, 50% of passengers pay less than \$350-\$500, a fare much lower than the 50% of passengers paying less than \$420-\$600 in 2008. While there is a longer tail in 1993, such that that a small percent of passengers paid a fares not seen in 2008, the bulk of passengers paid a limited range of fares compared with 2008.

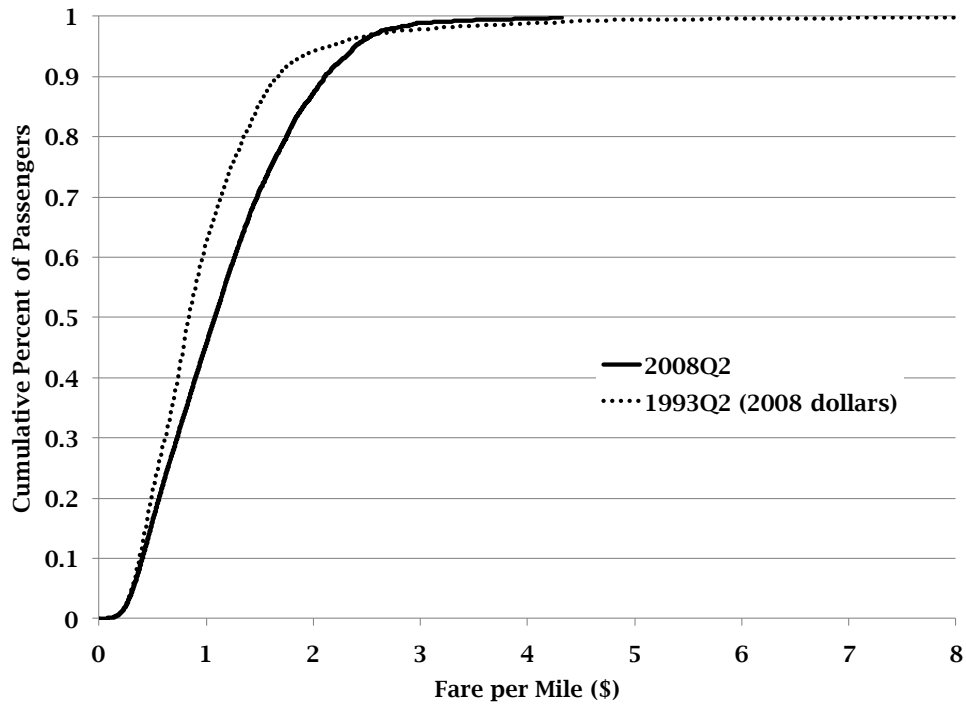


Figure 1.9 Distribution of total system passenger one-way fares per mile.

1.4 Central Planner Response to a Fuel Price Increase

In considering the actions available to a central planner in responding to a fuel price, we define two categories of responses. The first is input substitution within the production process of a vehicle combination. The second is induced technological change, which is the movement to a lower cost production process brought about by an environmental policy.

In the context of intercity transportation, we define production processes by the vehicle technologies that convert inputs to outputs. We will consider production processes to be a single vehicle technology or a mix of vehicle technologies. The production process is represented by a total logistics cost function such that the inputs considered are supplier vehicle inputs (such as fuel, labor, and capital) and user inputs (such as travel time and schedule delay). Some possible production processes, represented by vehicle technologies, inputs and output are shown in Figure 1.10. Each vehicle combination in Figure 1.10 turns the inputs into the output through a technically efficient production process. These vehicle combinations, in the context of the intercity transportation system, are jets alone (J), turboprops alone (T), high speed rail alone (H), and a jet and turboprop mix (H and T), a high-speed rail and jet mix (H and J), and a turboprop and high-speed rail (T and H) mix.

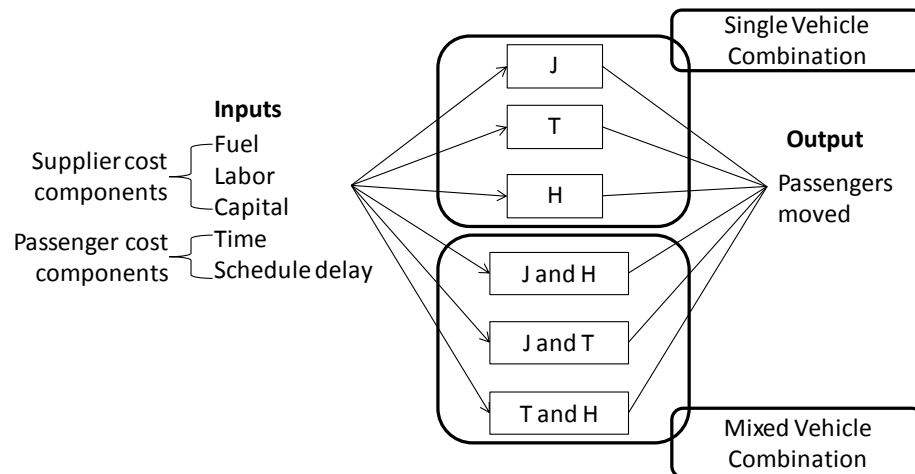


Figure 1.10 Inputs and output of single and mixed vehicle production processes.

For each vehicle combination in Figure 1.10, at a given level of factor prices (the prices associated with the inputs), there is a vehicle combination with the lowest total logistics cost. There are many technically efficient seat capacities associated with each possible vehicle combination. However, for each vehicle combination there is only one seat capacity (or set of seat capacities in the mixed case) that is both technically efficient and minimizes cost for a given level of factor prices. If a factor price were to increase, two possible actions are possible. The first is that, for each production process box in Figure 1.10, there will be a substitution of inputs and a move to another technically efficient seat capacity; this is input substitution. The second is that the production process that converts inputs to the output at the lowest cost changes; this represents induced technological change.

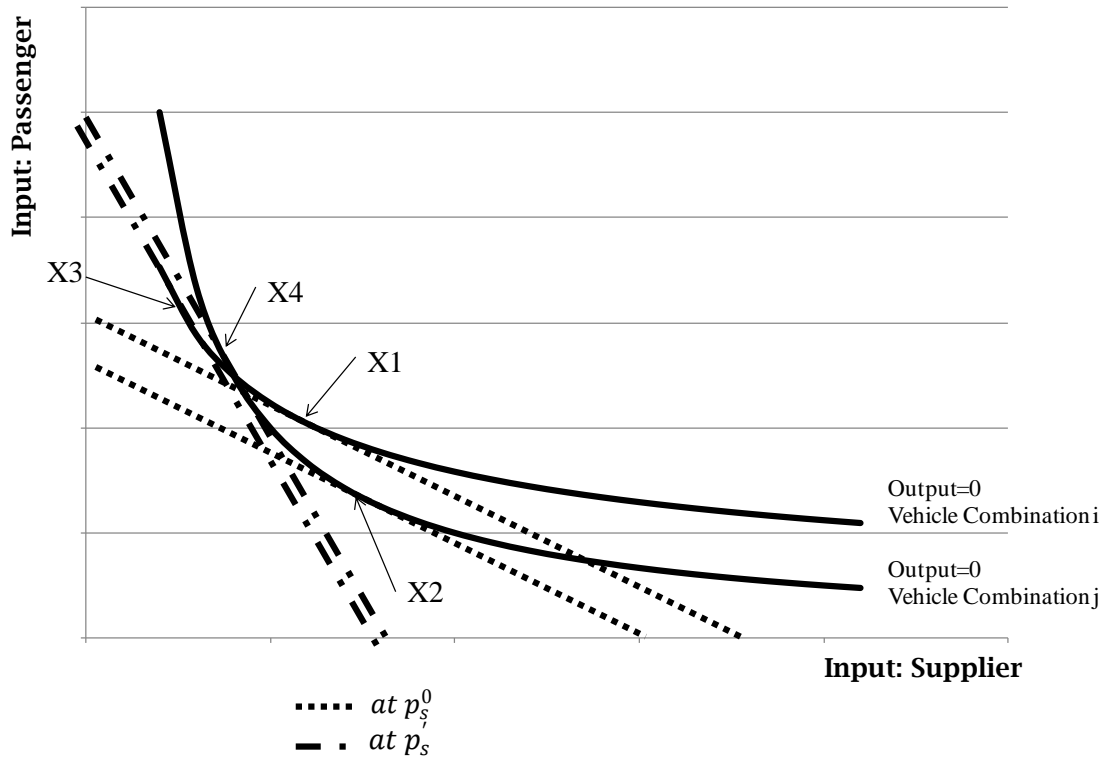


Figure 1.11 Illustration of input substitution and induced technological change.

Input substitution and induced technological change are illustrated in Figure 1.11, which depicts two isoquants each representing the total logistics cost to produce output O with either vehicle combination i or j . The production process depicted is a two input production process: one passenger input (P) and one supplier input (S). At a baseline factor price for all inputs, point $X1$ represents the optimal point of production for vehicle combination i ; point $X2$ represents the optimal point of production for vehicle combination 2. Let $C(X1)$ and $C(X2)$ represent the total logistics cost at the point of optimal production for vehicle combination i and j respectively. At a baseline (supplier) factor price of p_s^0 , $C(X2) < C(X1)$; vehicle combination j has a lower cost to produce the same output as vehicle combination i . This is illustrated in Figure 1.11, as point $X2$ is on a lower budget line than point $X1$. If there is an increase in the factor price of fuel (a supplier input) represented by p_s^1 , a new budget line and point of tangency exists for each vehicle combination. The shift from the optimal costs at p_s^0 to the optimal costs at p_s^1 – $C(X2)$ to $C(X4)$ and $C(X1)$ to $C(X3)$ – represents input substitution. Furthermore, at p_s^1 , $C(X3) < C(X4)$, such that optimal point of production for vehicle combination i is on a lower budget line than vehicle combination j . This change in vehicle combination with the lowest total logistics cost represents induced technological change.

In the following chapters we will explore the potential of the two categories of reduction strategies – induced technological change and input substitution – to manage costs due to a fuel price increase. In chapter 2 and 3, we investigate the potential of supplier-to-supplier input substitution (such that the production process is characterized by supplier inputs only), passenger-to-supplier input substitution (the production process is

characterized by supplier and passenger inputs), and induced technological change. Upon the finding that passenger-to-supplier input substitution and induced technological change have the greatest potential, chapter 4 develops a mathematical representation of intercity transportation that captures passenger-to-supplier input substitution and induced technological change. Chapter 5 presents a case study of an intercity transportation corridor by matching empirical models with the analytic models.

2.

The Potential of Turboprops for Reducing Aviation Fuel Consumption

In light of the wide range of future fuel price scenarios, we seek to understand how fuel price affects the comparative advantage of alternative air transport technologies and vehicles. While recent years have witnessed a shift away from turboprops toward regional jets, it may be that, since turboprops are more fuel efficient, increasing fuel prices could reverse this trend. The objective of this chapter is to compare representative aircraft for their operating costs and passenger costs over a range of fuel prices. The range of fuel prices reflects uncertainties about future market conditions as well as environmental policy choices.

In this chapter we compare the operating and passenger cost of turboprops, noted for their low fuel consumption, with two widely deployed aircraft, a regional jet and a narrow body jet. Operating costs include fuel, crew, maintenance, and airport costs. Passenger costs include travel time costs (flying time differences and schedule penalties) and the perceived disutility of flying on turboprops (relative to jets). By combining passenger and operating costs in a single function, this study takes a total logistics cost approach. This allows vehicles with different cost structures and service attributes to be compared. Homogenous fleets of each vehicle category are compared for operating and passenger costs over a range of fuel prices and route distances and the minimum cost fleet mix is determined. This study will perform these comparisons over wide ranges of distances and fuel prices to identify the combinations of values of these parameters at which the different aircraft models can serve segments with the lowest cost.

Several previous studies model and compare operating costs for airlines. These studies employ models to look for aircraft with the lowest operating costs as a function of segment characteristics such as stage length and market density. Douglas and Miller (1974) develop comparative aircraft cost models that divide operating costs which vary per user into fixed and variable costs. Using cost models developed in this manner, with fixed components and components that vary with distance and traffic, aircraft costs are compared. When discussing an efficient airline market, Douglas and Miller (1974) qualitatively discuss fleet assignment based on passenger preferences but stop short of developing an integrated passenger and operating cost model. In a similar study, Oster and McKey (1984), compare the operating costs of different commuter aircraft and perform a parametric analysis of operating cost versus stage length.

The importance of considering a total logistics cost function with passenger and operating cost rather than individual cost components is demonstrated in two studies by Wei and Hansen (2003; 2005). Wei and Hansen (2003) develop a translog cost model for jet aircraft operating cost. It is found that airlines could decrease operating costs by up-gauging from the sizes they typically employed during the study period. Such findings are balanced with the conclusions of a second study by Wei and Hansen (2005). Using a nested logit model, the study finds that an airline's market share experiences greater increases from increasing vehicle frequency rather than aircraft size. These findings point to the importance of balancing airline operating cost and passenger preference costs when choosing fleet mix and determining flight schedules.

2.1 Model Formulation

Let the total logistics cost per passenger to serve a segment with aircraft type i be $L_i(f, \vec{p}, d, q, \ell)$ where f is fuel price, \vec{p} is a vector of other input prices, d is segment distance, q is passenger flow per day, and ℓ is load factor—the fraction of aircraft seats occupied by passengers. While \vec{p} is clearly an essential argument of the logistics cost function, our interest here is the variation of cost with f assuming other factor prices are fixed at present-day levels. Values for some of these prices—for example passenger travel time—are explicitly assumed in our formulation. Other factor prices—particularly those related to aircraft operating cost—are implicitly contained in industry cost data used to implement the model.

We decompose L_i into an aircraft operating cost component C_i and a passenger component P_i . The carrier component is further divided into a fuel component F_i , a pilot component R_i , a cabin crew component S_i , a maintenance component M_i , and an airport landing fee component A_i . The passenger cost is decomposed into a flight time component T_i and a schedule delay component D_i . Thus we have:

$$L_i = C_i + P_i \quad (2.1)$$

$$C_i = F_i + R_i + S_i + M_i + A_i \quad (2.2)$$

$$P_i = T_i + U_i + D_i \quad (2.3)$$

We assume that fuel required for a given aircraft type to fly a particular segment is independent of fuel price, that is that possibilities for factor substitution involving fuel are negligible. We also assume that fuel required for the segment can be approximated by a constant term corresponding to the fuel used for take-off and landing, and a linear distance term corresponding to cruise. Thus we have:

$$F_i = f \cdot (\alpha_i + \beta_i d) / (\ell \cdot s_i) \quad (2.4)$$

where s_i is seat capacity of aircraft type i , making $\ell \cdot s_i$ the total passengers per flight. Estimation of the parameters α_i and β_i as well as the validity of the linear approximation are discussed below.

Pilot costs, cabin crew costs, and maintenance costs are all assumed to be proportional to block hours required to fly the segment, $B_i(d)$, which, like fuel burn, is assumed to be approximated by a constant term (γ_i) and linear distance-varying term (λ_i):

$$B_i(d) = \gamma_i + \lambda_i d \quad (2.5)$$

The proportionality constants for pilot and maintenance costs (ρ_i and η_i) are obtained from airline data reported to the US Department of Transportation, which specify costs per block hour by airline and aircraft type in each of these categories. For cabin crew, we assume a constant block-hour cost per crew member (σ), which we multiply by the minimum number of cabin crew required for the aircraft type, N_i . Thus we have:

$$R_i = \rho_i \cdot B_i(d) = \rho_i \cdot (\gamma_i + \lambda_i d) / (\ell \cdot s_i) \quad (2.6)$$

$$M_i = \eta_i \cdot B_i(d) = \eta_i \cdot (\gamma_i + \lambda_i d) / (\ell \cdot s_i) \quad (2.7)$$

$$S_i = \sigma \cdot N_i \cdot B_i(d) = \sigma \cdot N_i \cdot (\gamma_i + \lambda_i d) / (\ell \cdot s_i) \quad (2.8)$$

The final component of carrier cost considered in this analysis is airport landing fees, which are proportional to maximum aircraft take-off weight, w_i , yielding:

$$A_i = p_a \cdot w_i / (\ell \cdot s_i) \quad (2.9)$$

where p_a is the landing fee per unit weight.

Passenger travel time costs are proportional to total passenger flying time for the segment. We ignore access, processing, and boarding time, which we assume are independent of aircraft type. Total passenger time cost is then given by:

$$T_i(\cdot) = p_t \cdot B_i(d) = p_t \cdot (\gamma_i + \lambda_i d) \quad (2.10)$$

where p_t is the cost to passengers of flight travel time.

As will be discussed below, passengers exhibit preferences for particular aircraft types, in particular for jet service as compared to turboprop service. Thus the passenger cost function includes a monetization of this preference, U_i .

Finally, we introduce schedule delay cost, which captures the value of more frequent service that results from serving a given passenger flow with smaller aircraft. Schedule delay is defined as the time difference between when a passenger would like to fly and when a flight is available. The average schedule delay in a market depends on the distribution of passengers' desired flight times and the times when flights are scheduled. Empirical relationships, based on representative distributions of desired flight times and flight schedules, have been developed based on flight frequency. Thus:

$$D_i(\cdot) = q \cdot p_d \cdot g(f_i) \quad (2.11)$$

where p_d is the cost of schedule delay, $g(\cdot)$ is the schedule delay function, and f_i is the frequency with which aircraft type i would serve the market. f_i is calculated by finding the number of flights, each carrying passengers $\ell \cdot s_i$, required to serve the given flow:

$$f_i = q/(\ell \cdot s_i) \quad (2.12)$$

2.2 Aircraft Operating Cost Model

To determine how short haul fleet mixes might be configured in response to changing fuel costs, we consider three aircraft categories: turboprop, regional jet, and narrow body aircraft. Specific aircraft are chosen to represent the three categories on the basis of their large presence in the market and the availability of data. Details of these aircraft are shown below in Table 2.1 (ATR (2008), Boeing Company (2008), and Embraer (2008)).

Table 2.1 Details of representative aircraft.

Aircraft Category	Aircraft Model	Manufacturer	Seats	Maximum Takeoff Weight (lb)	Runway Length Requirement
Narrow Body Jet	B737-400	The Boeing Company	137	149,710	2,012 m
Regional Jet	ERJ 145	Embraer	44	44,070	1,951 m
Turboprop	ATR 72-200	EADS & Alenia Aeronautica	72	50,265	1,408 m

2.2.1 Carrier Component Costs

Fuel consumption for the three aircraft over fixed distances is reported by European Environmental Agency (EEA) (2006).² Using this data, individual relationships between fuel consumption and distance are developed for each aircraft model. These are the estimates for α and β in (2.4). The estimates indicate that the turboprop has substantially lower fuel burn than either jet, including a fixed component per flight that is over 50% less and a variable component that is over 60% less.

For the jet aircraft, data to develop a relationship between flying time and distance is collected from the US Department of Transportation Form 41, summarized by aircraft

² The EEA (2006) has data for a variety of jet and turboprop aircraft models. This data includes the fuel consumed, the travel time, and other metrics over a variety of travel distances lengths. To calculate fuel burn, Project Interactive Analysis and Optimization (PIANO), a parametric aircraft design model, was used. This model uses aircraft characteristics, such as number of engines and fuel type, to estimate fuel consumption for a distance by using standard values for thrust at different stages of flight and assuming a standard Landing Take-Off Cycle. Their methodology calculates fuel consumption from the entire gate-to-gate operation for a flight of a defined distance.

model. For each aircraft model there are carrier-specific reports on average miles per flight, total block hours operated in a day, and the number of departures that aircraft completes in a day.³ From these variables, block time in hours for an individual flight is extracted. The block times for the turboprop are reported by the EEA for a range of distances; these observations are used in lieu of Form 41 due to low observation count. A relationship in the form of (2.4) is estimated for each aircraft model individually, with block time as the dependent variable and average distance from Form 41 as the independent variable. When this equation is used for flying time, γ represents the time lost during taxi, take-off, climb out, landing and descent, while λ is time that varies with distance. While the turboprop has considerably lower lost time than the jets, the distance-varying time is over twice as large compared with the jets.

Flight crew costs per block hour, denoted ρ in (2.6), are available from Form 41. Form 41 reports these statistics for all carriers operating an aircraft type. To achieve a single value for crew costs, the carrier average for each aircraft model is used.⁴ Cabin crew, while not typically included in cost analyses, are included in this study because the aircraft necessitate different number of cabin crew, denoted N in (2.8). While one cabin crew could be sufficient for the regional jet, a minimum of two is necessary on the other aircraft (and two per aircraft type are assumed). Cabin crew costs (σ), are fixed at \$20/block hour. The total crew costs are the largest for the narrow body, with the costs for the regional jet and the turboprop being roughly half of the narrow body crew costs.

Maintenance costs per block hour (η in (2.7)) are also available from Form 41. The average direct maintenance plus maintenance burden costs per block hour for all airlines operating an aircraft model are used as the maintenance costs. Direct maintenance is labor and materials. Maintenance burden costs are overhead, such as maintenance administration, planning, and supervising (Bureau of Transportation Statistics, 2008). Maintenance per block hour is the largest for the narrow body and the smallest for the regional jet, with the value for the turboprop being roughly equal to the average of the two jet costs.

Landing fees are fees levied by an airport on an arriving aircraft to capture value of providing service in the terminal airspace. Landing fees incorporate a charge for using the airfield. The most common landing fee is levied in proportion to aircraft weight (Odoni and de Neufville, 2003). The determination of landing fees varies airport to airport; in this study, fees are based on maximum takeoff-weight and are charged the existing landing fee at San Francisco International Airport (\$3.01/1000 lbs) for illustrative purposes (San Francisco International Airport, 2007). This is the value of p_a in (2.9). The

³ Block hours are the number of hours to complete a gate-to-gate operation. As block time does not include aircraft processing time at the gate (or turn time), block times are a measure of flight time that are relatively not specific to an airline.

⁴ A shortcoming to using the carrier average is that it is sensitive to different carrier operating procedures. If network and low-cost airlines operate the same aircraft, the average will be skewed downward than if all network airlines operate the aircraft in question. In the data used, there is only one low-cost carrier present, and that is for the ERJ 145 regional jet; it is then possible that the regional jet carrier average for crew costs is skewed downward.

airport-related costs therefore are linearly related to the weight of the aircraft, with the narrow body being the heaviest and the regional jet being the lightest.

By combining the operating cost components including fuel, operating cost equations are derived for all aircraft models. Operating cost equations are presented as per operation and per passenger. Evaluating operating cost per passenger allows for a cost direct comparison for operating one seat on each aircraft. Aircraft seat capacity is shown in Table 2.1, and a load factor of 75.6% is assumed for each aircraft (Bureau of Transportation Statistics, 2007). Fuel price and distance are left as variables to facilitate a parametric analysis of the two variables in the following section. The equations for operating cost per passenger are shown in the latter part of Table 2.2. The values in Table 2.2 are categorized by their coefficient: fuel price (f), distance multiplied by fuel price ($d \cdot f$), distance (d), and a fixed value per flight.

Table 2.2 Operating cost equations, total and per passenger.

Coefficient Value				
Aircraft Category	Fuel Price (f)	Distance · Fuel Price ($d \cdot f$)	Distance (d)	Fixed
Per Operation				
Narrow Body	$2.7 \cdot 10^2$	2.1	2.6	$1.3 \cdot 10^3$
Regional Jet	$1.9 \cdot 10^2$	1.9	1.2	$5.9 \cdot 10^2$
Turboprop	$4.5 \cdot 10^1$	$6.5 \cdot 10^{-1}$	3.8	$3.7 \cdot 10^2$
Per Passenger				
Narrow Body	2.5	$2.0 \cdot 10^{-2}$	$2.5 \cdot 10^{-2}$	$1.2 \cdot 10^1$
Regional Jet	5.6	$5.7 \cdot 10^{-2}$	$3.6 \cdot 10^{-2}$	$1.8 \cdot 10^1$
Turboprop	$8.1 \cdot 10^{-1}$	$1.2 \cdot 10^{-2}$	$7.0 \cdot 10^{-2}$	6.6

When the values in Table 2.2 are considered on a per operation basis, the turboprop exhibits a lower fixed cost and a lower cost that varies with fuel consumption than the jet aircraft. However, the cost that varies with distance alone is higher for the turboprop, due to greater variable travel time. The two jet aircraft have similar costs, yet their constants are greatly different due to the difference in airport-related costs and fixed travel time. When costs are considered on a per passenger basis the regional jet has consistently higher values than the narrow body. The lower seat capacity of the regional jet means costs are spread among fewer passengers. The costs that vary with distance alone are still highest for the turboprop, and therefore, while all other costs are lower, distance appears to be the factor which will constrain the turboprop from offering the lower costs. We now explore how these differences translate into the minimum cost homogenous vehicle fleet based on operating cost.

2.2.2 Parametric Operating Cost Comparison

We use the operating cost functions in Table 2.2 to compare the costs of the three aircraft models over a range of distances and fuel prices. Difference in operating cost per

passenger for two pairs of aircraft, the regional jet and the turboprop and the narrow body and the turboprop, are compared using contour curves representing a percent difference in operating cost. The calculations of percent difference in operating cost are done for varying distance and fuel price. Such a procedure allows for simple identification of the combinations of fuel price and distance for which a given aircraft has a cost advantage. In each chart, the middle dashed line represents the two aircraft being compared having an equal operating cost per passenger. The region under the middle dashed line represents the fuel price-stage length region where a turboprop has a lower cost per passenger; the region above the middle dashed line represents the fuel price-stage length region where the jet aircraft being compared has a lower cost per passenger. The percentage labels are based on the jet aircraft in comparison to the turboprop: 20% means the jet has a 20% higher operating cost than the turboprop, while -20% means the jet has a 20% lower operating cost than the turboprop.

A fuel price and distance combination (for distances under-1000 miles) for which the regional jet has a lower or equal operating cost per passenger compared with the turboprop does not exist because the regional jet has a higher operating cost per passenger than the turboprop for all fuel prices and stage lengths. Therefore, Figure 2.1 shows a contour plot for the regional jet and turboprop comparison with two curves, one for where the regional jet has a 50% higher operating cost per passenger than the turboprop, and the other for 30% higher. This is atypical because the regional jet consistently has a higher operating cost per passenger due to the higher per passenger fuel consumption and fixed block time for the regional jet.

The figure also shows a contour plot for the narrow body and turboprop comparison. In this case, there are fuel price and distance combinations for which the two aircraft models have an equal operating cost. This equal operating cost curve exists in the sub-1000 mile distance region for fuel prices up to \$4.00/gallon. The curves above and below the zero percent difference curve represent the narrow body holding a 20% higher and lower operating cost compared with the turboprop, respectively. The narrow body has a 20% higher operating cost per passenger than the turboprop for all stage lengths up to 1000 miles when the fuel price equals levels seen in the summer of 2008, \$4.30/gallon. At a price of \$2.00/gallon, the situation is significantly different, with the narrow body jet having a lower cost per passenger than the turboprop for stage lengths greater than 300 miles. As anticipated, the turboprop is very cost competitive over short distances because of the lower fixed and larger variable costs with distance.

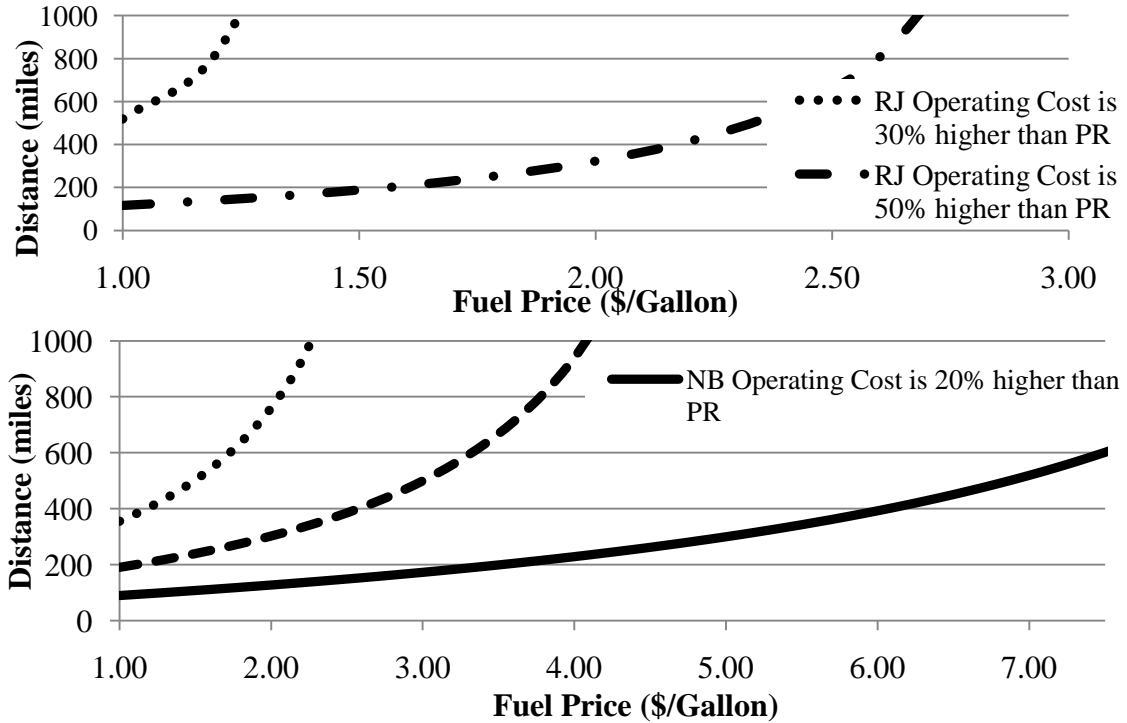


Figure 2.1 Percent difference operating cost per passenger contour curve for regional jet and turboprop comparison and narrow body and turboprop comparison.

There are additional factors beyond operating cost to be considered when comparing aircraft economics.

2.3 Passenger Cost Model

We now consider the passenger cost component of the total logistics function, P , described in section 2.1. The cost of flying time for each aircraft type is the flying time function multiplied by a passenger value of time, p_t in (2.10), to produce a cost per time-passenger. The willingness to pay not to travel on a turboprop, U , incorporates the perceived negatives of flying on a turboprop, including increased passenger noise and potential safety concerns. Estimates for the passenger disutility of traveling on a turboprop and the cost of travel time can be found in Adler et al. (2005). The authors also find that business travelers are 43% of the population with the remaining 57% non-business. The value of flying time and disutility for turboprop travel were estimated separately for both groups using a mixed logit model. The weighted average of these values finds values of \$47.75/hour-passenger for travel time and \$29.17/operation-passenger for the disutility of turboprop service.

The disutility of turboprop travel and the value of passenger flying time costs are included in the operating cost equations to produce a combined total logistics cost of aircraft operation. The operating and passenger cost per operation and per passenger equations are defined in Table 2.3.

The turboprop continues to exhibit the lowest costs that vary with fuel price (and distance multiplied by fuel price) on a cost per passenger basis. However, the turboprop disutility which is a fixed cost per operation, and flying time which varies with distance make the turboprop less advantageous in comparison to the operating cost results presented in Table 2.2. Turboprops have a slower flying time and an added disutility per passenger per operation which is reflected in the relative increase in costs compared with Table 2.2. The inclusion of passenger costs will further limit the range for which the turboprop offers the lowest cost.

Table 2.3 Operating and passenger cost equations, total and per passenger.

Aircraft Category	Coefficient Value			
	Fuel Price (f)	Distance · Fuel Price ($d \cdot f$)	Distance (d)	Fixed
Per Operation				
Narrow Body	$2.7 \cdot 10^2$	2.1	$1.3 \cdot 10^1$	$4.6 \cdot 10^3$
Regional Jet	$1.9 \cdot 10^2$	1.9	4.2	$1.8 \cdot 10^3$
Turboprop	$4.5 \cdot 10^1$	$6.5 \cdot 10^{-1}$	$1.7 \cdot 10^1$	$2.8 \cdot 10^3$
Per Passenger				
Narrow Body	2.5	$2.0 \cdot 10^{-2}$	$1.2 \cdot 10^{-1}$	$4.4 \cdot 10^1$
Regional Jet	5.6	$5.7 \cdot 10^{-2}$	$1.3 \cdot 10^{-1}$	$5.3 \cdot 10^1$
Turboprop	$8.1 \cdot 10^{-1}$	$1.2 \cdot 10^{-2}$	$3.0 \cdot 10^{-1}$	$5.1 \cdot 10^1$

2.3.1 Parametric Operating and Passenger Cost Analysis

Similarly to the contour plots in Figure 2.1, Figure 2.2 displays percent different contours for total logistics cost for the two aircraft comparison pairs. When passenger costs are introduced, a zero percent difference contour emerges between the regional jet and turboprop in the fuel price – distance space between \$1.50/gallon and 100 miles and \$3.50/gallon and 1000 miles. At \$3.00/gallon, the regional jet has a lower cost for stage lengths greater than 400 miles, an increase of \$0.50/gallon leads regional jets have a higher total cost per passenger for all stage lengths up 1000 miles. In short, fuel price peaks similar to the 2007-2008 run-up in fuel prices completely alter the competitive balance between regional jets and turboprops in the under-1000 mile market.

The lower section of Figure 2.2 presents a similar analysis for narrow body jet and turboprops. Narrow body jets have a lower total cost per passenger than the turboprop for all distances and fuel prices up to \$4.00/gallon. The zero percent difference contour curve does not extend to stage lengths over 400 miles, even at fuel prices as high as \$15.00/gallon. It is clear from the operating and total cost fleet comparisons that the comparative advantage of narrow body jets over turboprops is strongly dependent on the monetization of passenger costs. Considering this total logistics cost, narrow body jets have a lower cost per passenger compared to turboprops under a wide range of fuel prices and distances. When only operating costs are considered, narrow body jets have a higher

operating cost per passenger when compared with turboprops for fuel costs above \$4.00/gallon.

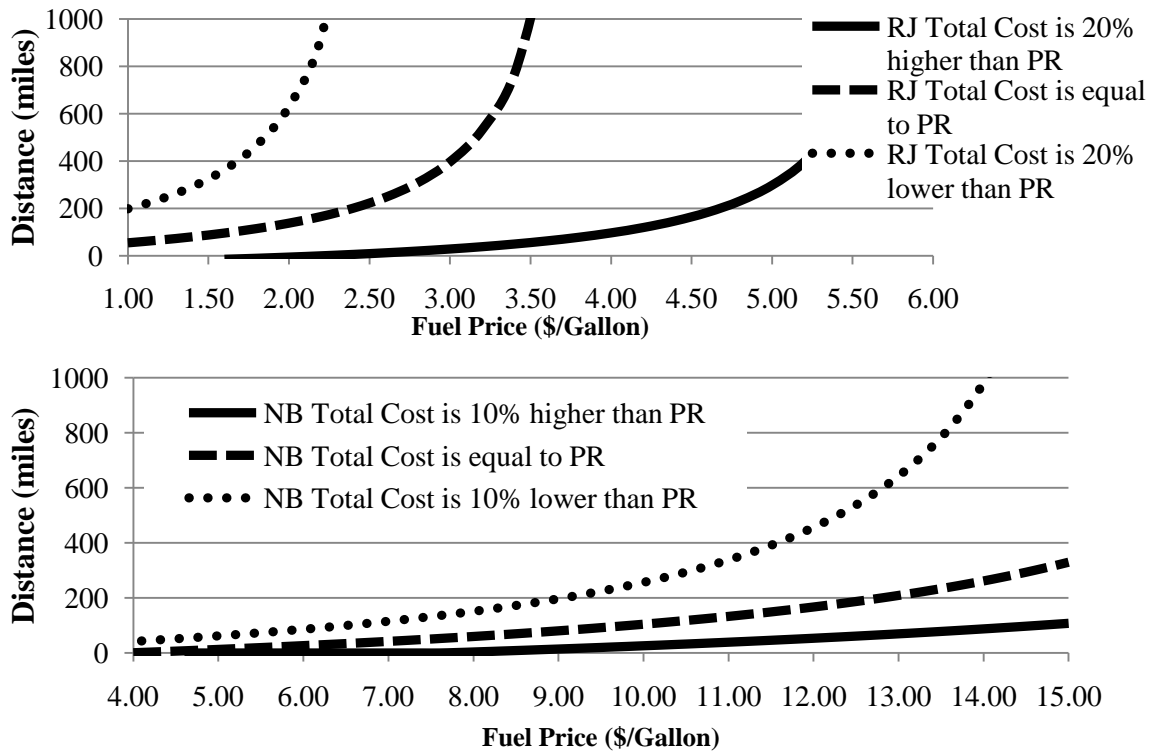


Figure 2.2 Percent difference in total cost per passenger contour curve for regional jet and turboprop and narrow body and turboprop comparison.

2.3.2 Value of Frequency

The inclusion of frequency highlights the difference in operating aircraft with a wide range of seat capacities. The range of seating capacities means that a fixed number of passengers can be served by a different number of flights depending on the fleet selection. As passengers place value on the difference between desired arrival time and actual arrival time, the frequency of service is included into passenger costs. The value of the difference between a passenger's desired arrival time and actual arrival time, termed schedule delay, is estimated by Adler et al. (2005). Passenger value of frequency is captured through passenger willingness to pay for flights of varying flight times around the desired time and is denoted p_d in (2.11). Delays in either direction (early or late) were considered to be equally onerous.

To capture the impact of providing more frequent service a relationship between frequency and schedule delay must be identified. Abrahams (1983) reviews a relationship developed by Eriksen (1978) for schedule delay based on flight frequency. The equation was estimated to account for schedule peaking and does not assume that flights are uniformly distributed in time. Equation (2.13) shows the schedule delay function for a given route, termed $g(\cdot)$ in (2.12), in hours developed by (Eriksen, 1978). The equation for flight frequency (2.12) is determined by q_i the passenger flow per day between a given origin and destination per day, the seat capacity of aircraft type i (s_i), and the load

factor (ℓ). The schedule delay determined from these variables is multiplied by the weighted average of schedule penalties for both business and non-business travelers (p_d), which is \$15.77/hour (Adler et al., 2005). As the result (2.13) does not depend on distance or fuel price, the new cost equations only differ from those previously defined by a constant. The constant term varies with market density; five representative market densities are chosen for analysis purposes.

$$g(f_i) = 5.7 / (f_i) \quad (2.13)$$

The zero percent difference contour curves between aircraft pairs after the introduction of schedule delay are shown for a range of market densities in Figure 2.3. The area under each curve represents the fuel price – distance space where the turboprop has the lower cost per passenger.

When the turboprop is compared with the regional jet, increasing market density increases the fuel price – distance space where the turboprop offers a lower cost per passenger. Because the regional jet has a smaller seat capacity, its use necessitates more frequent service than the turboprop. At lower market densities, the schedule delay incurred by the regional jet is lower compared with the turboprop due to this more frequent service. As market density increases, the discrepancy in schedule delay is decreased, and the difference is overtaken by the higher operating cost of the regional jet. The highest fuel price in the upper half of Figure 2.3 is \$3.50, which indicates that even after the introduction of schedule delay, the regional jet still offers a higher cost per passenger for a range of fuel prices, including those seen in the summer of 2008.

The narrow body jet and the turboprop (lower half of Figure 2.3) exhibit a reverse relationship regarding market densities and cost per passenger than the regional jet and turboprop. Because the narrow body has almost twice the seats of a turboprop, it serves the same market density with less frequent service, increasing the schedule delay incurred from using this aircraft. As market density increases, the cost impact of schedule delay decreases, and the fuel price – distance space where a turboprop offers a lower cost per passenger shrinks and tends toward higher fuel prices. Most of the market density curves begin at fuel prices of \$4.60 to \$7.60/gallon. At the highest fuel price shown, \$14.80/gallon, the curves terminate at stage lengths between 400 and 600 miles. For a wide range of fuel prices and stage lengths, the narrow body exhibits a lower cost per seat despite higher schedule delays.

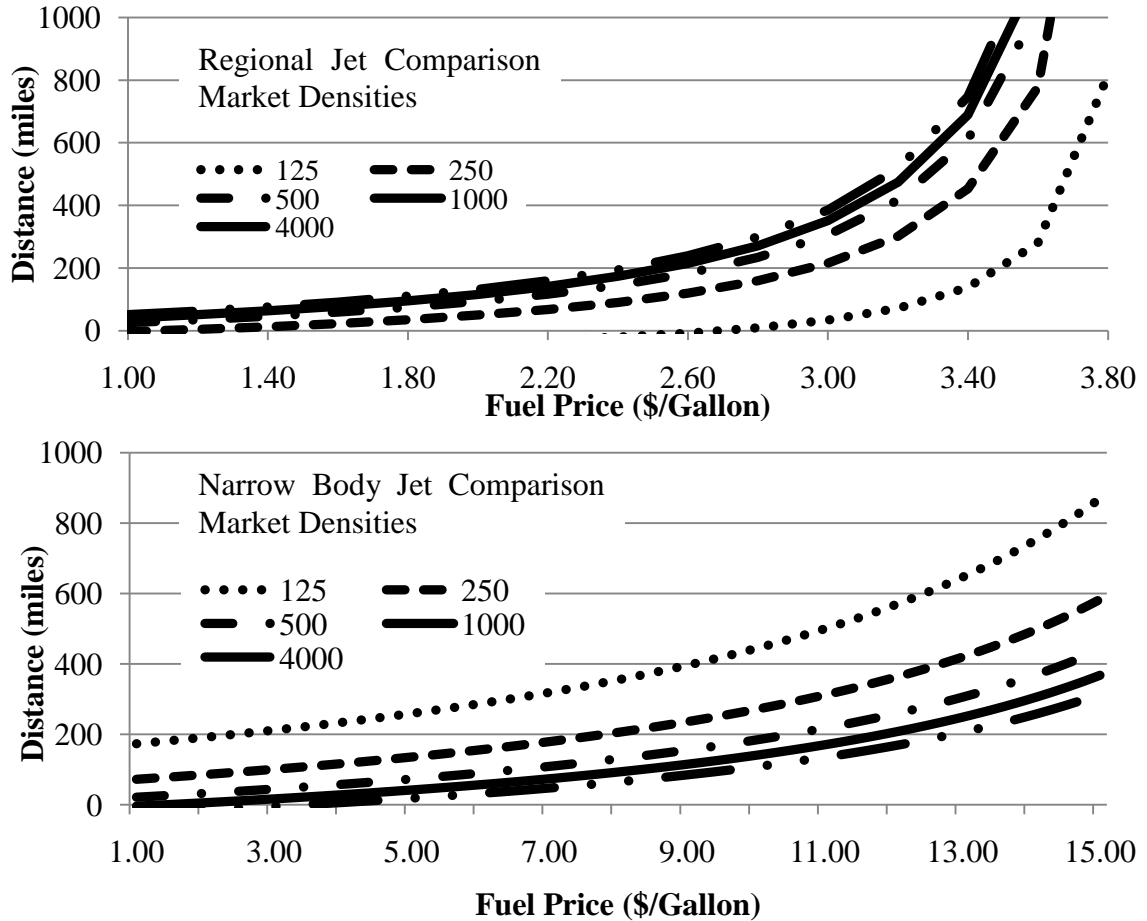


Figure 2.3 Zero percent difference total cost including schedule delay per passenger contour curve for regional jet and turboprop, and narrow body and turboprop comparison.

The inclusion of schedule delay has finalized the fuel price – distance space where the turboprop has a lower cost per passenger.

2.4 Market Penetration Analysis

Here we put the minimum cost aircraft type analysis in the context of actual operations and passengers moved. We use data from the T100 Database collected by the Department of Transportation Bureau of Transportation Statistics. Each record corresponds to a service segment s , defined by an airport pair $p(s)$, airline $a(s)$, and aircraft type $i(s)$, and specifies the number of monthly passengers flown $z(s)$ for April 2008.⁵ Thus each s corresponds to a $(d(s), z(s))$ pair, where $d(s)$ is the distance between airport pair $p(s)$. For

⁵ Only segments under 1000 miles were collected to stay consistent with the study scope. Any segments flown less than 30 times in that month, or flights solely for freight were eliminated, as were those flown less than 40 miles. The aircraft type notation $i(s)$ may encompass more than the three types introduced in Section 3, whereas the aircraft type i is restricted to the three study types.

each $(d(s), z(s))$ pair, the $L_i(f, \vec{p}, d, q, \ell)$ is calculated $\forall i$ (turboprop, regional jet, narrow body $\ni i$) for a range of fuel prices f . Let $M_{PR}(s, f)$ be an indicator function equal to 1 if the turboprop (PR) is the aircraft type for which $L_i(f, \vec{p}, d, q, \ell) = \min L_i(f, \vec{p}, d, q, \ell) \forall i$ and equal to zero otherwise. For each f the fraction of passengers carried per day who would be served at the minimum cost on a turboprop at a given fuel price, $\sum_s z(s) * M_{PR}(s, f) / \sum_s z(s)$, is calculated. In addition to this aircraft comparison across all three aircraft types, the same method is used to compare the turboprop with each jet aircraft type individually.

Figure 2.4 shows $\sum_s z(s) * M_{PR}(s, f) / \sum_s z(s)$ vs. f , the fraction of passengers on a representative day for each fuel price where the turboprop has a lower operating plus passenger cost (total cost hereafter) per passenger compared with the regional jet or the narrow body. Compared with the regional jet, at fuel prices under \$2.00/gallon, the share of passengers transported where the turboprop has the lower total cost per passenger does not pass 5%. However, this share increases rapidly as fuel prices surpass \$2.00/gallon; at a fuel price of \$4.00/gallon almost 90% of passengers flown per day could be carried with a lower total cost per passenger on a turboprop compared with the regional jet. When considering the comparison between the turboprop and narrow body, at fuel prices under \$2.00/gallon, the fraction of passengers which could be carried on a turboprop with less total cost per passenger than the narrow body is 20%. As fuel prices increase, the fraction increases slowly, ultimately reaching 80% at \$15.00/gallon.

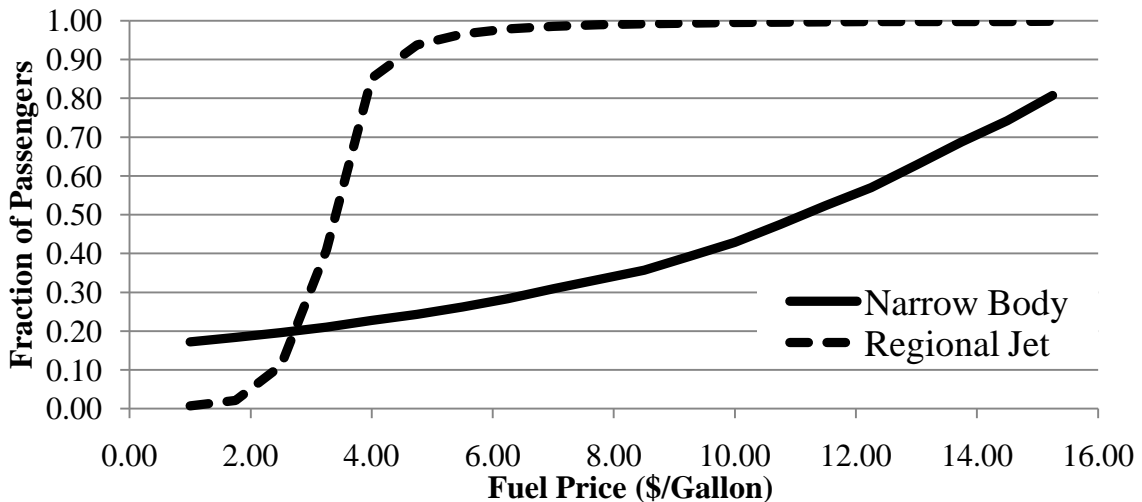


Figure 2.4 Potential fraction of passengers served by a turboprop with the lowest total cost per passenger compared with a regional jet and a narrow body.

Beyond the aircraft pair comparisons shown in Figure 2.4, a comparison between the three aircraft (Figure 2.5) gives an overall picture of the fraction of passengers that can be served on a turboprop at the minimum total cost per passenger. This fraction begins at one percent for a fuel price of \$2.00/gallon, increases to 10% at a fuel price of \$4.00/gallon, and reaches 80% at \$15.00/gallon. As the slope between \$3.00/gallon and \$5.50/gallon is the steepest slope in Figure 2.5, a carbon tax instituted on fuel prices in this will range yield the largest percent increase in the fraction of passengers that can be served on a turboprop at the minimum total cost per passenger. For example, for fuel

prices of \$4.00/gallon plus a \$1.00/gallon carbon tax, the percent of passengers carried for the least cost on a turboprop would jump from 10% to 20%.

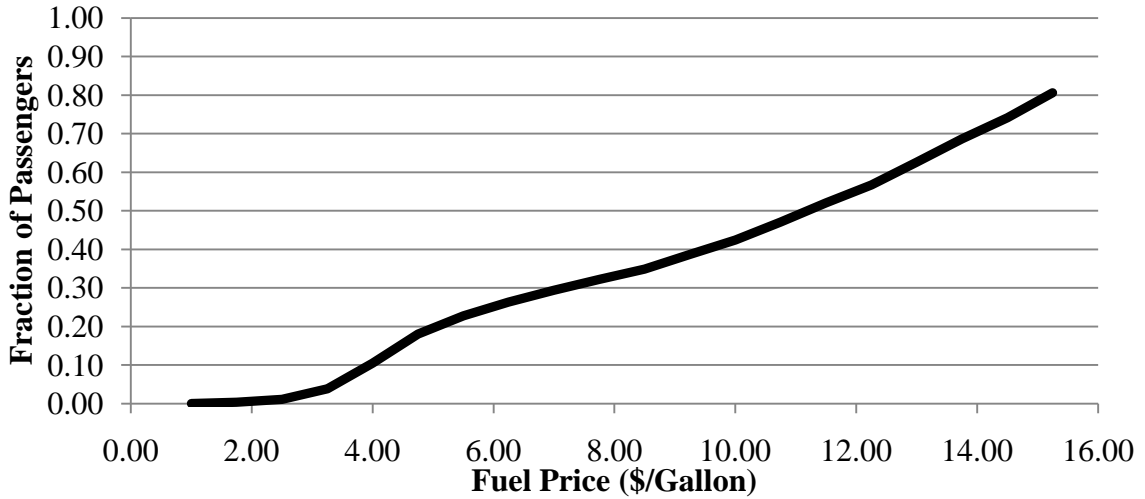


Figure 2.5 Potential fraction of passengers served on a turboprop for the lowest comparative total cost per passenger.

2.5 Conclusions

This analysis shows that the determination of minimum cost aircraft operations over distances of 1000 miles or less is highly sensitive to fuel prices and passenger costs. The results of this study show that the popularity of regional jets is due to their relatively low passenger costs when compared with turboprops, and the popularity of narrow body jets is due to their ability to balance operating and passenger costs when fuel prices are below those commonly seen during the study period. We have seen that in 2007 turboprops made up less than 5% of the sum of turboprops, regional jets, and narrow body jets, down from 20% in 1996. Our results show that increasing fuel prices could reverse the trend of regional jets replacing turboprops in short haul markets. While aircraft adoption and deployment decisions are made for a variety of reasons, this study shows that high fuel costs can overshadow the importance of passenger costs. The inclusion of other costs based on fuel consumption, such as environmental costs, would tip the advantage to the turboprop. Such a finding allows for the consideration of additional taxes, such as carbon taxes, to encourage airline fleet selection to consider environmental and fuel preservation.

3.

The Impact of Fuel Price on Jet Aircraft Operating Costs

In this chapter, we perform statistical cost estimation to investigate the relationship between aircraft operating cost and fuel price. Toward this end, we develop empirical jet aircraft operating cost models using published airline data. The most complicated of these models, the translog, provides the most complete representation of the empirical relationship between fuel cost and operating cost, allowing for substitution, scale, aircraft age, and other effects – including interactions – to be captured. The simpler models (Leontief and linear models) are more transparent, require fewer inputs, and allow the contribution of a single factor, such as fuel price, to operating cost to be more easily isolated. The development of multiple models and comparison of their predictions allows us to investigate the importance of the effects the translog uniquely captures, and thus to assess the tradeoffs between using a complicated but flexible cost model and a simpler but highly restrictive one in the subsequent research.

The models developed in this chapter follow a large body of literature in empirical aircraft cost modeling, well described by Wei and Hansen (2003), that includes Caves et al., (1984), Hansen et al. (2001), and more recently Chau et al. (2005). Wei and Hansen (2003) develop a translog econometric operating cost model for jet aircraft allowing for variable aircraft size at the airline-aircraft level. The authors find that, keeping all inputs constant, there exists a unique aircraft size that minimizes operating cost. This finding supports the concept that schedule delay is not the only driver of aircraft size, but rather there are cost efficiencies in operating smaller aircraft. The authors also find that if pilot salaries are considered endogenous, the aircraft size that minimizes operating cost is significantly smaller than if pilot salaries are exogenous. In this chapter, we seek to both update and improve upon the model of Wei and Hansen (2003) and to consider in more detail the effect of fuel price. In improving the model, we use econometric methods that account for correlation across airlines, aircraft, and time. We also estimate on a larger and more up-to-date data set, which includes a broader range of aircraft types and explanatory variables. Our dataset includes aircraft sizes from regional to heavy jets. We also consider additional explanatory variables, such as aircraft age.

The translog functional form allows for detailed analysis on the interactions between the drivers of operating cost. It can also be used to model the impact of fuel price on the aircraft size that minimizes operating cost; however, the detailed nature of the translog model (hereafter, TM) makes it challenging to minimize a more complete function of costs, such as a total logistics cost function. As in subsequent chapters we will be looking

to minimize a total logistics cost function, we develop operating cost models with more simple functional forms than the translog model and compare the results. The first model with a simple functional form considers aircraft to be Leontief technologies. These functions are developed in the previous chapter to study aircraft comparative costs under fuel price uncertainty. Hereafter we will refer to such a model as a Leontief Model, or LM for short. The second is a linear operating cost model based on the same dataset as the translog operating cost model.

Leontief technology cost models assume that inputs of a cost model, such as labor, fuel, and materials, must be used in fixed proportions regardless of their prices. Because the inputs are assumed to be in fixed proportions, these models are specific to an aircraft type. This produces a set of models rather than a single, generalized model. However, as there is currently a wide range of aircraft types, of varying size, on the market, it is appropriate to consider aircraft size as a continuous variable.⁶ In an attempt to generalize aircraft cost models that are not specific to an aircraft type but retain the simplicity of Leontief models, Swan and Adler (2006) develop two jet aircraft operating cost models using Boeing and Airbus aircraft data. One is for single aisle aircraft while the other is for double aisle aircraft. Limiting the data source to these two airframe manufacturers implicitly limits the aircraft types considered to mid-size and large aircraft. Furthermore, as the model is based on aircraft size and distance traveled, it is not able to capture cost changes due to economic forces such as fuel price changes. In this study a third operating cost model is developed, a simple econometric model with a linear functional form, to represent operating cost relationships in a more simple way while allowing aircraft size to vary continuously. The comparison of the Leontief model and the linear model to the translog operating cost model sheds light on the importance of capturing the factor substitution of inputs and other effects in predicting operating costs.

The remainder of this chapter is organized as follows: The following section reviews the data collected for the development of the translog model and the modeling approach. Regularity conditions of the estimated TM are explored, and coefficient estimates are presented and interpreted based on the objective of the study. In the following section, predictions from the translog model and LM are compared. Finally, we present estimation results for linear model that allows for variable vehicle size while retaining the simple form of an LM, and compare the linear model with the translog.

3.1 Translog Operating Cost Model

The operating cost per operation (O) function has the form:

$$O = f(p, z, q, c, g) \tag{3.1}$$

where p is a vector of input prices including fuel price; z is a vector of airline-aircraft outputs—specifically average seat capacity and segment length; q is the value capturing the time in year-quarter; c is the vector of airline designations; and g is the vector of aircraft age variables. Along with the fuel price, the vector p includes measures for pilot

⁵ This was not always the case. Viton (1986) expresses an interest in modeling costs with aircraft size as a continuous variable yet cites the limited aircraft sizes available during the study period as reason to perform an aircraft specific analysis.

cost and materials cost. The vector z includes the seat capacity per operation and average stage length per operation. While p and z are essential arguments of the operating cost function, this study will focus on the variation of operating cost with fuel price (*fuel*) and seats per operation (*seat*). The vector g includes variables to measure the age of the aircraft, the length of time an airline has been operating a certain aircraft model, and the number of hours operated in a quarter per airline per aircraft. The value q is one of a set of ordinal values signifying year-quarter values. We denote airlines by c and aircraft by n , such that each observation has a unique combination of c , n , and q . We capture airline fixed effects with c , where $c = 1$ if the observation is for airline i , 0 otherwise.

The model specification used is a translog model to estimate the operating cost per departure (O_{cnq}). The translog model is widely used in cost modeling (for example, Wei and Hansen, 2003; Caves et al., 1984; Hansen et al., 2001); as a second order Taylor series expansion, it is able to approximate many different model specifications.

$$\begin{aligned}
\ln O_{cnq} = & \alpha q_{cnq} + \sum_c \phi_c + \sum_i \omega_i \ln p_{cnq}^i + \sum_i \delta_i \ln z_{cnq}^i \\
& + \sum_i \varphi_i g_{cnq}^i + \frac{1}{2} \sum_i \sum_{j \geq i} \beta_{ij} \ln p_{cnq}^i \ln p_{cnq}^j \\
& + \frac{1}{2} \sum_i \sum_{j \geq i} \pi_{ij} \ln z_{cnq}^i \ln z_{cnq}^j \\
& + \sum_i \sum_{j \geq i} \gamma_{ij} g_{cnq}^i g_{cnq}^j \\
& + \sum_i \sum_{j \geq i} \rho_{ij} \ln p_{cnq}^i \ln z_{cnq}^j \\
& + \sum_i \sum_{j \geq i} \theta_{ij} \ln p_{cnq}^i g_{cnq}^j \\
& + \sum_i \sum_{j \geq i} \tau_{ij} \ln z_{cnq}^i g_{cnq}^j + \varepsilon_{cnq}
\end{aligned} \tag{3.2}$$

Where

i, j index elements in p , z , g , or c

$\alpha, \phi_c, \omega_i, \delta_i, \varphi_i, \beta_{ij}, \pi_{ij}, \gamma_{ij}, \rho_{ij}, \theta_{ij}, \tau_{ij}$ are coefficients to be estimated

3.2 Data for Operating Cost Model

To estimate the operating cost model in (3.2), data from the US Department of Transportation (DOT) Form 41 are collected. Form 41 provides quarterly cost data and operating statistics per airline and per aircraft type. The dataset includes a large set of explanatory variables and a date range from 1996-2006 inclusive. Data for 26 airlines (c) (network, regional, and low cost) that operated jet aircraft during the study period were collected (Appendix A1.1). Across the airlines there were 23 unique jet aircraft types (n) operated (Appendix A1.1) in this period. The panel data used in this model has airline-aircraft designators in vector k over a set of year-quarters (q). Because the set of k values represented in the data vary across q , the panel is unbalanced. The total number of observations is 1657 covering 66 unique aircraft-airline combinations. The dependent and

independent variables are presented in Table 3.1, and procedures for calculating these variables are discussed below.

Table 3.1 Variables of the operating cost model.

Vector	Variable Label	Variable Name	Variable Units	Variable description (specific to aircraft-airline pair, year-quarter)
	<i>O</i>	Operating cost	\$/Departure	Direct operating cost per departure
<i>z</i>	<i>seat</i>	Seats	Seats/Departure	Average aircraft seat capacity per departure
	<i>asl</i>	Average stage length	Miles/Departure	Average stage length traveled per departure
<i>p</i>	<i>pilot</i>	Pilot unit price	\$/Block Hour	Ratio of pilot and copilot salaries to the amount of block hours
	<i>fuel</i>	Fuel price	\$/Gallon	Ratio of the amount spent on fuel to the amount consumed
	<i>ppi</i>	Materials price	Unitless	Producer price index, proxy for materials price
<i>g</i>	<i>util</i>	Utilization	Hours/Quarter	Number of hours an aircraft is operated in a quarter
	<i>aage</i>	Airline-Aircraft age	Years	Number of years an airline operates a particular aircraft model
	<i>tage</i>	Technology age	Years	Time elapsed since the first year of entry in service across domestic airlines for a specific aircraft type

The input prices and the independent variable, operating cost per operation (O_{cnq}), are collected from US DOT Data in Form 41 Schedule P-5.2. Ownership costs related to depreciation and rentals were eliminated from this total to capture direct operational costs only. The data collected to develop input prices includes expenditures on aircraft fuels and pilots and copilots salaries. Aircraft operating statistics are collected from Form 41 Schedule P05B.⁷ These statistics, collected for scheduled and non-scheduled service, include gallons of fuel used; available seat miles; revenue aircraft miles; departures performed; and block hours, or the sum of actual hours an aircraft spends from gate to gate. From these prices and statistics, the unit price of fuel and pilots, the average stage length, and seat capacity are derived.⁸

⁷ It is important to note that aircraft fuels is the actual cost of the fuel, without fuel taxes, any additional costs for the act of fueling the aircraft, or other charges. It is not the total cost related to fuel consumption, but rather the actual cost of fuel. The fuel tax exclusion has little impact as the tax on commercial aviation fuel was constant and minimal through at the study period at \$0.044/gallon.

⁸ Many airlines operate identical aircraft types with different seat capacities determined by their business models. For example, a network carrier looking to lure business passengers may operate an aircraft with fewer seats and more differentiated service classes, while a low cost carrier may use a one-class configuration. To exclude any cost impacts to operating different configurations of the same aircraft, each aircraft type is assigned the weighted average seat capacity for that aircraft type.

Data on aircraft age and utilization are collected from Form 41, Schedule B-43, which includes the total number of each aircraft model in service per airline per year, and the year in which the airline began to operate that aircraft model. The utilization (*util*) variable is derived from these statistics, as well as the number of years an airline operates a particular aircraft model (*aage*). Collected from the aircraft manufacturers is the first year of entry in service across domestic airlines for a specific aircraft type; these data are used to calculate the technology age (*tage*) of the aircraft, or the time elapsed between the earliest entry year in domestic service of an aircraft type and 2006.

To capture the materials price, the Producer Price Index is collected from the Bureau of Labor Statistics; a similar method is employed in the work of Caves et al. (1984) as well as Hansen et al. (2001) to develop airline cost functions. Instead of converting costs and prices for each year of data into constant dollars, this study follows Hansen et al. (2001) and uses the Producer Price Index as both a proxy for materials cost and a gauge of changes in inflation. Furthermore, as the third factor price in the set with labor and fuel, it acts as a “catch-all” term such that all non-fuel and non-pilot and copilot costs are captured by the producer price. The PPI is entered into the model to capture the cost of maintenance materials, but as a “catch-all,” it also captures maintenance labor costs, which does not have a direct relationship with materials price.

Table 3.2 includes the summary statistics for each independent variable, including the mean, median, standard deviation, and maximum and minimum values.

Table 3.2 Summary statistics of variables in the operating cost model.

	Mean	Standard Deviation	Median	Minimum	Maximum
Seats	155.79	59.81	148.15	49.02	359.75
Average stage length	1055.37	467.30	1057.59	125.11	2686.33
Pilot price	419.56	165.04	414.87	11.02	1169.35
Fuel price	1.07	0.53	0.84	0.35	2.56
Utilization	803.06	227.63	835.30	13.87	1395.13
Materials price	1.56	0.18	1.61	1.19	1.83
Airline-Aircraft age	7.13	4.54	6.21	1.00	23.09
Technology age	15.60	6.14	17.00	2.00	24.00

3.3 Operating Cost Model Estimation

Following the model definition and the data description, the translog operating cost model is estimated in this section. The data are demeaned such that the dependent variable and the independent variables are estimated about the mean values in the dataset. The process of demeaning ensures the resulting first order coefficients estimates are equal to the elasticities. At the sample mean, the elasticity of the operating cost respect to factor price i is ω_i , the first order coefficient of factor price i . Therefore, the process of demeaning the data enables straightforward interpretations of the results: the effect at the sample mean of each independent variable is the parameter estimate.

To properly estimate the model in equation (3.1), we must take into account that the data form an unbalanced panel. The data is a panel of airline-aircraft pairs, and it is possible that different airline-aircraft pairs have different error variances. To test for the presence of heteroskedasticity, we test the null hypothesis of homoskedasticity against the alternative hypothesis that the residual variances depend on two key independent variables: fuel price, seat capacity, or both variables. The Breusch-Pagan, Cook-Weisberg test for heteroskedasticity finds p-values for both variables to be zero, which leads to a rejection of the null hypothesis and necessitates correction for heteroskedasticity. Furthermore, we expect to see autocorrelation; because the data is in a time series, we expect the error terms of a particular airline-aircraft pair to be correlated over time. Using the Wooldridge test for autocorrelation, we reject the null hypothesis that it is not present and therefore must include a correction in the model for autocorrelation. To estimate the model, we use ordinary least squares with panel-corrected standard error estimates and assuming first-order autocorrelation within panels.

We estimate the full model, termed model 1, on the full set of variables (3.1). We also estimate model 2, in which coefficients that do not have statistical significance at least at the 10% level in model 1 are eliminated. Estimation results for both models are shown in Appendix A1.2. The coefficient estimates generally have the expected signs and most are significant at the five or one percent level. Prior to discussing estimation results, we first assess the conformance of the estimated model to regularity conditions.

3.3.1 Regularity Conditions

According to Diewert and Wales (1987), a translog cost function should satisfy certain regularity conditions. These regularity conditions ensure that a cost function is consistent with cost minimization. The five necessary regularity conditions are reviewed in Chua (2005); like Diewert and Wales (1987), we will focus on two conditions here. The first is that the cost function is linearly homogeneous; if all input prices, $p_i \forall i$, are scaled by the same proportion, the cost function will be similarly scaled by the same proportion. The second condition is that the cost function is concave in the input prices p_i , such that the matrix of second derivatives is negative semidefinite. This is expected because as an input price increases, a cost-minimizing production process would substitute away from that input.

Before exploring linear homogeneity and concavity in input prices, we consider their relevance in our setting. The conditions are necessary if the decision-making unit, in our case an airline-aircraft pair, is a cost-minimizing unit. In much the cost literature reviewed in this chapter (for example, Caves et al. (1984) and Hansen et al. (2001)), the decision-making unit is at the airline level. It is clear that at the airline level that cost minimization is a valid assumption, as an airline is at the firm level. However, it is less clear that an airline-aircraft pair is a cost-minimizing unit. To consider this, we explore a possible scenario where an increase in cost for a particular airline-aircraft pair could lead to a decrease in costs for an airline. It is possible that a coupling of processes for different aircraft types could result in such a phenomenon. For example, standardization of a particular maintenance process across aircraft models could increase costs for one aircraft

model but decreases costs for all others, thus leading to a violation of the cost-minimizing assumption at the aircraft type level. In this instance, one particular aircraft model could experience an increase in the use of an input with an increase in factor price.

Because we are not certain if the assumption of cost-minimization must hold for our airline-aircraft level model, we do not impose regularity condition constraints. The practice of constraining an airline-level operating cost model to exhibit linear homogeneity is widespread in the empirical literature, for example, Caves et al. (1984), Hansen et al. (2001) and the recent work of Zou and Hansen (2010). Empirical studies that constrain an airline operating cost model to exhibit concavity in input prices are limited, and include the work of Chua et al., (2005). Instead of imposing constraints on either condition, we investigate how well our unconstrained airline-aircraft operating cost model conforms to these conditions.

Linear Homogeneity

Diewert and Wales (1987) discuss that a model exhibits linear homogeneity if the conditions in equation (3.3) and equation (3.4) hold. Equations (3.3) and (3.4) ensure that a proportionate increase in all factor prices produces a similar increase in operating cost; for example, a 10% increase in all factor price leads to a 10% increase in operating costs. Equation (3.3) states that the first order coefficients for the factor prices sum to one. Together with the condition in (3.4) that the second order coefficients involving factor price must add to zero, scaling factor prices by k will lead to a proportional increase in operating costs.

$$\sum_i \omega_i = 1 \quad (3.3)$$

$$\sum_i \beta_{ij} = \sum_j \beta_{ij} = \sum_i \rho_{ij} = \sum_i \theta_{ij} = 0 \quad \forall i, j \quad (3.4)$$

Table 3.3 shows the results of calculating equation (3.3) and equation (3.4) for model 1 and model 2 for the second order coefficients that include p_{cnq}^i . This is calculated for constant j and $i \in (fuel, materials, labor)$.

The equation (3.3) holds approximately for both models. We see that the condition from equation (3.4) nearly holds for $\sum_i \rho_{ij}, \sum_i \theta_{ij}$ and most combinations of $\sum_i \beta_{ij}$, but does not hold for the second order coefficient on fuel price. The interpretation is, at the sample means, a factor price increase of k will lead to a proportional increase in operating cost. However, at values other than the sample mean, the function will not strictly exhibit linear homogeneity, such that a factor price increase of k may lead operating costs to increase by more or less than k . The behavior of operating cost with respect to a factor price increase is therefore data dependent and cannot be stated generally for the cost function.

Table 3.3 Linear homogeneity regularity conditions calculation.

Term	Coefficient Sum	j	Model 1	Model 2
	$\sum_i \omega_i$		1.006	1.121
$\sum_i \sum_{j \geq i} \beta_{ij} \ln p_{cnq}^i \ln p_{cnq}^j$	$\sum_i \beta_{ij}$	Fuel	-0.541	-0.279
		Materials	0.161	-0.316
		Pilot	-0.050	-0.054
$\sum_i \sum_{j \geq i} \rho_{ij} \ln p_{cnq}^i \ln z_{cnq}^j$	$\sum_i \rho_{ij}$	Fuel	0.032	0.127
		Materials	0.304	0
		Pilot	-0.118	-0.097
$\sum_i \sum_{j \geq i} \theta_{ij} \ln p_{cnq}^i g_{cnq}^j$	$\sum_i \theta_{ij}$	Fuel	-0.013	-0.016
		Materials	0.046	0.044
		Pilot	0.018	0.012

Concavity

The cost function must be concave in prices, such that, as an input price increases, less of that input is employed. It is known that concavity in prices holds if and only if the Hessian matrix of the cost function is negative semidefinite. This is clearly a data-dependent property, as the second order derivative depends on the data. As described by Diewert and Wales (1987), the Hessian (H) matrix of second derivatives is equal to:

$$H = A - \hat{s} + ss^T \quad (3.5)$$

A is the matrix of factor price coefficients: $A = \begin{bmatrix} \beta_{ff} & \beta_{fm} & \beta_{fl} \\ \beta_{mf} & \beta_{mm} & \beta_{ml} \\ \beta_{lf} & \beta_{lm} & \beta_{ll} \end{bmatrix}$. s is the share vector,

$s = [s_f \quad s_m \quad s_l]^T$. Each component of the share vector, s_i , is $s_i = \frac{p_i x_i}{O}$, where p_i is the factor price of i , x_i is the quantity of that factor used (per departure), and O is the operating cost per departure, all for a cnq combination. The values of x_i for fuel and labor are captured directly from each observation; the value of x_i for materials is captured as the operating cost minus the fuel and pilot labor costs, as it is a “catch-all” for materials price and labor. The matrix \hat{s} is a diagonal matrix with the shares on the diagonal. We have three input prices, fuel (f), materials price (m), and pilot cost (l , for labor), such that $i \in (f, m, l)$. The resulting Hessian matrix (H) is:

$$H = \begin{bmatrix} \beta_{ff} - s_f + s_f^2 & \beta_{fm} + s_f s_m & \beta_{fl} + s_f s_l \\ \beta_{mf} + s_f s_m & \beta_{mm} - s_m + s_m^2 & \beta_{ml} + s_m s_l \\ \beta_{lf} + s_f s_l & \beta_{lm} + s_m s_l & \beta_{ll} - s_l + s_l^2 \end{bmatrix} \quad (3.6)$$

As we have two models, we have two values for A , A_1 for model 1 and A_2 for model 2.

$$\begin{matrix} A_1 & A_2 \\ \begin{bmatrix} 0.155 & -0.582 & -0.114 \\ -0.582 & 0.717 & 0.026 \\ -0.114 & 0.026 & 0.038 \end{bmatrix} & \begin{bmatrix} 0.134 & -0.316 & -0.097 \\ -0.316 & 0 & 0 \\ -0.097 & 0 & 0.043 \end{bmatrix} \end{matrix}$$

As H is data dependent, we have a value of H for each of the 1657 observations. For each observation, we calculate the share vector and determine if the H matrix is negative semidefinite. For model 1, we find there are no observations with a negative semidefinite Hessian matrix; for model 2, this result improved to 37.4% of observations with a negative semidefinite Hessian matrix. While the results yield low percentages, they are consistent with the literature. In developing an empirical cost model to explore the cost implications of airline alliances, Chua et al. (2005) find concavity with respect to input prices in 39.3% of their observations. Caves et al. (1984) find that 50% of the observations yield a negative semidefinite Hessian matrix. While Caves et al. (1984) find that the observations that do not conform generally fall in extreme data ranges, we do not find that in our study.

Chua et al. (2005) discuss that the majority of transportation literature in which an empirical operating cost model is developed do not constrain the Hessian to be negative semi-definite; in a departure from the literature, the authors develop a separate set of estimates with a concavity constraint. The authors find that the 39.3% of observations that exhibit concavity in input prices increases to 83.1% with the constraint. This puts in perspective the 37.4% found in this study and the 39.3% found using the unconstrained model in Chua et al. (2005).

In light of the failure of both models developed in this study to exhibit concavity in input prices, we focus on the individual input prices. We investigate if the second derivative of each input price is negative for all data points, such that, as the input price increases, the quantity of that input used is decreased. We do this by calculating the functions on the diagonal of the Hessian matrix, which are the second derivatives of operating cost with respect to each factor price i , $\beta_{ii} - s_i + s_i^2$. The percent of data points for which $\beta_{ii} - s_i + s_i^2 < 0$ is reported in Table 3.4.

Table 3.4 Negative second derivatives (%) with respect to factor prices.

Factor Price	Model 1	Model 2
Fuel	96.3%	99.5%
Materials	0%	100%
Pilot	99.5%	99.5%

We see that the key variable in this study, fuel price, along with pilot price, has consistently high percentages of negative second derivatives across models. The results suggest that aircraft operations exhibit the expected behavior of substituting away from inputs whose prices increase; in practice, this substitution is limited to clear operational needs and requirements. We notice that materials price exhibits starkly different results from model 1 to model 2. The second order coefficient on materials price is statistically insignificant in model 1, and as such, it is eliminated from model 2. Therefore the relevant entry in the Hessian matrix for model 2 is simply $s_m^2 - s_m$; as $s_m < 0$, $s_m^2 - s_m < 0$. The inconsistent behavior and the statistical insignificance may be related to PPI acting as a “catch-all” variable, and therefore does not have a direct relationship with maintenance labor costs. It is possible that materials price in the form of PPI should

be further decomposed to more accurately capture the difference between maintenance materials and maintenance labor.

In summary, we find in this section that our models do not strictly adhere to the regularity conditions set forth by Diewert and Wales (1987). However, we also discuss potential reasons why regularity conditions based on an assumption of cost-minimizing behavior do not fully apply to the model. Moreover, we confirm that operating cost is concave in the key variable of fuel price. In light of this we conclude that the estimated model is credible and therefore proceed to interpreting the estimation results.

3.3.2 Interpretation of TM Results

Table 3.5 contains select estimation results for model 1 (estimation results for both model 1 and model 2 can be found in Appendix A1.2). As neither model was found to fully conform to regularity conditions, we choose to analyze model 1 because it contains the complete set of explanatory variables. The evaluation of the relationship between aircraft size and fuel price begins with the first order coefficient on aircraft size. The coefficient implies operating cost economies of aircraft size; a ten percent increase in aircraft size would increase operating cost by 4.4 percent. The first order coefficient of fuel price, 0.408, implies that at the sample mean, a ten percent increase in fuel price would increase operating cost by 4.08%. As we found that model 1 exhibits linear homogeneity at the sample mean, we conclude that the share of operating cost attributed to fuel costs is 40.80%. Beyond our two key variables of *seat* and *fuel*, we find the expected magnitudes and signs for the coefficients of *asl*, *pil*, *util*, and *ppi*. While previous studies have excluded the age variables, the model estimates show that the inclusion of these variables is warranted by their significant effect. The first order terms on technology age and airline-aircraft age are positive and statistically significant, and imply that, all else being equal, costs are greater for an aircraft developed in an earlier year.

The higher order coefficients provide insight into how the independent variables interact, and how inputs are substituted due to factor price increases. The second order coefficient of the seat variable is positive and implies that aircraft economies of scale attenuate for aircraft sizes larger than the average size. The second order coefficient estimate on fuel price, 0.155, implies that the 4.08% increase in operating cost due to a 10% increase in fuel price would increase with fuel price greater than the sample mean. The interaction term between fuel price and aircraft size, 0.123, tells us that as fuel prices increase, economies of scale due to aircraft size diminish slightly. In sum, high fuel prices reduce cost economies of aircraft size. With regard to aircraft age, the negative interaction term between airline-aircraft age and fuel price is unexpected, but may result from learning curve effects. As an airline gains experience with an aircraft, it learns the optimal fuel loads, flying speeds, and altitudes. Such benefits are found by Southwest Airlines and their one aircraft type fleet (Gittell, 2002). The interaction between aircraft size and average aircraft age shows that smaller aircraft show the signs of age more quickly.

Table 3.5 Select operating cost model empirical results.

Variables	First Order Term	Second Order Term	Variable Interactions	First Order Term
Seats	0.400*** (0.083)	0.206*** (0.062)	Seats – Average stage length	-0.162*** (0.079)
Average stage length	0.803*** (0.054)	0.126*** (0.033)	Seats – Fuel price	0.123*** (0.048)
Pilot price	0.296*** (0.038)	0.038*** (0.012)	Average stage length – Fuel price	9.88×10^{-5} (0.030)
Fuel price	0.408*** (0.037)	0.155*** (0.034)	Airline-aircraft age – Fuel price	-0.014*** (0.005)
Utilization	-0.124*** (0.036)	-0.011 (0.007)	Airline-aircraft age – Seats	-0.021** (0.010)
Materials price	0.302 (0.210)	0.717 (0.632)		
Airline-aircraft age	0.037*** (0.007)	1.08×10^{-3} *** (4.4×10^{-4})		
Technology age	0.004** (0.002)	1.28×10^{-3} *** (3.49×10^{-4})		

Where

***Variables are significant at the 1% level

**Variables are significant at the 5% level

*Variables are significant at the 10% level

3.3.3 Translog Operating Cost Prediction

In this section, we evaluate the impact of fuel price on the aircraft size that minimizes operating cost per seat-mile. This analysis enables an understanding of how a fuel price increase might influence jet aircraft size from a purely operating cost perspective.

We estimate operating cost per seat-mile for selected stage lengths over a range of aircraft sizes and fuel prices using the TM model 1 coefficient estimation results. We develop operating cost predictions using Delta Airlines as the base airline, and use the Delta Airlines average values for all variables except fuel price, stage length and seat capacity. The results presented are parametric over seats, fuel price and stage length; combinations of these three variables will be specified inputs. This will enable an interpretation of how the aircraft size that minimizes operating cost per seat-mile changes with the key input price of fuel.

Figure 3.1 presents the operating cost per seat-mile over seats for three representative fuel prices. The fuel price values range from a minimum value (\$0.50/gallon) and a maximum value (\$5.00/gallon), double the maximum value experienced in the dataset.⁹ For constant distance flown, as fuel price increases, the aircraft size that minimizes operating cost per seat mile decreases. This reflects the positive interaction term between seats and fuel price. We also observe that for each stage length – fuel price combination, there is a

⁹ Note that the minimum and maximum fuel price range in the data is \$0.35-2.56/gallon; predictions out of this range may be less reliable.

unique aircraft seat capacity that minimizes operating cost per seat mile. This is represented by the large black data point on each curve in Figure 3.1, and presented in the table in the lower right hand panel. The aircraft seat capacities that minimize cost are much larger, in most cases, than aircraft technology that exists today. While we confirm the finding of Wei and Hansen (2003) that there exists a unique aircraft size that minimizes operating cost per seat-mile, we depart from their finding that the technology size is in a range of existing aircraft technologies. Therefore, in the context of existing technologies, aircraft size should be maximized to minimize operating cost per seat-mile.

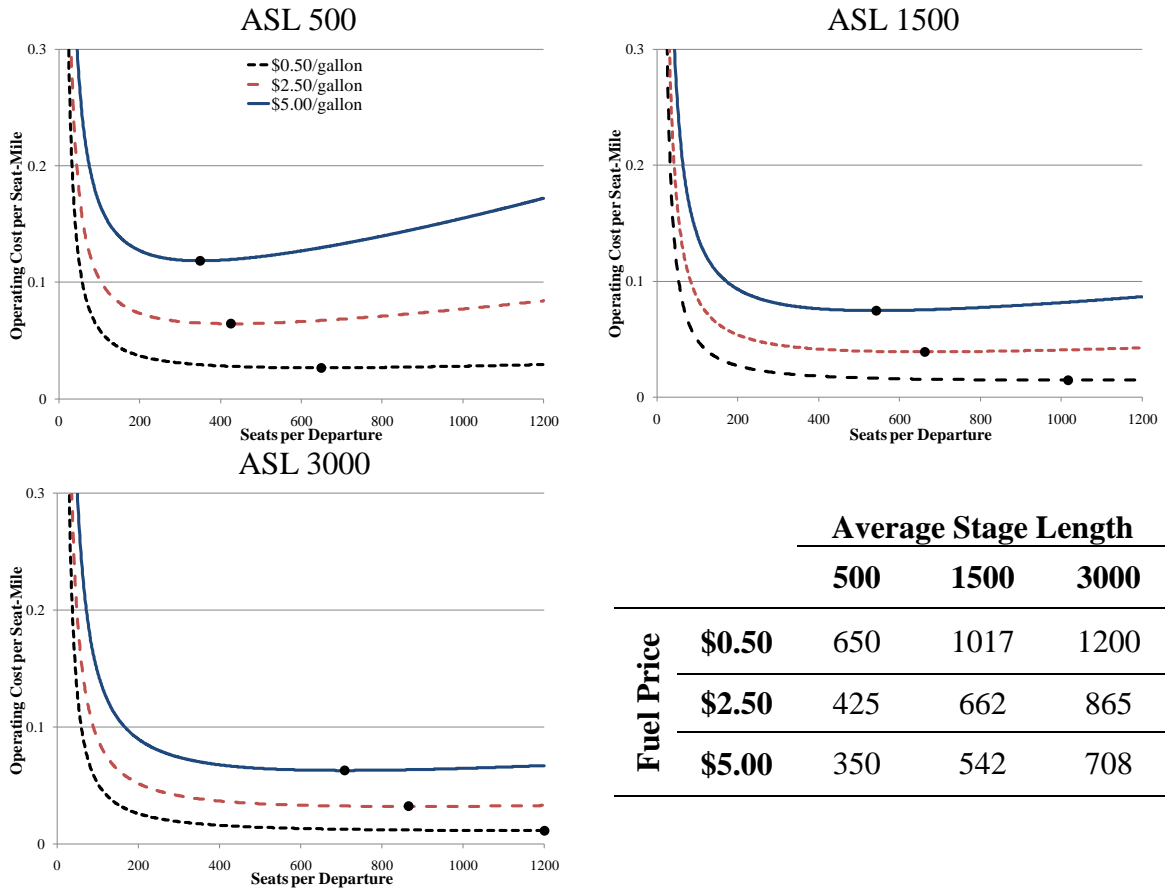


Figure 3.1 Seat capacity corresponding to the minimum operating cost per seat mile for a range of fuel prices and distances.

A possible explanation for the large aircraft seat capacities that minimize operating cost is that airlines consider pilot costs to be endogenous, as suggested by Wei and Hansen (2003). To determine the impact of endogenously considering labor costs on cost-minimizing seat capacity, we construct a relationship between the unit price of labor and aircraft seat capacity. The following is the resulting equation estimated using the dataset on which the translog model was estimated, with both coefficients significant at the one percent level. To be consistent in the estimation method, we estimate using ordinary least squares and panel specific standard errors and assumed autocorrelation within panels. As we are predicting operating costs for the year 2006, we deflate all data points to be in constant 2006 dollars. The estimation results are in A2.2.

$$pilot\ price_{cnq} = \gamma + \delta * seat_{cnq} + \sum_c \phi_c \quad (3.7)$$

Where

$seat_{cnq}$ is the seat capacity of aircraft n operated by airline c in year-quarter q
 γ, ϕ_c, δ are coefficients to be estimated

For comparison purposes, the results in Figure 3.1 assume a labor price of about a 250 seat aircraft, representative of a large model such as a Boeing 757 or a Boeing 767. Using equation (3.7) we calculate labor price for seat capacities between one and 1200 and predict operating cost from this augmented dataset. We see in Figure 3.2 that when labor price is endogenous to the model, the seat capacity that minimizes operating cost is reduced. However, aircraft technologies are still larger than exist in the system today for stage lengths greater than about 1500 miles. For stage lengths less than 1500 miles, the aircraft sizes that minimize operating cost per seat-mile exist in the system today, however, they are not typically flown for missions less than 1500 miles.

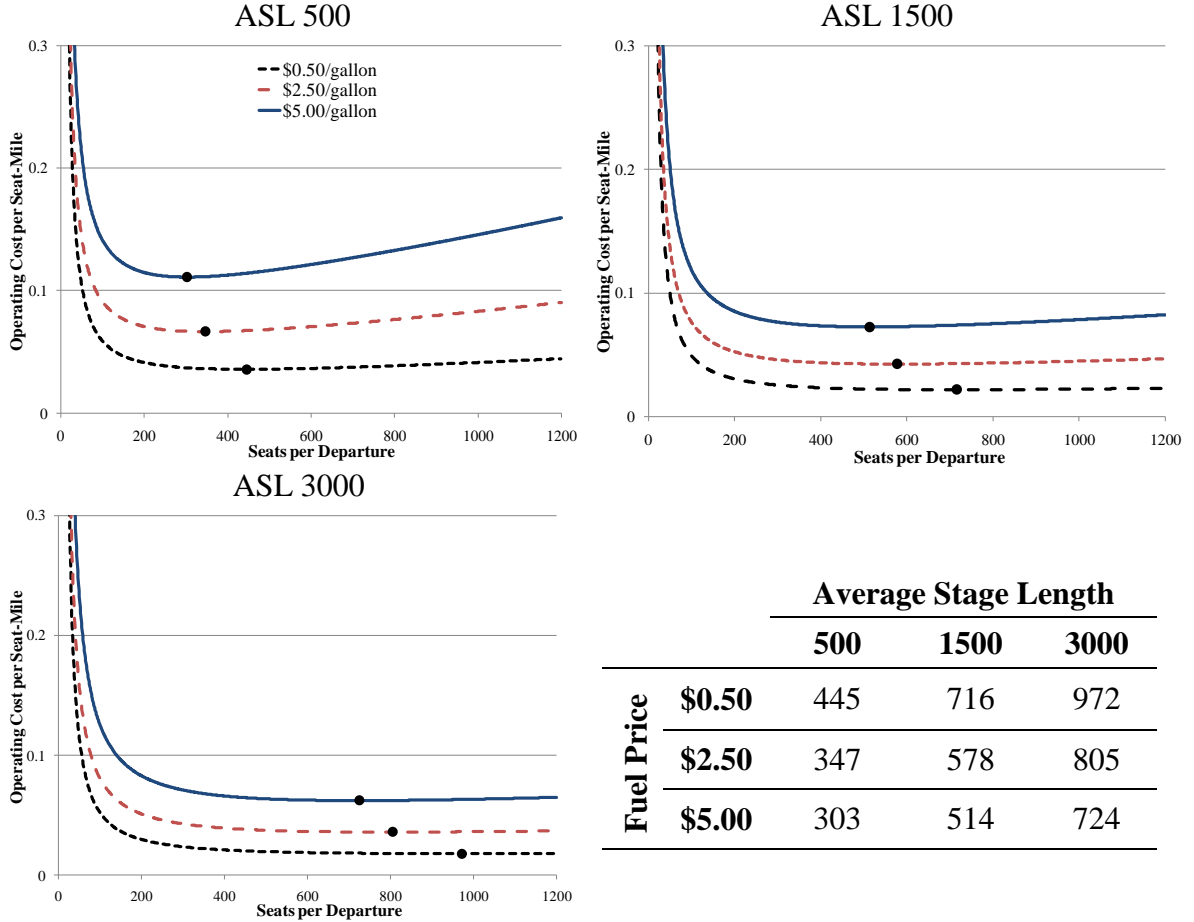


Figure 3.2 Seat capacity corresponding to the minimum operating cost per seat mile for a range of fuel prices and distances, labor price considered endogenous.

The use of the translog function enables investigation of the consequence of variable interactions. We find there is a unique aircraft size that minimizes operating cost per seat-mile, and that fuel price plays a large role in determining this aircraft size. We also find that fuel price increases could lead to a reduction in aircraft size, if cost minimization is the goal. However, it is possible that relationships between our key variables of interest – seat capacity and the unit price of fuel – can be captured by simpler functional form for operating cost. In the following section, we examine two such functional forms: the Leontief Technology operating cost model and the linear operating cost model.

3.4 Leontief and Translog Operating Cost Model Comparison

This section will investigate the difference in predicted values between the Leontief technology model (LM) developed in chapter 2 and translog model (TM). The LM was developed in the previous chapter using average values from the same data set used in the current study but a later year (2007). In chapter 2, three specific aircraft models are chosen for cost calculation, two of which are jet aircraft: an ERJ 145 regional jet and a Boeing 737-400 narrow body. The key cost categories – fuel, labor, and maintenance – are summed based on statistical relationships between fuel burn and distance traveled and travel time and distance traveled.¹⁰ The values, presented in chapter 2, are reported in Table 3.6 in units of \$/operation. Using the same methodology, the cost coefficients for a mid-sized aircraft (182 seats), the narrow body Boeing 757-200, are determined.

Table 3.6 Leontief Technology model operating cost coefficients.

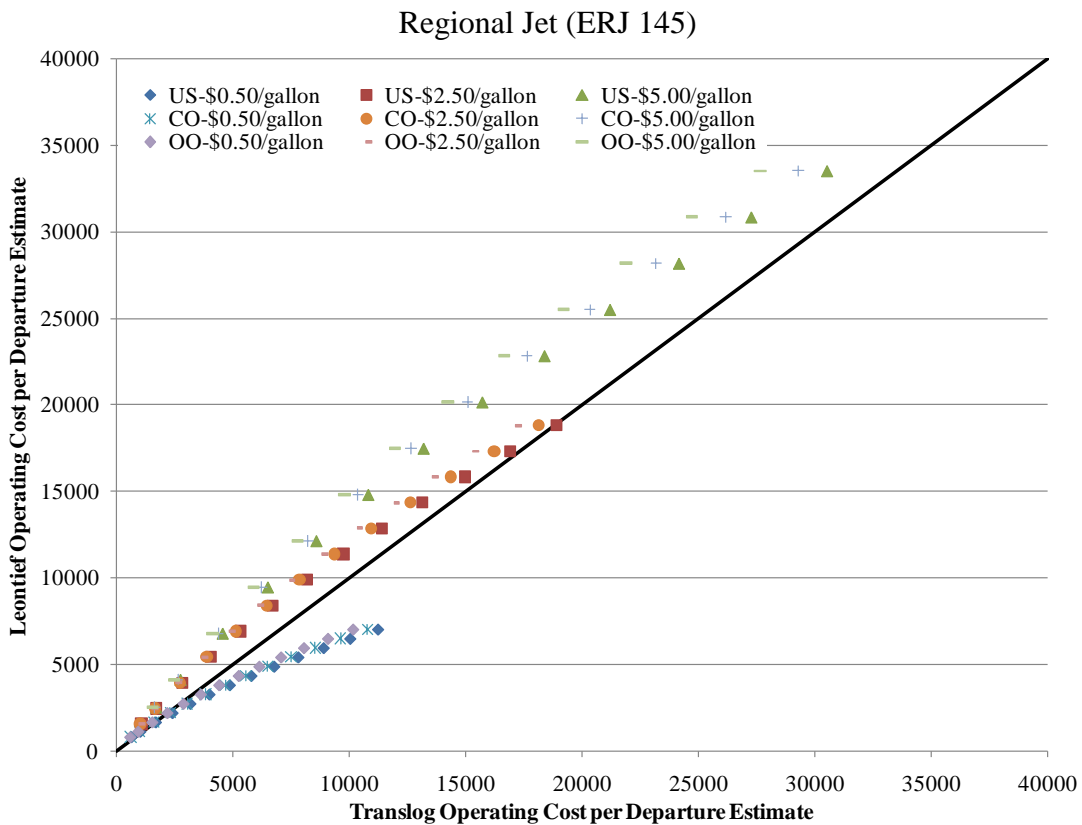
Aircraft Category	Coefficient Value			
	Fuel Price (f)	Distance · Fuel Price (d · f)	Distance (d)	Fixed
B757-200	5.1*10 ²	2.0	2.5	9.4*10 ²
B737-400	2.7*10 ²	2.1	2.6	8.8*10 ²
ERJ 145	1.9*10 ²	1.9	1.2	4.8*10 ²

We perform the comparison of LM and TM results by estimating operating cost per departure with both models and plotting the results. The inputs needed for estimation with the LM are simply fuel price and distance traveled. We choose three sample fuel prices and 13 stage lengths between 100 and 3000 miles. For the translog model, beyond fuel price and stage length we need all inputs shown in Table 3.1. To identify values for these inputs, we calculate average values specific to each aircraft type (ERJ 145, Boeing 737-400 and Boeing 757-200) using the original dataset on which the translog model was estimated (deflated to 2006 values). For the value of seats, the seat capacities for the aircraft in the LM are equal to the aircraft averages; this value is used. Finally, we need to identify a base airline for which we estimate operating costs with the TM. We choose three representative airlines for the estimation: SkyWest (OO), Continental (CO), and USAir (US). We chose these airlines based on the coefficient estimates of the airline fixed effects (Appendix 1.2). SkyWest represents the 1st quartile, Continental the median,

¹⁰ It should be noted that the model in the previous chapter also includes airport charges as part of the operating costs; these are eliminated for this analysis because they are not part of the direct operating costs.

and USAir the 3rd quartile of the fixed effect coefficient estimates. For comparison, the operating cost per departure estimates from the LM and TM are plotted against each other along with a 45-degree equality line for the three aircraft types.

We begin our discussion of Figure 3.3 by considering the effect of fuel price. While for most aircraft sizes at most fuel prices the predictions are relatively linear along a 45-degree equality line, we do see trends in over-prediction and under-prediction that highlight the difference between Leontief technology models and translog models. At relatively low fuel prices, the LM predictions are significantly less than the TM predictions. At relatively high fuel prices, this relationship shifts such that the LM predictions are either higher than the TM predictions (for the regional jet and the Boeing 737), or relatively higher compared with lower fuel prices. These effects reflect the technology assumptions behind the TM and LM. The LM considers aircraft to be a Leontief technology, in which all inputs must be used in fixed proportions. The TM model allows substitution between inputs when factor prices change. The LM was developed at a time when the operators of a 737-400 were paying an average of \$2.01/gallon; the operators of a 757-200 were paying an average of \$1.99/gallon. It therefore follows that when the TM and LM are applied at fuel prices close to this \$2.00/gallon average, the TM predictions and the LM predictions will be very similar. For fuel prices above this average, the LM estimates should be relatively higher than the TM estimates. This is because the TM allows for input substitution: as fuel prices increase, airlines will take steps to use fuel more efficiently by leveraging other inputs, a phenomenon that the LM cannot capture.



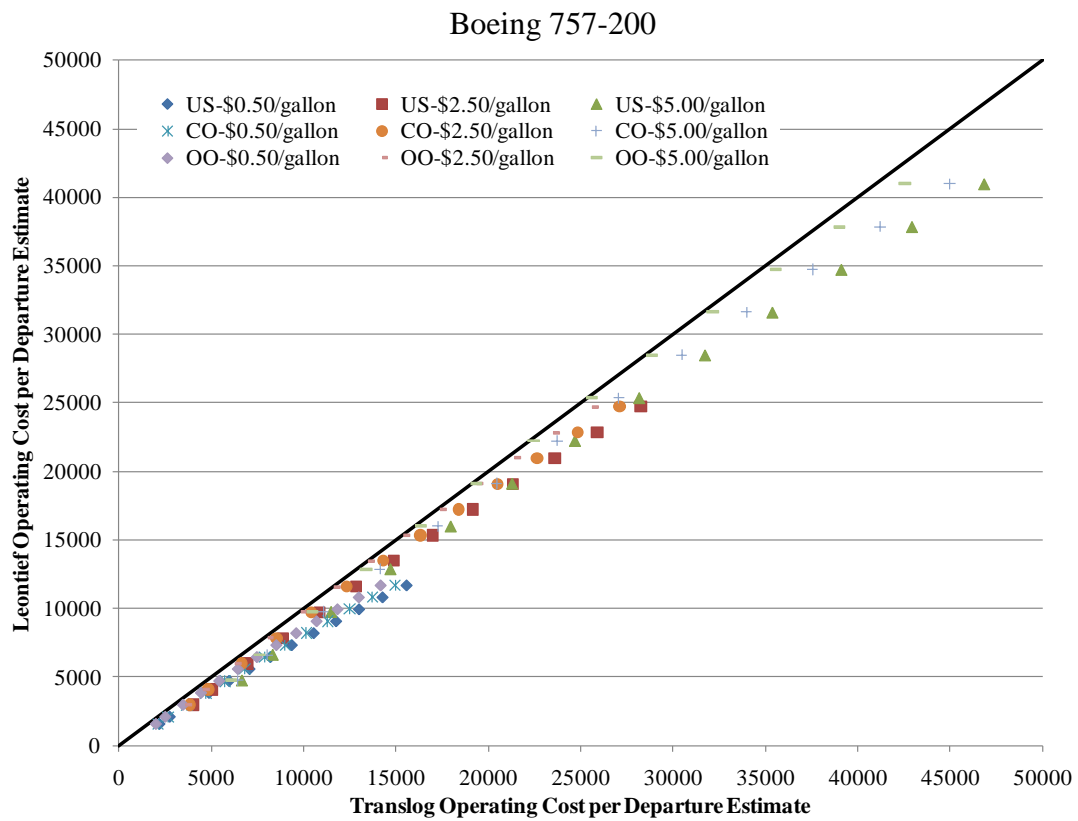
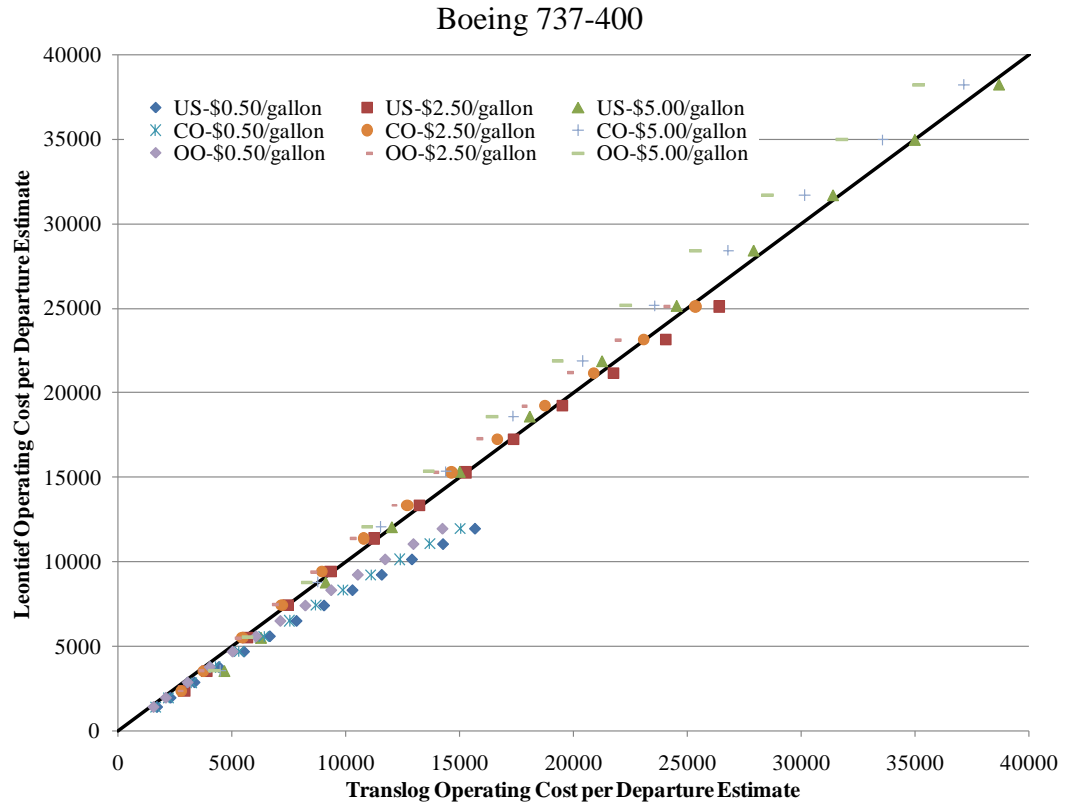


Figure 3.3 Predicted operating cost per departure, Leontief Technology vs. translog operating cost model.

Similarly, one might expect that the TM would predict lower costs a low fuel prices, in this case a result of substituting cheap fuel for other inputs. Figure 3.3 does not bear this out however. Indeed, when low fuel prices are assumed the LM predictions are highest relative to the TM predictions. These results reinforce our previous conclusion that classical economic assumptions are not strictly applicable to operating costs for individual aircraft types.

Moreover, these patterns aside, Figure 3.3 shows a relatively linear relationship along the 45-degree equality line between the LM and TM for the two larger jet aircraft. This implies that, while there is a small under- and over-prediction trend, the potential for supplier input substitution for fuel is rather modest. Thus, while we are able to glean insights into variable interactions from the translog model, it is not essential to capture these interactions in order to accurately predict operating costs.

This section finds that the Leontief technology operating cost model is able to accurately predict operating costs, despite sacrificing the estimation of variable interactions. In the final section, we explore a linear operating cost model, also transparent and takes few inputs like the LM, yet can capture variations in seat capacity and fuel price in a single model.

3.5 Linear Operating Cost Model

In developing the translog operating cost model, we were able to glean insights into the contribution of individual variables along with variable interactions. However, we found by comparing the LM and TM that operating costs can be accurately captured by models with less complexity. As there are instances when a less complicated, simple representation of operating costs is necessary, we explore a representation of operating cost that retains the simplicity of the LM but includes seat capacity as a variable.

Estimating a linear model of operating costs proved to be a challenge. One possible reason for this challenge is the relationship between fuel efficiency (measured by seat-miles per gallon of fuel) and seat capacity, shown in Figure 3.4. The fuel efficiency of an aircraft peaks around an aircraft size of 200 seats, which is generally the separation between narrow body and wide body aircraft. The TM is able to capture this through the positive interaction term between fuel and seat capacity, yet the linear model is unable to capture the parabolic relationship between fuel efficiency and seat capacity. As the focus of this research is on short haul transportation, we will restrict the dataset on which the linear model is estimated to include aircraft with seat capacities below 200 seats.

Even with the restriction on seat capacity, estimating an operating cost model still presents a challenge. We therefore experiment with a model that treats operating cost without fuel – mainly fuel and maintenance – and operating cost due to fuel separately. We develop two models, one to capture the operating cost without fuel (O'_{cnq}) and one to capture fuel consumption (F_{cnq}) for jet aircraft with seat capacities below 200 seats. The

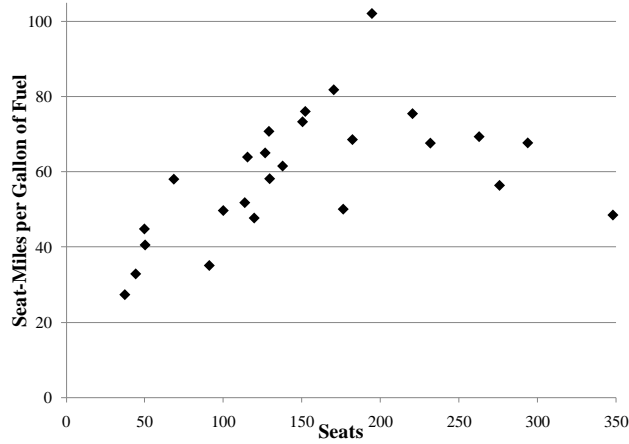


Figure 3.4 Seat-miles per gallon of fuel vs. seats.

final operating cost per departure function (O_{cnq}) is the sum of these two functions, where *fuel* is the unit price of fuel.

$$O_{cnq} = fuel * F_{cnq} + O'_{cnq} \quad (3.8)$$

We develop an econometric operating cost model (3.9) and an econometric fuel consumption model (3.10), with the key variables of seats per departure (*seat*), average stage length traveled (*asl*), and airline fixed effects (*c*). We do not include labor explicitly in the operating cost component but rather let it be endogenous to aircraft size. Similar to the estimation of (3.7) we deflate the cost values to be in constant 2006 dollars. We estimate this model on a dataset from the same source as the original dataset for the translog model, but with a slightly different date range: 2003-2009 inclusive. To estimate the TM on the full list of variables, the date range was limited to no later than 2006 because of data availability; as the models in (3.9) and (3.10) includes three variables, we are able to use a more recent dataset. As the dataset is still an unbalanced panel, we estimate using ordinary least squares and panel specific standard errors and assumed autocorrelation within panels as we did with the translog model.

$$O'_{cnq} = \alpha + \sum_c \phi_c + \omega seat_{cnq} + \delta asl_{cnq} + \varphi seat_{cnq} asl_{cnq} + \varepsilon_{cnq} \quad (3.9)$$

$$F_{cnq} = \beta + \theta seat_{cnq} + \delta sl_{cnq} + \rho seat_{cnq} asl_{cnq} + \varepsilon_{cnq} \quad (3.10)$$

Where

$seat_{cnq}$ is the seat capacity of aircraft *n* operated by airline *c* in year-quarter *q*

asl_{cnq} is the average distance traveled by aircraft *n* operated by airline *c* in year-quarter *q*

$seat_{cnq} asl_{cnq}$ is the interaction term between seats per operation and distance per operation

$\alpha, \phi_c, \omega, \delta, \varphi$ are coefficients to be estimated in (3.9)

$\beta, \gamma, \theta, \delta, \rho$ are coefficients to be estimated in (3.10)

In estimating (3.9) and (3.10) (estimation results shown in Appendix A1.4 and A1.5, respectively), we find in both cases some key coefficients are statistically insignificant. Beginning with O'_{cnq} , we find that ω is marginally significant, with a t-statistic of -1.71. For F_{cnq} , the coefficient estimate of δ is negative and insignificant. However, instead of dropping the variable of distance in both functions, we instead preserve the first order terms in both equation (3.9) and (3.10). This is for two reasons. The first is to preserve consistency with the analytic total logistics cost model to be presented in chapter 4. The second is to preserve the scale economies of aircraft size found with the translog model. We therefore define the preferred model as including only the main terms and not the interaction term or the constant. We find the coefficient estimates are significant and of the expected signs. The linear operating cost model is then the function in (3.8) with the parameter estimates of the preferred model.

To evaluate the estimation performance of the linear model, we compare the estimates of the linear model and the TM. We predict values using both models at three fuel prices: \$0.50/gallon, \$2.50/gallon, \$5.00/gallon; for 13 distances between 100 and 3000 miles; and with Delta Airlines as the base airline. For the additional variables in the TM, we use those consistent with the year 2006 and the Delta Airlines average. In general, when both models are estimated for relatively high fuel prices (above \$2.50/gallon), the estimates from the linear model exceed those from the TM. This is further demonstrates that the TM captures input substitution in the case of fuel. The percent difference in estimates is smallest in the 100-200 seat range, with the TM predictions between 25% lower to 10% greater than the linear model predictions; this trend was also observed in the relationship between the LM and TM. For seat capacities close to the sample mean in the translog model, the TM and linear model estimates are fairly close. We demonstrate that a linear model restricted to a range of data is able to estimate operating costs within 0-25% of the estimates from the translog model.

3.6 Conclusions

In this chapter we develop three empirical operating cost models for jet aircraft based on a similar data set. In developing the translog model, we establish a detailed portrait of the relationship between aircraft operating cost and the variables that influence cost. We find relationships between seat capacity, fuel price, and other key variables not documented in previous literature. However, we find that the simpler functional forms of the LM and the linear model yield predictions of operating costs that are similar to the predictions of the TM. Through the comparison of the LM, which assumes the mix of inputs required to operate a given air vehicle is insensitive to factor price, and the translog operating cost model, we establish the limited role of supplier input substitution in managing fuel-related cost. The linear model is developed such that the coefficients are parameters in an analytically tractable total logistics cost function in the next chapter. Here we establish that the simple linear formulation is able to predict operating costs that are similar to the predictions of the translog operating cost model. The LM and linear models have many strengths, including transparency, few inputs, and ease of prediction. While translog, Leontief technology, and linear models all play an important role in aviation cost modeling, this study suggests that use of the linear model is unavoidable for tractability.

4.

System Optimal Mathematical Models of Intercity Transportation

In this chapter, we develop a parametric optimization model for intercity passenger transport in a given corridor, in which the parameter of central interest is effective fuel price. Toward this end, we consider a central planner minimizing the total logistics cost, including those to vehicle operators, passengers, and the environment. The goal of the central planner is to find the optimal (least cost) service mix, defined by the vehicles to operate and the headway at which to operate. We must therefore develop a total logistics cost function for an intercity transportation corridor. Vehicle types, headways, sizes, and passenger assignment to vehicles are chosen to minimize total logistics cost. Uniquely, the model allows for the use of mixed fleets—i.e. a slow inexpensive vehicle and a fast expensive one—and travelers with different values of time.

Logistics scheduling literature considers how a central planner should schedule freight vehicle deployments to minimize costs. Smilowitz and Daganzo (2007) consider an integrated package delivery network and determine optimal service frequency using a total logistics cost function that considers all related operating costs. Daganzo and Newell (1993) develop an operating cost function to study delivery strategies as they relate handling costs. Neuman and Smilowitz (2002) consider the benefit of coordinating drayage movements in the Chicago Intermodal Freight Interchange. A planner's perspective is taken in all these studies. Instead of considering the incentives and motivations of the multiple operators and customers involved, least-cost routes, frequencies, and homogenous vehicle assignments are determined as if there were a central operator able to coordinate deployments. Neuman and Smilowitz (2002) find that considerable cost savings could be gained from central planner coordination of drayage movements due improved vehicle utilization. Hansen (1991) uses a total logistics cost function in an aviation context that includes social and private costs to compare two vehicle types in order to serve passengers with homogenous values of time. The costs considered in the total logistics cost function are passenger costs (airport access time, travel time, and schedule delay) and aircraft operating and ownership cost.

While the previously mentioned studies assumed all customers have the same value of time, Viton (1986) and Keeler et al. (1975) note their skepticism with using one value of time to represent all passengers and situations due to multiple time classifications (travel time, schedule delay) and varying values of passenger time (high-valued business travelers, low-valued leisure travelers). Using a combination of revealed and stated

preference surveys of air transportation users, Adler et al. (2005) find the existence of significant variation in passenger value of time as well as differences between the value of schedule delay and on-time performance. Their study uses a mixed logit model and assumes all non-fixed parameters are normally distributed. Another study pointing to the existence of passenger heterogeneity is Berry et al. (1996). By assuming that preferences for prices and flight characteristics are correlated, they estimate two sets of coefficients for two passenger groups using a random utility model.

Related research in logistics include exploratory, high level routing studies that consider both heterogeneous vehicles and passenger value of time. The delivery of packages with heterogeneous time values over a transport network has been studied by Smilowitz et al. (2003). In the study, the authors investigate the potential of serving two classes of packages – high value express and lower value deferred packages – on an integrated network instead of separating their distribution. The research compares two vehicles for service, aircraft for high value-of-time packages and truck ground transportation, and finds that cost savings can be achieved by using underutilized space on aircraft to serve the deferred packages.

In this study, we will consider vehicle and input substitution in the same function. Total logistics cost functions that consider multiple vehicle types are well-explored in the literature, as are ones that address input substitution; however we lack an integrated analytic model that captures both effects fully in one function in the context of intercity passenger transportation. To this end, we develop mathematical models that capture airline costs and passenger costs in a total logistics cost function and assigns passengers to the most appropriate vehicle based on their value of time and preferred time of departure. The models allow for mixed-vehicle as well as single-vehicle services. Section 4.1 presents the assumptions and structure of the total logistics cost function methodology. In section 4.2, we construct total logistics cost functions for single and mixed vehicle combinations considering passenger groups defined by demand and value of time. We describe the model assumptions and setup, and achieve an analytic solution for operational frequency and vehicle size. In sections 4.3 and 4.4 we consider passenger time to have a distribution, thus generalizing the representation of heterogeneous passengers.

4.1 Total Logistics Cost Function Assumptions and Structure

In this research we consider passengers who desire to travel on an intercity corridor. Service on this corridor is represented on an infinite timeline with vehicles scheduled to serve a single origin-destination pair. There is no limit on the number of vehicles available and therefore on the schedule frequency. We model three scenarios with varying assumptions regarding passenger characteristics and assignment:

1. Passengers fall into discrete groups, each of which is characterized by a demand rate and value of time; passengers must be served in the headway in which they desire to depart.

2. Passenger value of time follows a continuous distribution; passengers must be assigned to a vehicle bounding the headway in which they desire to depart.
3. Passenger value of time follows a continuous distribution; passengers are assigned to the most appropriate vehicle, which in some cases may not bound the headway in which they desire to depart.

We consider fleets consisting of one or two vehicle types (or technologies). In the case of a single vehicle fleet, we define the vehicle type to be i where $i \in I = \{\text{jet, turboprop, highspeed rail}\}$. If the fleet contains two vehicle types, we define the vehicle pairs to be c where $c \in C = \{\{\text{turboprop and jet}\}, \{\text{high speed rail and jet}\}, \{\text{turboprop and high speed rail}\}\}$. c is thus a set containing two vehicles, which are in turn elements of set I . We therefore have $i \in I$ or $i \in c$ and use the index i to generally refer to a vehicle technology whether it is part of a single- or two-vehicle fleet.

Each vehicle operation on technology i – whether $i \in I$ or $i \in c$ – generates a cost to the service provider and a cost to the passengers on-board. There are two costs incurred by the supplier to operate vehicle type i : a fixed component (α_i) which does not depend on the passenger load and a variable component (β_i) which represents the marginal cost of carrying an additional passenger on a vehicle operation. Both α_i and β_i are functions of fuel price f , distance d , and other supplier factors. If i is the index representing the vehicle technology used for the operation in question, and assuming full vehicle occupancy, then the cost associated with an operation on a per passenger basis: $\frac{\alpha_i}{s_i} + \beta_i$, where s_i is the number of seats per departure on vehicle type i .

Each passenger incurs two costs associated with traveling on the intercity transportation system. The first is the time spent in-vehicle, which is the travel time for a given distance on vehicle type i (m_i). The second is schedule delay, the expected value of for a passenger of type n on vehicle type i is denoted $w_{i,n}$. This is the expected difference between when a passenger of type n desires to depart and the actual departure time of vehicle i . The time costs are monetized through multiplication by the passenger value of time λ_n .

We will explore the scenarios in the following sections. In all scenarios we assume that passenger demand is exogenous, because our focus is on the supply side rather than the demand side of the system.

4.2 Total Logistics Cost Models for Passenger Scenario One

Under scenario 1 we segment passengers into groups. The index for passenger groups is n , and passenger groups are defined by a value of time λ_n and an exogenous demand, Q_n . The sum of all passenger groups is the total demand, $\sum_n Q_n = Q_t$. Furthermore in scenario 1 each passenger group has a desired departure time that is uniformly distributed and passengers must be served in the headway in which they desire to depart. Said another way, the rate in which passengers would hypothetically “arrive” for a vehicle departure is a constant value (Q_n). This is the wished for arrival rate as discussed in Daganzo and Garcia (2000). Vehicle operation schedules are based on these passenger

assumptions. The Continuum Approximation method described by Daganzo (1999) illustrates that with a stationary wished for arrival curve and the passenger assumptions made here, vehicles are scheduled uniformly to minimize schedule delay. In other words, vehicles are scheduled over time at a constant headway, such that a single frequency (the inverse of headway) of vehicle departures over time holds.

In this section we develop a total logistics cost function for a corridor served by a single vehicle technology and a mixed vehicle technology. We begin by defining notation for parameters and decision variables.

Parameters:

α_i	Vehicle fixed cost, function of fuel price (f) and distance (d), $\$/\text{Operation}$
β_i	Vehicle variable cost, function of fuel price (f) and distance (d), $\$/\text{Passenger}$
m_i	In-vehicle travel time, function of distance (d), $\text{Time}/\text{Passenger}$
Q_t	Total flow of passengers, $\text{Passenger}/\text{Time}$
Q_n	Flow of passengers in group n , $\text{Passenger}/\text{Time}$
λ_n	Passenger value of time for group n , $\$/\text{Passenger} - \text{Time}$
$w_{i,n}$	Expected schedule delay for a passenger of type n on vehicle type i , Time
τ_n	Critical departure time, Time
$Z_{i,n}$	Time interval for departure, Time
$X_{i,n}$	Generalized cost (time) differential, Time
$P(R_n)$	Probability a passenger is of type n
$P(V_i)$	Probability a passenger is on vehicle type i
$P(R_n V_i)$	Conditional probability that a passenger on vehicle type i is of passenger type n
$P(V_i R_n)$	Conditional probability that a passenger is assigned vehicle type i given they are of type n
s_i	Seats per operation on vehicle type i , $\text{Seats}/\text{Operation}$

Decision Variable:

The decision variable is vehicle frequency, F , for the two possible vehicle combinations:

F_i	Vehicle frequency (single technology combination), $\text{Operations}/\text{Time}$
F_c	Vehicle frequency (mixed technology combination), $\text{Operations}/\text{Time}$

In both the single and mixed vehicle cases, the passenger cost is dependent on the vehicle type on which a passenger is traveling. Quantities must be developed to capture this vehicle assignment: the proportion of passengers on each vehicle type i , and the proportion of passengers of each type n on each vehicle type i . We then define two events: event V_i , which is the event that a passenger is assigned to vehicle type i ; and R_n , the event that a passenger is of type n . $P(V_i)$ defines the proportion of passengers on vehicle type i . $P(R_n|V_i)$ is the conditional probability that a passenger on vehicle type i is of passenger type n .

The three quantities related to passenger allocation, $P(V_i)$, $P(R_n|V_i)$, and $w_{i,n}$, can be expressed in terms of parameters $\alpha_i, \beta_i, \lambda_n$, and m_i . We begin by considering how passengers are assigned to vehicles in both the single and mixed vehicle case. In the problem formulation, user optimal vehicle assignment and system optimal vehicle assignment are identical if we assume that passengers pay variable vehicle operating cost as well as time costs. When assigning passengers to a vehicle, the central planner seeks to minimize the sum of the generalized cost of each passenger. The generalized cost is a function of travel time, vehicle variable cost, expected schedule delay, and passenger value of time. Vehicle variable cost, β_i , is included so passengers internalize the marginal cost their vehicle choice imposes on the system. If passengers internalize the marginal cost they impose on the system in choosing which vehicle departure to take, the solution is system and user optimal.

Passengers are defined by two indices: their passenger group (demand and value of time) n and the vehicle type on which they are assigned i . We will consider the passenger generalized cost, which is the cost incurred by a single passenger in units of time. We now construct an expression for the generalized cost. Consider Figure 4.1 and Figure 1.1, which depict an interval of time between two scheduled departures—i.e a headway. Figure 4.1 shows the single vehicle case for a vehicle technology $i \in I$. Figure 1.1 displays the mixed vehicle case, in which the two vehicles form the set $c \in \{j, k\}$. In both cases the expected total time (generalized, to include money costs) faced by a passenger desiring to depart during this headway (of time length $\frac{1}{F_i}$ or $\frac{1}{F_c}$) is the sum of the travel time, m_i , the variable cost divided by value of time, $\frac{\beta_i}{\lambda_n}$, and the expected schedule delay, $w_{i,n}$. (We assume here, without loss of generality, that the passenger pays the variable cost and chooses which vehicle to take in order to minimize her generalized cost. However, as explained above, we obtain the same results if the supplier — or anyone else — pays these costs and passengers are assigned to vehicles by the central planner.) To find the point in time when passengers are indifferent between two vehicles we find the *critical departure time* τ_n , or the instant in time in which the generalized cost for both vehicles are equal. We assume that passengers are indifferent to departures scheduled t units before or t units after the preferred time. Therefore, to find τ_n we draw lines of slope 1 representing the schedule delay cost for either vehicle and find their point of intersection. The x-coordinate of the intersection is the *critical departure time* τ_n . The y-coordinate is the generalized cost at τ_n , which is also the maximum cost a passenger of type n would face in utilizing the system.

We can now define the *time interval for departure* on vehicle i by passenger of type n ($Z_{i,n}$), which is the time interval between the departure time of vehicle i and τ_n . If a passenger of type n desires to depart in the region $Z_{i,n}$ she will be assigned to vehicle type i . Because passengers of type n have desired departure times that are uniform over time (and therefore over $Z_{i,n}$), the expected wait time for passengers of type n is $\frac{Z_{i,n}}{2}$. It follows that $Z_{i,n}$ is one-half the headway when vehicles are of a single type (Figure 4.1); however, when the vehicles are different technologies (Figure 4.2), this region may be either larger or smaller than one-half the headway due to vehicle and passenger attributes. We term the difference between $Z_{i,n}$ and $\frac{1}{2F_c}$ as the *generalized cost differential*, $X_{i,n}$. $X_{i,n}$ is the additional time region beyond one-half the headway in which a passenger of type n will be assigned to a vehicle of type i ; $X_{i,n}$ is zero in the single vehicle case, and expressed in terms of the performance parameters vehicle type j and type k for the mixed vehicle case. This is shown in (4.1); the equation for $w_{i,n}$ follows in (4.2) (in which an unsubscripted F is used to represent both F_c and F_i).

$$X_{j,n} = \frac{m_k \lambda_n + \beta_k - m_j \lambda_n - \beta_j}{2\lambda_n}; X_{k,n} = -X_{j,n} \quad (4.1)$$

$$w_{i,n} = \frac{Z_{i,n}}{2} = \frac{1}{2} \left(\frac{1}{2F} + X_{i,n} \right) \quad (4.2)$$

Figure 4.1 shows the generalized cost vs. time for the single vehicle case. Figure 4.2 shows this for the mixed vehicle case.

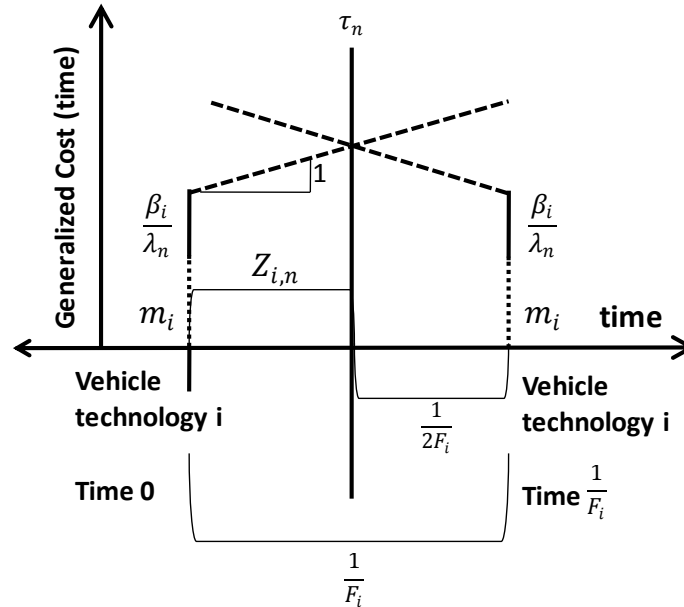


Figure 4.1 Generalized cost (time) and related quantities for the single vehicle case, passenger scenario 1.

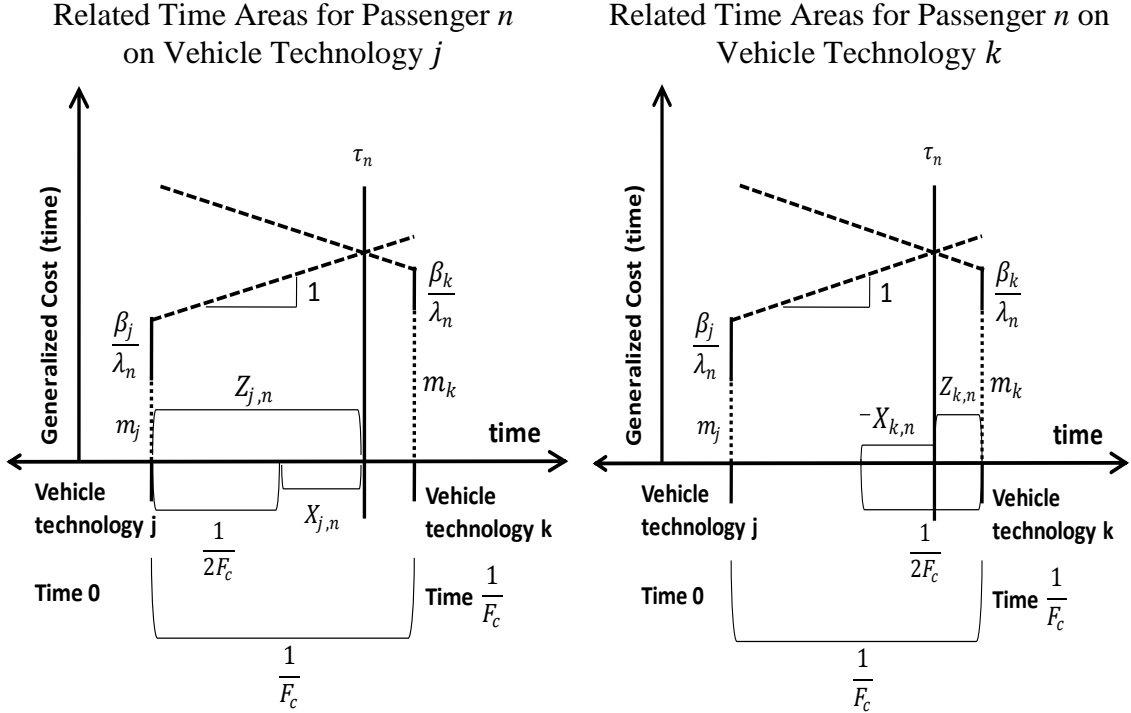


Figure 4.2 Generalized cost (time) and related quantities for the mixed vehicle case, passenger scenario 1.

We can now define values for $P(V_i)$ and $P(R_n|V_i)$. By the total probability theorem, the unconditional probability of a passenger being on vehicle type i , $P(V_i)$, is the sum of the conditional probability that a passenger is assigned vehicle type i given they are of type n , $P(V_i|R_n)$, multiplied by the probability they are a passenger of type n , $P(R_n)$. $P(V_i|R_n)$ is the ratio of the passenger vehicle assignment region for passengers of type n on vehicle i and the headway. This is the passenger assignment region divided by the vehicle headway: $P(V_i|R_n) = FZ_{i,n}$. It directly follows from the above definitions that $P(R_n) = \frac{Q_n}{Q_t}$.

$$P(V_i) = \sum_n P(V_i|R_n)P(R_n) = \frac{F \sum_n Q_n Z_{i,n}}{Q_t} \quad (4.3)$$

From Bayes' theorem, the conditional probability that a passenger is of type n given they are on vehicle type i , $P(R_n|V_i)$, is the ratio of passengers of type n assigned to vehicle type i to the total passengers assigned to vehicle type i .

$$P(R_n|V_i) = \frac{Q_n Z_{i,n}}{\sum_m Q_m Z_{i,m}} \quad (4.4)$$

Recall that the supplier cost associated with each operation is $\alpha_i + \beta_i s_i$, where s_i is the number of seats per departure on vehicle type i . Assuming a load factor of one, the seats per operation is equal to the number of passengers on each vehicle

$$s_i = Q_t P(V_i) \quad (4.5)$$

Having determined these relationships, we can now specify the total logistics cost per passenger for the single and the mixed vehicle case.

4.2.1 Single Vehicle Fleets

For single vehicle fleets, we define the objective function as the total logistics cost of an intercity transportation corridor served by a vehicle i where $i \in I$. The difference in cost between the two vehicles whose departures bound the headway is zero, as they are identical. Also, when considering single vehicle fleets, vehicle headways are simply the inverse of frequency. It follows that the expected passenger wait time is independent of passenger group n and simply one-quarter of the inverse of frequency (4.6).

$$w_{i,n} = \frac{1}{4F_i} \quad (4.6)$$

The objective function is to minimize the total logistics cost per passenger. It will be convenient to superscript the decision variable and the total logistics cost (TLC) at optimal frequency with the passenger scenario and the letter b to designate base case: F_i^{1-b} and z_i^{1-b} .

The TLC is defined by the following:

$$\begin{aligned} z_i^{1-b} &= \frac{F_i^{1-b} \alpha_i}{Q_t} + P(V_i) \left(\beta_i + \frac{\sum_n \lambda_n Q_n \left(m_i + \frac{1}{4F_i^{1-b}} \right)}{Q_t} \right) \\ &= \frac{F_i^{1-b} \alpha_i}{Q_t} + \beta_i + \frac{1}{Q_t} \sum_n \lambda_n Q_n \left(m_i + \frac{1}{4F_i^{1-b}} \right) \end{aligned} \quad (4.7)$$

In this function, two costs are related to the decision variable F_i^{1-b} . The fixed supplier cost is positively related to the decision variable (more vehicle operations, higher fixed cost), while the passenger cost is negatively related to F_i^{1-b} (increased vehicle operations reduces schedule delay). Daganzo (1999) discusses this cost tradeoff in the logistics literature, where the decision variable is the shipment size (termed the Economic Order Quantity (EOQ)). The formulation of (4.7) defines the decision variable as the frequency of “shipments” or vehicle operations.

As the total logistics cost function is non-linear and convex, we can determine the optimal value of frequency:

$$F_i^{1-b*} = \left(\frac{\sum_n \lambda_n Q_n}{4\alpha_i} \right)^{\frac{1}{2}} \quad (4.8)$$

Which is a true minimum as $\frac{d^2 z_i}{d(F_i^{1-b})^2} = \frac{\sum_n \lambda_n Q_n}{2(F_i^{1-b})^3} > 0$.

The frequency that minimizes TLC is inversely proportional to fixed vehicle cost and positively related to passenger flow and value of time, capturing the EOQ tradeoff costs.

We can now develop a function for the vehicle-specific TLC per passenger at optimal frequency.

$$z_i^{1-b^*} = \beta_i + \frac{(\sum_n \alpha_i \lambda_n Q_n)^{\frac{1}{2}} + \sum_n m_i \lambda_n Q_n}{Q_t} \quad (4.9)$$

The quantity $(\sum_n \alpha_i \lambda_n Q_n)^{\frac{1}{2}}$ and the value of optimal frequency (4.8) represent the primary competing forces in intercity transportation: economies of scale and passenger preference for customized service. As fixed costs increase, then, all else equal, frequency decreases, because of the greater cost penalty for operating more flights. Conversely, as passenger value of time and/or demand increases, then, all else equal, frequency of operations increase as passengers – either individually or collectively – derive more value from frequent service.

4.2.2 Mixed Vehicle Fleets

The objective function is now for the total logistics cost of an intercity transportation corridor served by vehicles in set C . The decision variable is the frequency of the mixed vehicle fleet per unit time which, following the deployment assumption above, is equally divided across the two available vehicle types (identified by j and k hereafter). For each vehicle pair, the following inequalities are assumed to hold: $\beta_j \geq \beta_k, m_k \geq m_j$.

The notation for the decision variable is F_c^{1-a} , where 1 is the passenger scenario and a corresponds to the case number $a \in A = \{b, 1, 2, 3, 4, 5\}$. The following case will be designated the base case (b) for passenger scenario 1 and the key quantities will be designated F_c^{1-b} for the decision variable and z_c^{1-b} for the objective function.

We begin building the objective function assuming that a non-zero fraction of each passenger group is assigned to each of the two vehicle types. This means that no passenger group can have a *time interval for departure* that exceeds a full headway, which leads to the following condition in order for the objective function to be valid:

$$\left| \frac{1}{2X_{i,n}} \right| \geq F_c^{1-b}; \forall i, n \quad (4.10)$$

Cases $a = \{1, 2, 3, 4, 5\}$ for which this assumption is violated are discussed in the following section.

The supplier cost per passenger of the mixed vehicle fleet is $\sum_{i \in c} \frac{\alpha_i F_c^{1-b}}{2Q_t} + \beta_i P(V_i)$. The passenger cost is a function of the fraction of passengers of each type n on each vehicle type i , $P(V_i)P(R_n|V_i)$, and the passenger cost incurred by passengers of each group on that aircraft type, $\lambda_n(m_i + \bar{w}_{i,n})$. Thus, the passenger cost expression is $\sum_{i \in c} P(V_i) \sum_n P(R_n|V_i) \lambda_n(m_i + w_{i,n})$. By summing the passenger and supplier cost expressions, we achieve the objective function, the total logistics cost per unit time for the mixed technology case:

$$\begin{aligned}
z_c^{1-b} &= \sum_{i \in c} P(V_i) \left(\frac{\alpha_i F_c^{1-b}}{2P(V_i)Q_t} + \beta_i + \sum_n \lambda_n P(R_n|V_i) (m_i \right. \\
&\quad \left. + w_{i,n}) \right) \\
&= \sum_{i \in c} \left(\frac{\alpha_i F_c^{1-b}}{2Q_t} \right. \\
&\quad \left. + \frac{F_c^{1-b} (\sum_n Q_n Z_{i,n})}{Q_t} \left(\beta_i \right. \right. \\
&\quad \left. \left. + \sum_n \lambda_n \frac{Q_n Z_{i,n}}{\sum_m Q_m Z_{i,m}} \left(m_i + \frac{1}{4F_c^{1-b}} + \frac{X_{i,n}}{2} \right) \right) \right)
\end{aligned} \tag{4.11}$$

We now find the value of F_c^{1-b} that minimizes z_c . The optimum frequency is thus:

$$F_c^{1-b*} = \left(\frac{\sum_n \lambda_n Q_n}{2(\sum_{i \in c} \alpha_i - 2 \sum_n \lambda_n Q_n X_{jn}^2)} \right)^{\frac{1}{2}} \tag{4.12}$$

Which is a true minimum as $\frac{d^2 z_c^{1-b}}{d(F_c^{1-b})^2} = \frac{\sum_n \lambda_n Q_n}{2Q_t (F_c^{1-b})^3} > 0$.

The frequency that minimizes TLC is related to the sum of the fixed vehicle cost, passenger value of time, and the flow of passengers, reflecting the EOQ tradeoff. In this way, the optimal frequency is similar in the single and mixed vehicle cases. However, in the mixed case we also have a function of the assignment areas in the form of the generalized cost (time) differential X_{jn} . If $X_{jn}^2 = 0$, such that the vehicle have the same travel time and variable cost, and α_i is constant $\forall i$, then $F_c^{1-b*} = F_i^{1-b*}$. If $X_{jn}^2 \neq 0$ and α_i is constant $\forall i$, as the difference in generalized cost increases, the interpretation is that schedule delay is more onerous than travel time for passenger group n . Passengers in group n are less willing to wait for a particular vehicle, and therefore, the overall frequency increases.

Using F_c^{1-b*} we achieve a function for the minimum total logistics cost of a mixed vehicle fleet. The total logistics cost function at optimality shown in (4.13), again with a component capturing the trade between fixed cost and passenger value of time:

$$\begin{aligned}
&z_c^{1-b*} \\
&= \frac{\sum_n (\sum_i \beta_i + \lambda_n \sum_i m_i) Q_n + (2 \sum_n \lambda_n Q_n)^{\frac{1}{2}} (\sum_{i \in c} \alpha_i - 2 \sum_n \lambda_n Q_n X_{jn}^2)^{\frac{1}{2}}}{2Q_t}
\end{aligned} \tag{4.13}$$

Two components of this function that are directly related to two components of the single vehicle total logistics cost function: $\frac{\sum_i m_i \sum_n Q_n \lambda_n}{2Q_t}$, $\frac{\sum_i \beta_i}{2}$. Simply replacing m_i, β_i in the

single vehicle total logistics cost function with the weighted average of each value yields these two components, showing the similarity of the two functions. However, the function incorporates the generalized cost differential. As the generalized cost differential increases, the contribution of passenger flow and value of time decreases, as passengers are, if $X_{j,n}^2 \neq 0$, experiencing reduced schedule delay.

The optimal solution is (4.13) when conditions outlined in (4.10) are met; we term this the base case. However, there are five ways that these conditions can be violated. These groups are presented in two categories due to their similarities. Upon determining that the conditions in (4.10) are violated with the optimal value of frequency in (4.12), the appropriate case is determined using the optimal value of frequency $F_c^{1-b^*}$. Recall the case designation a , where a corresponds to the case number $a \in A = \{b, 1, 2, 3, 4, 5\}$. Case $a=b$ designates the “base case” when the conditions in (4.10) are met.

Group 1: All passengers on one vehicle type

Case 1-1 $F_c^{1-b^*} > \frac{1}{2X_{j,n}} > 0 \forall n$: All passengers assigned to vehicle type j

Case 1-2 $F_c^{1-b^*} > \left| \frac{1}{2X_{j,n}} \right|$ and $\frac{1}{2X_{j,n}} < 0 \forall n$: All passengers assigned to vehicle type k

Group 2: Some passengers are divided between vehicles

Assuming two vehicle types $i \in \{j, k\}$ and two passenger types $n \in \{l, h\}$

Case 1-3 $F_c^{1-b^*} > \left| \frac{1}{2X_{j,h}} \right|$ and $F_c^{1-b^*} < \left| \frac{1}{2X_{j,l}} \right|$: All passengers of type h are assigned to vehicle type j

Case 1-4 $F_c^{1-b^*} > \left| \frac{1}{2X_{j,l}} \right|$ and $F_c^{1-b^*} < \left| \frac{1}{2X_{j,h}} \right|$: All passengers of type l are assigned to vehicle type k

Case 1-5 $F_c^{1-b^*} > \left| \frac{1}{2X_{j,n}} \right| \forall n$ and $\frac{1}{2X_{j,n}} < 0 \forall n$: All passengers of type l are assigned to vehicle type k , and all passengers of type h are assigned to vehicle type j

A new function is developed for each case and a new optimal frequency determined, which is considered in the following sections.

Case 1-1 and 1-2

In case 1-1 and 1-2 there are no passengers divided between vehicle types, and all passengers are simply assigned to one vehicle type. These bounds represent the limitation of the assumption that passengers must be served in the headway in which they desire to depart. In the mixed vehicle case, when τ_n occurs *earlier than* the departure time of vehicle type j for all passenger groups n , the physical interpretation is that all passengers are willing to wait longer than a full headway for Vehicle k (case 1-1). Hence, $F_c^{1-b^*} > \frac{1}{2X_{j,n}} > 0; \forall n$. Case 1-2 is when τ_n is *later than* the departure time of Vehicle k for all passenger groups n , and passengers are willing to wait longer than a full headway for

Vehicle j . The mathematical representation of case 1-2 is $F_c^{1-b^*} > \left| \frac{1}{2X_{j,n}} \right|$ and $\frac{1}{2X_{j,n}} < 0; \forall n$. These two cases are illustrated in Figure 4.3.

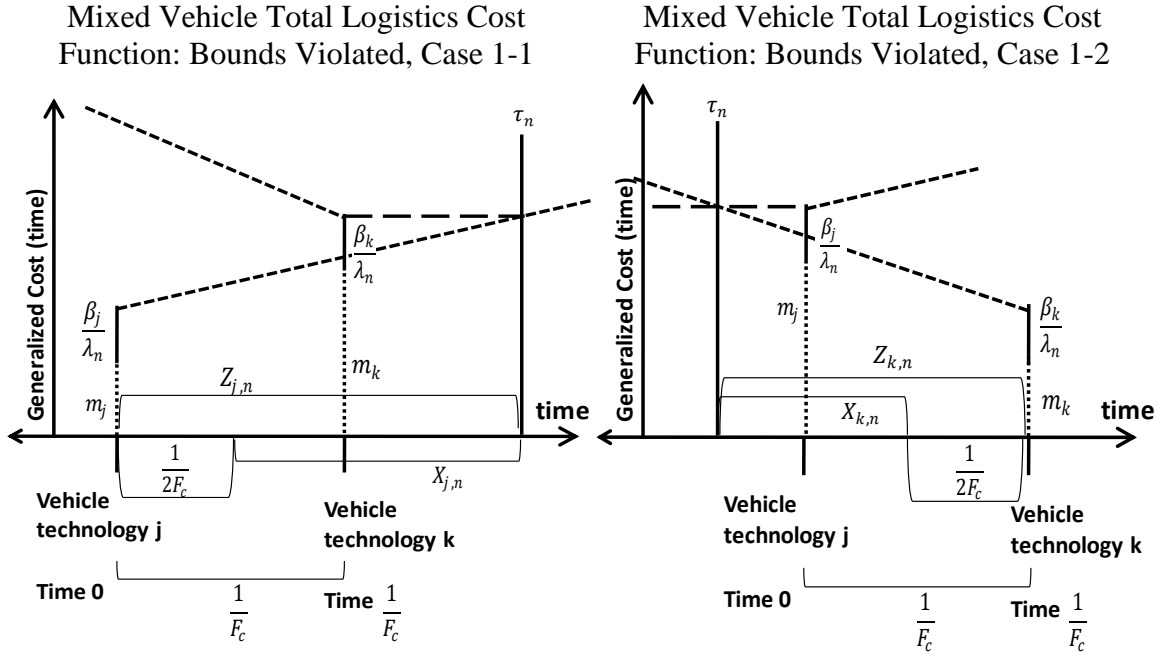


Figure 4.3 Generalized cost (time) and related quantities under the violated passenger assignment assumption, Case 1-1 and 1-2.

We can define a new total logistics cost function based on each of these two cases. In fact, except for a change of index, the function for both cases is the same. Define index i so that for case 1-1 $i=j$ and for case 1-2 $i=k$. The decision variable at optimality for case 1-1 is $F_c^{1-1^*}$, for case 1-2 $F_c^{1-2^*}$. The supplier cost is based on the fixed cost of both vehicles and the variable cost of the vehicle to which all passengers are assigned. Since all passengers are assigned to one vehicle, the expected value of schedule delay is one-half the headway, and the travel time is that of the vehicle to which all passengers are assigned.

$$z_c^{1-a} = \frac{\sum_{i \in C} \alpha_i F_c^{1-a}}{2Q_t} + \beta_i + \frac{\sum_n \lambda_n Q_n}{Q_t} \left(m_i + \frac{1}{2F_c^{1-a}} \right); a = \{1, 2\} \quad (4.14)$$

Similarly to (4.12), the frequency that minimizes (4.14) is:

$$F_c^{1-a^*} = \left(\frac{\sum_n \lambda_n Q_n}{\sum_{i \in C} \alpha_i} \right)^{\frac{1}{2}}; a = \{1, 2\} \quad (4.15)$$

Which is a true minimum as $\frac{d^2 z_c^{1-a}}{d(F_c^{1-a})^2} = \frac{\sum_n \lambda_n Q_n}{2Q_t (F_c^{1-a})^3} > 0$.

We expect the optimal frequency to resemble the optimal frequency from the single vehicle cost, as the schedule delay is equal in both cases. We find the TLC at optimal frequency to be a simple function of the variable cost and travel time on vehicle i and the sum of the fixed costs.

$$z_c^{1-a^*} = \frac{(\sum_{i \in c} \alpha_i (\sum_n \lambda_n Q_n))^{\frac{1}{2}} + m_i \sum_n \lambda_n Q_n}{Q_t} + \beta_i; a = \{1, 2\} \quad (4.16)$$

Case 1-1 and 1-2 are virtually the single vehicle case, as all passengers are assigned to one vehicle. The difference is in the sum of the fixed costs, which is reflected in the total logistics cost at optimal frequency. In further similarity to the single vehicle case, as passengers are directly assigned to vehicles, the solution is valid over the entire range. Therefore, cases 1.1 and 1.2 are terminal cases.

We note that for cases 1-1 and 1-2 the mixed fleet is never optimal, since the costs could be further reduced by not operating the class of vehicles that are empty. We present this “degenerate case” mainly for completeness.

Case 1-3 1-4, and 1-5

In cases 1-3; 1-4; and 1-5; we restrict our attention to cases with two passenger groups, one with a low value of time (indexed l) and the other with a high value of time (indexed h), so $\lambda_h > \lambda_l$. In case 1-3 and 1-4, one group of passengers $n \in \{l, h\}$ will divide between vehicle types while the other will not. In case 1-5, there are no passengers of type l assigned to vehicle type j , and no passengers of type h assigned to vehicle type k .

Case 1-3

In case 1-3 a passenger of type h experiences $Z_{j,h}$, the assignment area for a vehicle of type j , which is longer than a full headway, such that $F_c^{1-b^*} > \left| \frac{1}{2X_{j,h}} \right|$. Passengers of type l are divided between the two vehicle types such that $F_c^{1-b^*} < \left| \frac{1}{2X_{j,l}} \right|$. Case 1-3 is illustrated by Figure 4.4. Case 1-4 is very similar, with passengers of type h divided between vehicles ($F_c^{1-b^*} < \left| \frac{1}{2X_{j,h}} \right|$) and passengers of type l experiencing an assignment area for vehicle type k , $Z_{k,l}$, such that $F_c^{1-b^*} > \left| \frac{1}{2X_{j,l}} \right|$.

Mixed Vehicle Total Logistics Cost Function: Bounds Violated, Case 1-3

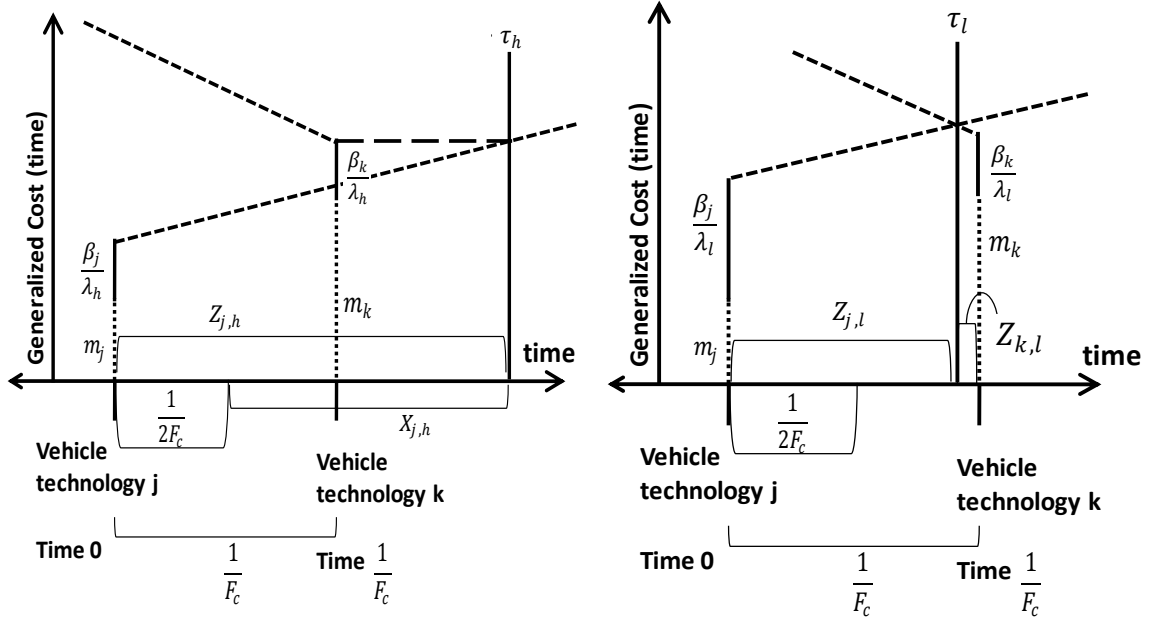


Figure 4.4 Generalized cost (time) and related quantities under the violated passenger assignment assumption, Case 1-3.

In case 1-3 there are no passengers of type h on vehicle type k . We need a new expression for $P(V_i)$, the proportion of passengers on vehicle type i . All passengers of type h are on vehicle type j and all passengers of type l who desire to depart in the assignment period $Z_{j,l}$ are on vehicle type j . Passengers of type l who desire to depart in assignment period $Z_{k,l}$ are on vehicle k . Hence:

$$P(V_j) = \frac{(Q_h + F_c^{1-3} Z_{j,l} Q_l)}{Q_t} \quad (4.17)$$

$$P(V_k) = \frac{(F_c^{1-3} Z_{k,l} Q_l)}{Q_t}$$

We also define the conditional probability that a passenger is assigned to vehicle type i given they are of type n :

$$P(V_j|R_h) = 1; P(V_k|R_h) = 0$$

$$P(V_i|R_l) = \frac{F_c^{1-3} Z_{i,l} Q_l}{Q_t} \quad (4.18)$$

We write the final total logistics cost function:

$$z_c^{1-3} = \sum_{i \in c} \left(\frac{\alpha_i F_c^{1-3}}{2Q_t} + P(V_i)\beta_i + P(V_i|R_l)\lambda_l(m_i + w_{i,l}) \right) + \frac{Q_h \lambda_h}{Q_t} \left(m_j + \frac{1}{2F_c^{1-3}} \right) \quad (4.19)$$

And the optimal frequency:

$$F_c^{1-3*} = \left(\frac{\lambda_h Q_h + \frac{\lambda_l Q_l}{2}}{\left(\sum_{i \in c} \alpha_i - 2X_{jl}^2 \lambda_l Q_l \right)} \right)^{\frac{1}{2}} \quad (4.20)$$

Which is a true minimum as $\frac{d^2 z_c^{1-3}}{d(F_c^{1-3})^2} = \frac{\lambda_h Q_h + \frac{\lambda_l Q_l}{2}}{(F_c^{1-3})^3 Q_t} > 0$.

We find the total logistics cost at optimal frequency by substituting for F_c^{1-3*} :

$$z_c^{1-3*} = \frac{1}{2Q_t} \left(Q_l \left(\sum_i \beta_i + \lambda_l m_i \right) + 2Q_h (\beta_j + \lambda_h m_j) + \left(2(2\lambda_h Q_h + \lambda_l Q_l) \left(\sum_{i \in c} \alpha_i - 2X_{jl}^2 \lambda_l Q_l \right) \right)^{\frac{1}{2}} \right) \quad (4.21)$$

We have the same components as the single vehicle case, yet the costs related to passengers of type h are weighted more heavily. These passengers do not divide between vehicle types, and their expected schedule delay is greater than for passengers of type l .

The bounds on this function are related to (4.10), such that $\left| \frac{1}{2X_{i,l}} \right| \geq F_c^{1-3*} \forall i$. If this holds, then case 1-3 is the optimal mixed vehicle case. It is possible that, upon solving for optimal frequency F_c^{1-3*} , that $\left| \frac{1}{2X_{i,l}} \right| < F_c^{1-3*} \forall i$. If this occurs, passengers of type l are no longer divided between vehicle types. Therefore, all passengers of type h are on vehicle type j , and all passengers of type l are on vehicle type j or k . Using the new value for optimal frequency F_c^{1-3*} , we determine which case, 1-1 or 1-5, to which the value of F_c^{1-3*} belongs.

In case 1-1 no passengers are assigned to vehicle type k . This is the case to be executed if $F_c^{1-3*} > \frac{1}{2X_{j,l}} > 0$.

In case 1-5, no passengers of type l are assigned to vehicle type j , and no passengers of type h are assigned to vehicle type k . This is the case to be executed if $F_c^{1-3^*} > \left\lfloor \frac{1}{2X_{j,l}} \right\rfloor$ and $\frac{1}{2X_{j,l}} < 0$.

As these two alternative cases are terminal cases, solving for case 1-1 or 1-5 would be the final step.

Case 1-4

In case 1-4, there are no passengers of type l on vehicle type j , as $F_c^{1-b^*} > \left\lfloor \frac{1}{2X_{j,l}} \right\rfloor$, and passengers of type h are split between vehicle types as $F_c^{1-b^*} < \frac{1}{2X_{j,h}}$. We need a new expression the quantities for $P(V_i)$. All passengers of type l in one headway are on vehicle type k . All passengers of type h who desire to depart in the assignment period $Z_{j,h}$ are on vehicle type j . Passengers of type h who desire to depart in assignment period $Z_{k,h}$ are on vehicle of type k . Hence:

$$P(V_j) = \frac{(F_c^{1-4} Z_{j,h} Q_h)}{Q_t} \quad (4.22)$$

$$P(V_k) = \frac{(Q_l + F_c^{1-4} Z_{k,h} Q_h)}{Q_t}$$

We also need the conditional probability that a passenger is assigned to vehicle type i given they are of type n :

$$P(V_i|R_h) = \frac{F_c^{1-4} Z_{i,h} Q_h}{Q_t} \quad (4.23)$$

$$P(V_j|R_l) = 0; P(V_k|R_l) = 1$$

We can write the final total logistics cost function:

$$z_c^{1-4} = \sum_{i \in c} \left(\frac{\alpha_i F_c^{1-4}}{2Q_t} + P(V_i) \beta_i + P(V_i|R_h) \lambda_h (m_i + w_{i,h}) \right) + \frac{Q_l \lambda_l}{Q_t} \left(m_k + \frac{1}{2F_c^{1-4}} \right) \quad (4.24)$$

And the optimal frequency:

$$F_c^{1-4^*} = \left(\frac{\lambda_l Q_l + \frac{\lambda_h Q_h}{2}}{\sum_{i \in c} \alpha_i - 2X_{jh}^2 \lambda_h Q_h} \right)^{\frac{1}{2}} \quad (4.25)$$

Which is a true minimum as $\frac{d^2 z_c^{1-4}}{d(F_c^{1-4})^2} = \frac{\lambda_l Q_l + \frac{\lambda_h Q_h}{2}}{(F_c^{1-4})^3 Q_t} > 0$.

We find the total logistics cost at optimal frequency:

$$z_c^{1-4*} = \frac{1}{2Q_t} \left(Q_h \left(\sum_i \beta_i + \lambda_h m_i \right) + 2Q_l (\beta_k + \lambda_l m_k) \right. \\ \left. + \left(2(2\lambda_l Q_l + \lambda_h Q_h) \left(\sum_{i \in c} \alpha_i - 2X_{jh}^2 \lambda_h Q_h \right) \right)^{\frac{1}{2}} \right) \quad (4.26)$$

Again we have the same components as the single vehicle case, yet the costs related to passengers of type l are weighted more heavily. These passengers do not divide between vehicle types, and their expected schedule delay is greater than for passengers of type h .

Similar to case 1-3 it is possible that, upon solving for optimal frequency F_c^{1-4*} , that $\left| \frac{1}{2X_{i,h}} \right| \geq F_c^{1-4*} \forall i$. If this occurs, passengers of type h are no longer divided between vehicle types. All passengers of type l are on vehicle type k , and all passengers of type h are on one vehicle type. Using F_c^{1-4*} , we determine which case, 1-2 or 1-5, for which the value of F_c^{1-4*} conforms.

In case 1-2 no passengers are assigned to vehicle type j . This is the case if $F_c^{1-4*} > \left| \frac{1}{2X_{j,h}} \right|$ and $\frac{1}{2X_{j,h}} < 0$.

In case 1-5, no passengers of type l are assigned to vehicle type j , and no passengers of type h are assigned to vehicle type k . This case occurs if $F_c^{1-4*} > \frac{1}{2X_{j,h}} > 0$.

As these two alternative cases are terminal cases, solving for case 1-2 or 1-5 would be the final step.

Case 1-5

In case 1-5, there are no passengers of type l assigned to the fast, expensive, vehicle type j , and no passengers of type h assigned to the slow, inexpensive, vehicle type k .

Therefore, the optimal frequency $F_c^{1-4*} > \left| \frac{1}{2X_{j,n}} \right|, n \in \{l, h\}$. In this case, illustrated by

Figure 4.5, a passenger of type h has a $Z_{j,h}$ that is longer than a full headway, and likewise for $Z_{k,l}$ for passengers of type l .

Mixed Vehicle Total Logistics Cost Function: Bounds Violated, Case 1-5

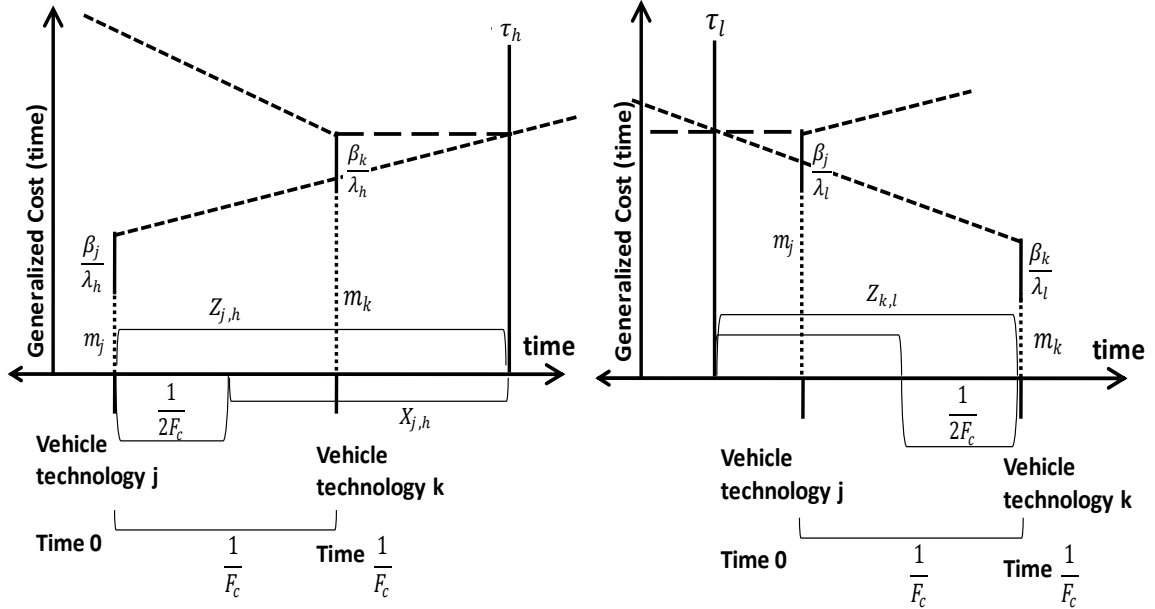


Figure 4.5 Generalized cost (time) and related quantities under the violated passenger assignment assumption, Case 1-5.

The total logistics cost function for case 1-5 reflects the fact that both passenger groups are assigned to dedicated vehicles. Therefore, the expected value of schedule delay is one-half the headway, and the travel time for a group is simply that of the vehicle to which it is assigned.

$$z_c^{1-5} = \frac{\sum_{i \in c} \alpha_i F_c^{1-5}}{2Q_t} + \frac{Q_h}{Q_t} \left(\beta_j + \lambda_h \left(m_j + \frac{1}{2F_c^{1-5}} \right) \right) + \frac{Q_l}{Q_t} \left(\beta_k + \lambda_l \left(m_k + \frac{1}{2F_c^{1-5}} \right) \right) \quad (4.27)$$

The frequency that minimizes z_c^{1-5} is identical to F_c^{1-1*} and F_c^{1-2*} :

$$F_c^{1-5*} = \left(\frac{\sum_n \lambda_n Q_n}{\sum_{i \in c} \alpha_i} \right)^{\frac{1}{2}} \quad (4.28)$$

Which is a true minimum as $\frac{d^2 z_c^{1-5}}{d(F_c^{1-5})^2} = \frac{\sum_n \lambda_n Q_n}{2(F_c^{1-5})^3 Q_t} > 0$.

The frequency is identical to F_c^{1-1*} and F_c^{1-2*} because in these three cases the schedule delay is equal for all groups, as is the fixed cost. We find the TLC at optimal frequency to be a simple function of the variable cost and travel time on each vehicle i incurred separately by each passenger group and the sum of the fixed costs. This is again very similar to cases 1-1 and 1-2 except that here only passengers of type h incur costs related to vehicle type j while passengers of type l incur costs related to vehicle type k .

$$z_c^{1-5*} = \frac{(\sum_{i \in c} \alpha_i \sum_n \lambda_n Q_n)^{\frac{1}{2}}}{Q_t} + \frac{Q_h}{Q_t} (\beta_j + \lambda_n m_j) + \frac{Q_l}{Q_t} (\beta_k + \lambda_l m_k) \quad (4.29)$$

Passenger groups are assigned to dedicated vehicles in this case, so the concept of assignment region does not apply. Therefore, case 1-5 is a terminal case.

Now that the single vehicle case, the mixed vehicle base case, and the five alternative mixed vehicle cases are solved, we present the solution algorithm.

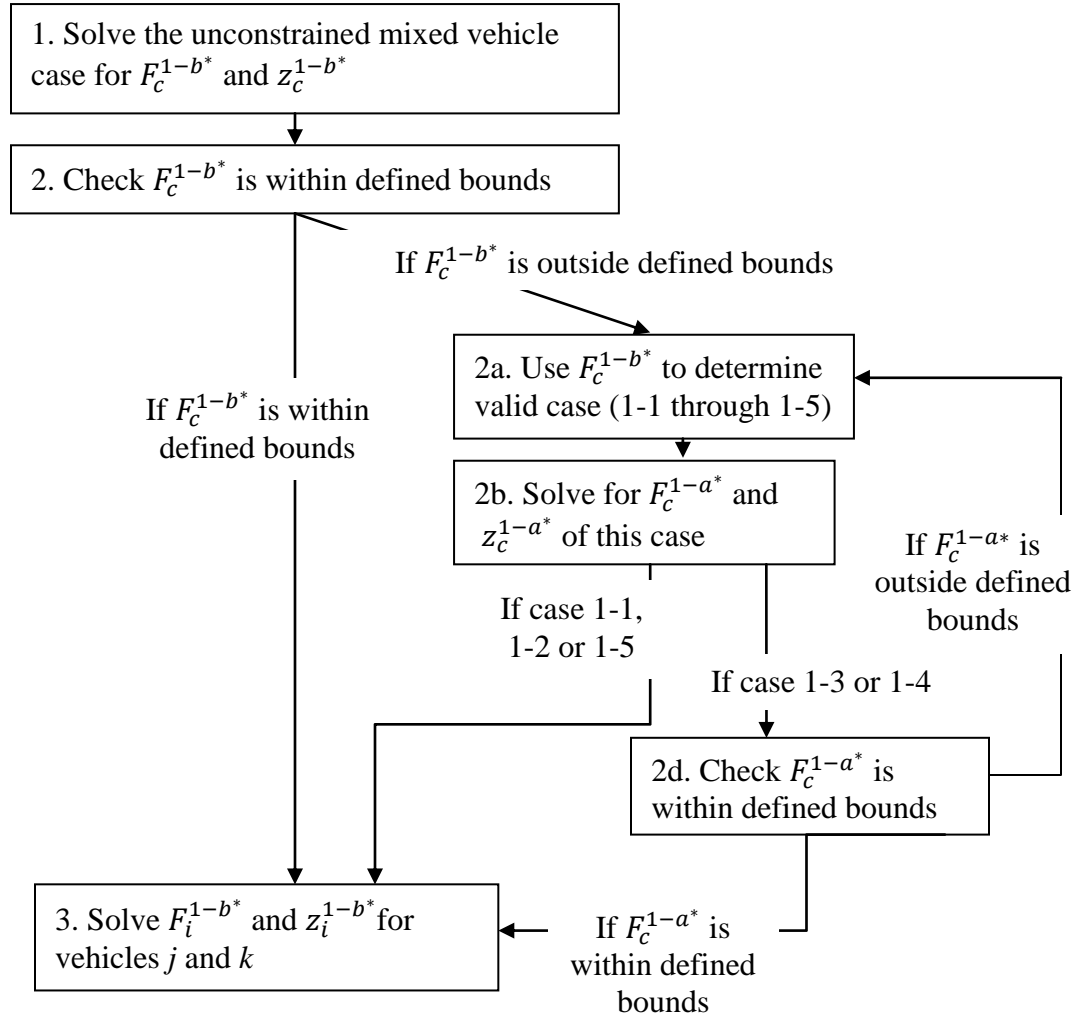


Figure 4.6 Passenger scenario 1 solution algorithm.

Upon solving for $z_i^{1-b*} \forall i$ (single vehicle case), and z_c^{1-a*} through the solution algorithm, we find the minimum total logistics cost combination (either single or mixed) by enumeration. In solving this function we are looking for the technology mix of both technology size and type that minimizes cost across all potential mixes.

If case 1-3, 1-4, or 1-5 occurs, it may be beneficial from a cost perspective to integrate the single and mixed vehicle cases such that all headways are not bound by vehicles of the same technology. This will be explored in passenger scenario 3, section 4.4.

4.3 Total Logistics Cost Models for Passenger Scenario Two

In passenger scenario 2 rather than having discrete passenger groups, we assume that passengers have a value of time that follows a continuous distribution. We consider that at each point t , a passenger will be assigned one of the two vehicle departures that bound the headway in which they desire to depart. They will be assigned based on their value of time, such that at each point t there is a breakeven value of time $\lambda(t)$. We define notation for parameters and decision variables:

Parameters:

α_i	Vehicle fixed cost, \$/Operation
β_i	Vehicle variable cost, \$/Passenger
m_i	In-vehicle travel time, Time/Passenger
Q	Total flow of passengers, Passenger/Time
t	Time
$\lambda(t)$	Indifference value of passenger time, \$/Passenger – Time
λ_1, λ_2	Minimum and maximum values for the distribution of value of time
$F(\lambda(t))$	Probability a passenger has a value of time below $\lambda(t)$

Decision Variable:

The decision variable is vehicle frequency, F , for the two possible vehicle combinations:

F_i	Vehicle frequency (single technology combination), Operations/Time
F_c	Vehicle frequency (mixed technology combination), Operations/Time

4.3.1 Single Vehicle Fleet

Consider one headway with a time of the first vehicle departure at 0 and the second vehicle departure at $\frac{1}{F_i}$, as shown in Figure 4.7. Both vehicles have the same non-schedule delay component, $m_i + \frac{\beta_i}{\lambda}$ for a passenger with value of time λ . Therefore, passengers who fall in $t, 0 \leq t \leq \frac{1}{2F_i}$ will be assigned to the vehicle that departs at time 0; passengers with $t, \frac{1}{2F_i} \leq t \leq \frac{1}{F_i}$, will be assigned to the vehicle that departs at $\frac{1}{F_i}$.

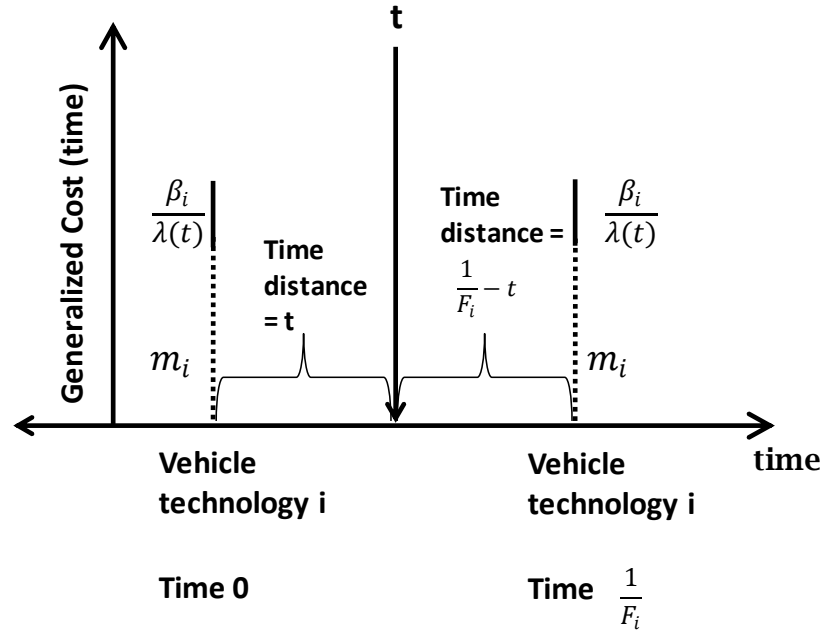


Figure 4.7 Generalized cost (time) and related quantities for the single vehicle case, passenger scenario 2.

The supplier cost per passenger has the same form as in (4.7). Using the superscript with the passenger scenario 2 and the base case designator, the number of passengers on each vehicle is $\frac{Q}{F_i^{2-b}}$. The supplier cost per passenger is the sum of the fixed and the variable cost per passenger.

$$\frac{F_i^{2-b} \alpha_i}{Q} + \beta_i \quad (4.30)$$

If value of time and desired departure time are independently and uniformly distributed, then the expected value of λ is a function of the upper (λ_2) and lower (λ_1) bounds. Because we are considering passenger cost on a per passenger basis, we consider the cost incurred by a passenger, $\frac{\lambda_2 + \lambda_1}{2} (m_i + t)$, over each time slice t weighted by the probability a passenger arrives at time t , F_i^{2-b} .

$$\int_0^{\frac{1}{F_i^{2-b}}} F_i^{2-b} \left(\frac{\lambda_2 + \lambda_1}{2} \right) (m_i + t) dt \quad (4.31)$$

The objective function is the sum of (4.30) and (4.31).

$$z_i^{2-b} = \frac{F_i^{2-b} \alpha_i}{Q} + \beta_i + \left(\frac{\lambda_2 + \lambda_1}{2} \right) \left(\frac{1}{2F_i^{2-b}} + m_i \right) \quad (4.32)$$

The total logistics cost function is non-linear and convex, and again we can determine the optimal value of frequency by minimizing z_i^{2-b} over the decision variable F_i^{2-b} .

$$F_i^{2-b*} = \left(\frac{Q(\lambda_2 + \lambda_1)}{4\alpha_i} \right)^{\frac{1}{2}} \quad (4.33)$$

Which is a true minimum as $\frac{d^2 z_i^{2-b}}{d(F_i^{2-b})^2} = \frac{\lambda_2}{4(F_i^{2-b})^3} > 0$.

The frequency that minimizes TLC under passenger scenario 2 is strongly reminiscent of the frequency that minimizes TLC under passenger scenario 1 (4.8). The optimum frequency depends on fixed vehicle cost, passenger flow, and the bounds on passenger value of time, again reflecting the EOQ tradeoff costs. We can now develop a function for the vehicle-specific TLC per passenger at optimal frequency, that is related to (4.9).

$$z_i^{2-b*} = \left(\frac{\alpha_i(\lambda_2 + \lambda_1)}{Q} \right)^{\frac{1}{2}} + \beta_i + \frac{m_i(\lambda_2 + \lambda_1)}{2} \quad (4.34)$$

As in (4.9), we see that the quantity $\alpha_i(\lambda_2 + \lambda_1)$ represents the trade between economies of scale and passenger preference for customized service.

4.3.2 Mixed Vehicle Fleet

In the mixed vehicle case, a passenger who desires to depart at time t , $0 \leq t \leq \frac{1}{F_c}$, will be assigned to either a vehicle of type k or j . We assume value of time and desired departure time are independently and uniformly distributed and consider a value of time unique to each departure time t for which passengers who arrive at t are indifferent to both vehicle types. This is termed the indifference value of time, $\lambda(t)$. The generalized cost of a passenger desiring to depart at time t is the sum of the vehicle travel time, m_i , the variable cost divided by the indifference value of time, $\frac{\beta_i}{\lambda(t)}$, and the schedule delay. The schedule delay is for a passenger who desires to depart at t would be t for vehicle type k or $\frac{1}{F_c} - t$ for vehicle type j (Figure 4.8). We find the indifference value of time (as a function of t) by setting the generalized cost incurred by a passenger on either vehicle to be equal:

$$m_k + \frac{\beta_k}{\lambda(t)} + t = m_j + \frac{\beta_j}{\lambda(t)} + \frac{1}{F_c^{2-b}} - t \quad (4.35)$$

$$\lambda(t) = \frac{\beta_j - \beta_k}{m_k - m_j + 2t - \frac{1}{F_c^{2-b}}} \quad (4.36)$$

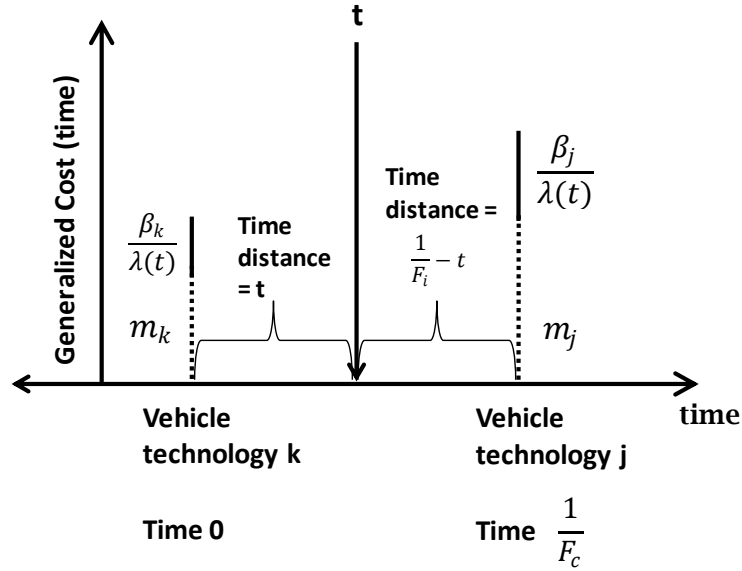


Figure 4.8 Generalized cost (time) and related quantities for the mixed vehicle case for passenger scenario 2.

A headway with a departure at $t = 0$ of vehicle type k and a departure at $t = \frac{1}{F_c}$ of vehicle type j is identical to a headway with the opposite vehicle departure profile. Therefore, we consider the headway shown in Figure 4.8 to be representative for the entire corridor.

Because passenger value of time follows a distribution, the probability that a passenger has a value of time below the critical value is the cumulative distribution function at $\lambda(t)$, $F(\lambda(t))$. The remaining $1 - F(\lambda(t))$ is the fraction of passengers with a time value greater than the indifference value of time.

As we consider passenger value of time to follow a uniform distribution, the following hold:

$$E(\lambda|\lambda < \lambda(t)) = \frac{\lambda(t) + \lambda_1}{2} \quad \lambda_1 < \lambda(t) < \lambda_2 \quad (4.37)$$

$$E(\lambda|\lambda > \lambda(t)) = \frac{\lambda(t) + \lambda_2}{2}$$

$$F(\lambda(t)) = \frac{\lambda(t) - \lambda_1}{\lambda_2 - \lambda_1} \quad \lambda_1 < \lambda(t) < \lambda_2 \quad (4.38)$$

In considering $\lambda(t)$ over the range $\lambda_1 < \lambda(t) < \lambda_2$ we are ensuring that $0 < F(\lambda(t)) < 1$ (we will explore cases when $\lambda(t)$ violates these bounds in the following section). The left pane of Figure 4.9 shows the range of the CDF, $F(\lambda(t))$, for which $\lambda_1 < \lambda(t) < \lambda_2$; the right pane of Figure 4.9 shows the graph of $\lambda(t)$ vs. t , over the range $\lambda_1 < \lambda(t) < \lambda_2$.

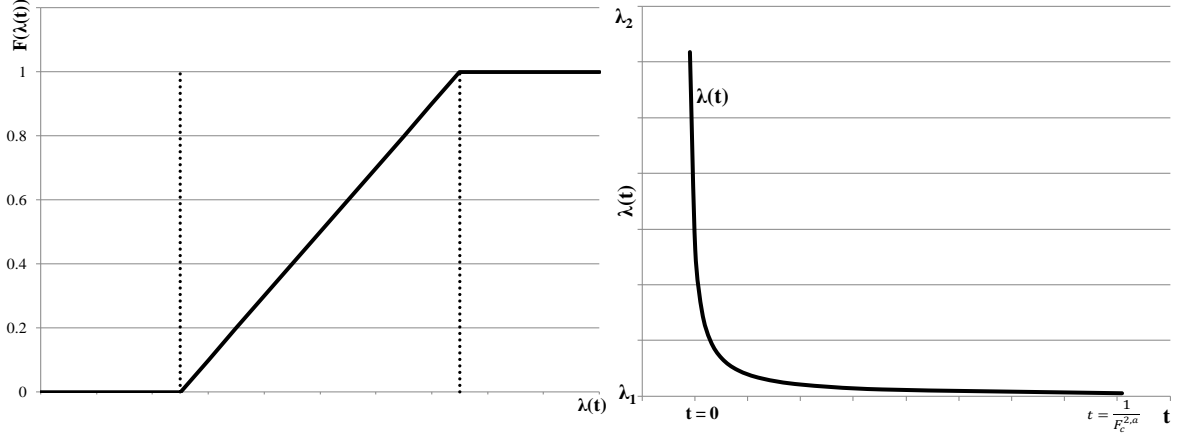


Figure 4.9 CDF and indifference value of time, mixed vehicle case.

As the case presented below is for when $\lambda(t) \in [\lambda_1, \lambda_2]$ we will term this the base case and use the notation F_c^{2-b} and z_c^{2-b} for the decision variable and the objective function, respectively.

The variable supplier cost and the passenger cost both involve the cumulative distribution function, and represent a weighted average passenger and variable supplier cost. It will be convenient to refer to the sum of the passenger cost and variable supplier cost as G^{2-a} where a represents the case designation. We integrate the sum over t over the interval $\left[0, \frac{1}{F_c^{2-b}}\right]$ and multiply the sum by F_c^{2-b} to consider the weighted average number of passengers that arrive in each time interval t .

$$G^{2-b} = F_c^{2-b} \int_0^{(F_c^{2-b})^{-1}} (1 - F(\lambda(t))) (\beta_j + ((F_c^{2-b})^{-1} - t + m_j)E(\lambda|\lambda > \lambda(t))) + F(\lambda(t))(\beta_k + (t + m_k)E(\lambda|\lambda < \lambda(t))) \quad (4.39)$$

$$G^{2-b} = \frac{\beta_j \lambda_2 - \beta_k \lambda_1}{(\lambda_2 - \lambda_1)} + \frac{\lambda_2^2(1 + 2F_c^{2-b}m_j) - \lambda_1^2(1 + 2F_c^{2-b}m_k)}{4F_c^{2-b}(\lambda_2 - \lambda_1)} + \frac{F_c^{2-b}(\beta_j - \beta_k)^2}{4(\lambda_2 - \lambda_1)} \ln \left(\frac{-1 + F_c^{2-b}(m_k - m_j)}{1 + F_c^{2-b}(m_k - m_j)} \right) \quad (4.40)$$

The total logistics cost function is the sum of the fixed cost, $\frac{F_c^{2-b} \sum_{i \in c} \alpha_i}{2Q}$, and G^{2-b} :

$$\begin{aligned}
z^{2-b} &= \frac{F_c^{2-b} \sum_{i \in c} \alpha_i}{2Q} + \frac{\beta_j \lambda_2 - \beta_k \lambda_1}{(\lambda_2 - \lambda_1)} \\
&\quad + \frac{\lambda_2^2(1 + 2F_c^{2-b} m_j) - \lambda_1^2(1 + 2F_c^{2-b} m_k)}{4F_c^{2-b}(\lambda_2 - \lambda_1)} \\
&\quad + \frac{F_c^{2-b}(\beta_j - \beta_k)^2}{4(\lambda_2 - \lambda_1)} \ln \left(\frac{-1 + F_c^{2-b}(m_k - m_j)}{1 + F_c^{2-b}(m_k - m_j)} \right)
\end{aligned} \tag{4.41}$$

Let us assume that the lower bound of the value of time distribution is zero ($\lambda_1 = 0$) and the resulting total logistics cost is:

$$\begin{aligned}
z^{2-b} &= \frac{F_c^{2-b} \sum_{i \in c} \alpha_i}{2Q} + \beta_j + \frac{\lambda_2}{4} \left(\frac{1}{F_c^{2-b}} + 2m_j \right) \\
&\quad + \frac{F_c^{2-b}(\beta_j - \beta_k)^2}{4\lambda_2} \ln \left(\frac{-1 + F_c^{2-b}(m_k - m_j)}{1 + F_c^{2-b}(m_k - m_j)} \right)
\end{aligned} \tag{4.42}$$

Upon setting $\lambda_1 = 0$, we see that z^{2-b} depends mostly on variables related to vehicle type j , with the exception of the fixed cost and the log component. Equation (4.40) in this form does not have an analytic solution. As there is a single component adding to the complication, $\frac{F_c^{2-b}(\beta_j - \beta_k)^2}{4\lambda_2} \ln \left(\frac{-1 + F_c^{2-b}(m_k - m_j)}{1 + F_c^{2-b}(m_k - m_j)} \right)$, we will explore the contribution of this component. We define upper and lower bounds of the following quantities: $(\beta_j - \beta_k)$, $(m_k - m_j)$, $F_c^{2,b}$, and λ_2 . We estimate the bounds for $(\beta_j - \beta_k)$ and $(m_k - m_j)$ by analyzing the dataset described in the previous chapter.¹¹ The bounds for λ_2 are drawn from the literature. The bounds for $F_c^{2,b}$ are determined by estimation of the single vehicle case using already established bounds.

We define two functions: the full model (4.42) and the truncated model (4.43), which is the full model without the log term.

$$\widetilde{z_c^{2-b}} = \frac{F_c^{2-b} \sum_{i \in c} \alpha_i}{2Q} + \beta_j + \frac{\lambda_2}{2} \left(\frac{1}{2F_c^{2-b}} + m_j \right) \tag{4.43}$$

Values for each quantity, evenly spaced across the defined interval are chosen; for all value combinations we calculate z_c^{2-b} and $\widetilde{z_c^{2-b}}$ and find an average percent difference (-4.10%), maximum percent difference (-13.19%), and 90th percentile percent difference (-7.02%). These values are relatively small, especially considering the overall purpose of the model is to develop qualitative insights than precise values. To gain insights from an analytic form, we use the truncated model. We find the frequency that minimizes total logistics cost by minimizing the total logistics cost function over the decision variable $\widetilde{F_c^{2-b}}$.

¹¹ Aircraft operating statistics and costs collected by the Department of Transportation from 2003-2008, on a per airline, per aircraft type, per year-quarter basis.

$$\widetilde{F_c^{2-b^*}} = \left(\frac{\lambda_2 Q}{2 \sum_{i \in c} \alpha_i} \right)^{\frac{1}{2}} \quad (4.44)$$

Which is a true minimum as $\frac{d^2 \widetilde{z_c^{2-b}}}{d(\widetilde{F_c^{2-b}})^2} = \frac{\lambda_2}{2(\widetilde{F_c^{2-b}})^3} > 0$.

We see that the frequency that minimizes $\widetilde{z_c^{2-b}}$ is of a very similar form to $F_c^{1-1^*}$ and $F_c^{1-2^*}$, the mixed vehicle case for passenger scenario 1 when all passenger groups are assigned to one vehicle type.

The total logistics cost function at optimal frequency is a function of the variable cost and the travel time on vehicle j , the sum of the fixed cost, and the upper bound of the value of time distribution. The fixed cost captures the cost of both vehicle types, while the variable cost and the travel time are only dependent on vehicle type j . When approximating the passenger scenario 2 base case with $\widetilde{z_c^{2-b^*}}$, we are implicitly assuming all passengers are assigned to vehicle type j without violating the boundary conditions. The values β_k and m_k factor into the function in the full form of z_c^{2-b} , but also in the bounds for which $\widetilde{z_c^{2-b^*}}$ is valid.

$$\widetilde{z_c^{2-b^*}} = \left(\frac{\sum_{i \in c} \alpha_i \lambda_2}{2Q} \right)^{\frac{1}{2}} + \beta_j + \frac{\lambda_2 m_j}{2} \quad (4.45)$$

As we set $\lambda_1 = 0$, the optimal solution in (4.45) is valid when $0 < \lambda(t) < \lambda_2$. However, the conditions can be violated when $\lambda(t) < 0$ (note $\lambda(t)$ can never be equal to zero due to construction) or $\lambda(t) \geq \lambda_2$. Upon determining that the conditions are violated, the appropriate case is determined using the indifference value of time. There are five ways that these conditions can be violated, that yield two mathematically unique solutions. Therefore, the cases are presented in two groups, case 2-1 and case 2-2; each group has sub-cases and one unique mathematical solution. For all cases, we consider t on the interval $\left[0, \frac{1}{F_c}\right]$ and passengers with a value of time λ on the interval $[0, \lambda_2]$.

Case 2-1: All passengers are assigned to vehicle type k

Case 2-1(a) $\lambda(t) < 0 \forall t$

Case 2-1(b) $\lambda(t) \geq \lambda_2 \forall t$

Case 2-1(c) Combination of case 2-1(a) and case 2-1(b)

Case 2-2: Some passengers are divided between vehicle types

Case 2-3(a) $\lambda(t) > 0$: Combination of case 2-1(b) and the base case

Case 2-3(b) $\lambda(t) \in \mathbb{R}$: Combination of case 2-1(a), 2-1(b), and the base case

A new function is developed for each case.

Case 2-1

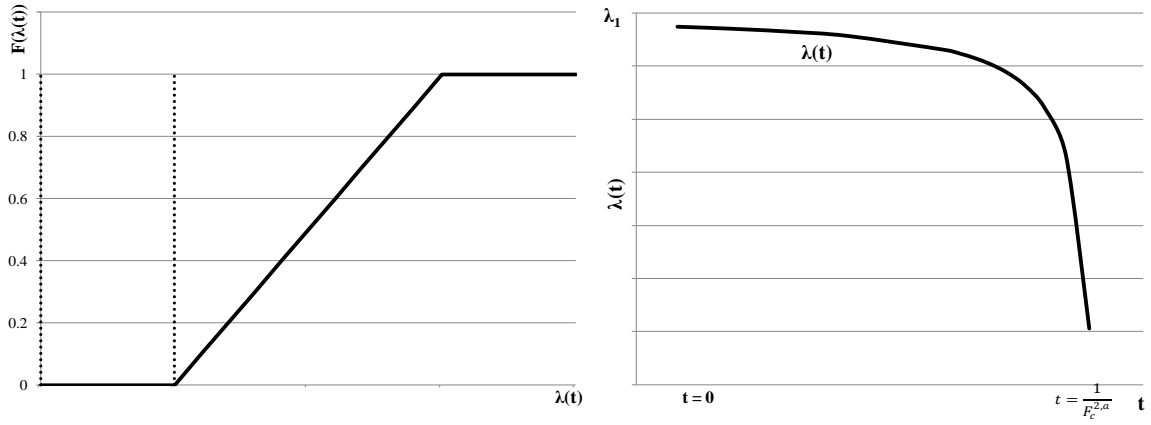
If $\lambda(t) < 0 \forall t$ or $\lambda(t) \geq \lambda_2 \forall t$, there are no passengers divided between vehicle types, and all passengers are simply assigned to one vehicle type. In case 2-1(a), $\lambda(t) < 0 \forall t$, such that for all wished-for departure times t , the indifference value of time is negative. This means that, when schedule delay is taken into account, vehicle j takes longer than the less expensive vehicle k . Since we assume that no passengers would be willing to spend more for a longer trip, all passengers will choose vehicle k in this case. Case 2-1(b) is when $\lambda(t) \geq \lambda_2 \forall t$, such that passengers have an indifference value of time that is greater than the upper bound. This means no passenger is willing to pay the extra cost required to take the fast, more expensive vehicle. Thus they are all assigned to vehicle type k . In case 2-1(c), some values of t make it such that $\lambda(t) < 0$, while for other values $\lambda(t) \geq \lambda_2$. Despite the discontinuity, case 2-1(c) identical to (a) and (b) such that all passengers are assigned to vehicle type k . These three cases are illustrated in Figure 4.10, which shows the range of $F(\lambda(t))$ each case captures and the graph of $\lambda(t)$ vs t .

In both cases, as no passengers are divided between vehicle types, the expected value of time is $\frac{\lambda_2}{2}$. The total logistics cost function is then a very simple function of the supplier and passenger cost:

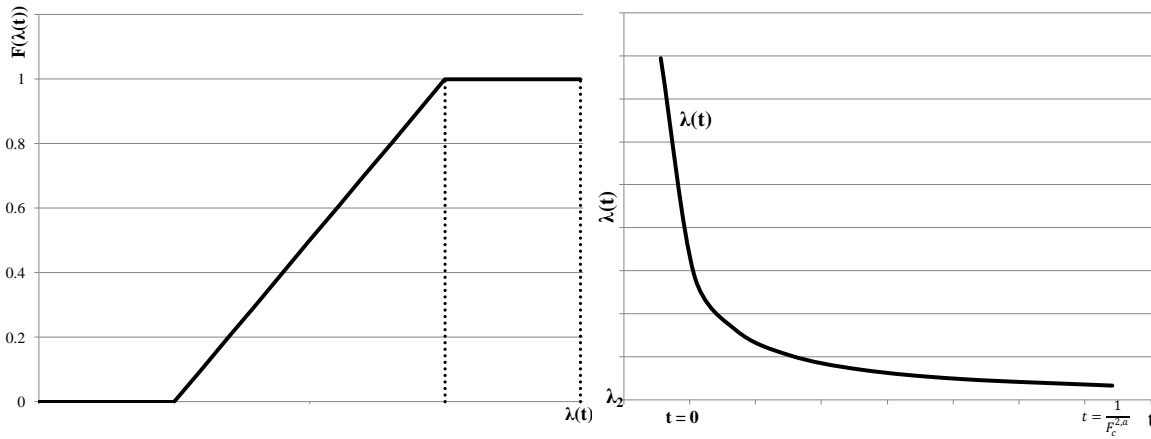
$$z_c^{2-1} = \frac{F_c^{2-1} \sum_{i \in c} \alpha_i}{2Q} + \beta_k + \frac{\lambda_2}{2} \left(\frac{1}{2F_c^{2-1}} + m_k \right) \quad (4.46)$$

This function is identical to the unbounded case truncated model, except k is the vehicle incurring costs of β and m . This follows directly from our understanding of $\widetilde{z_c^{2-b^*}}$, as we are implicitly assuming all passengers are assigned to one vehicle type. Because this function is identical to $\widetilde{z_c^{2-b}}$, then $F_c^{2-1^*} = \widetilde{F_c^{2-b^*}}$. It is therefore not possible for passengers to further reduce costs by dividing between vehicles. As such, case 2-1 is a terminal case, such that if, upon solving for the base case, it is determined that $\lambda(t)$ is outside $(0, \lambda_2)$, then case 2-1 is the final case to be solved.

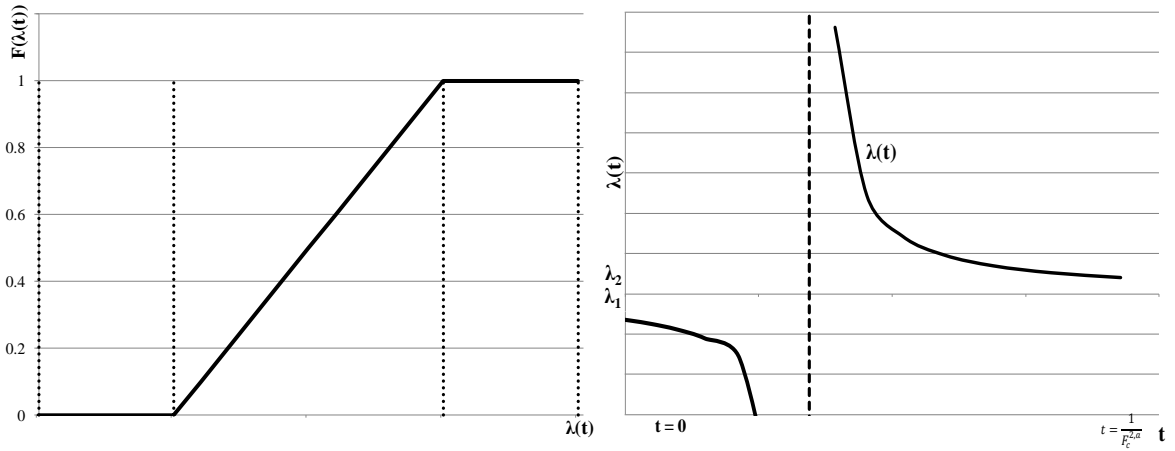
Case 2-1(a)



Case 2-1(b)



Case 2-1(c)



Case 2-2

For case 2-2, two different scenarios yield mathematically the same result. The cases are identical, as passengers are assigned to vehicle type k until a time for which $\lambda(t) = \lambda_2$; after this point in time passengers are divided between vehicles.

In case 2-2(a), passengers arrive at certain times t for which $\lambda_2 \leq \lambda(t)$, with the indifference value of time that is equal to or greater than the upper bound, such that they are assigned to vehicle type k . Passengers arriving at t such that $0 < \lambda(t) < \lambda_2$ will be divided between vehicles.

In case 2-2(b), $0 < \lambda(t) < \lambda_2$ for some t such that passengers are divided between vehicles; while $\lambda(t) \geq \lambda_2$ for some t and $\lambda(t) < 0$ for some t such that passengers are all assigned to vehicle type k . At the discontinuity (shown in the lower panel of Figure 4.10) all passengers continue to be assigned to vehicle type k as $\lambda(t)$ approaches 0^+ , as $\lambda(t) \geq \lambda_2$. The region of the CDF for which these sub-cases fall, and the graph of $\lambda(t)$ vs. t are shown in Figure 4.10.

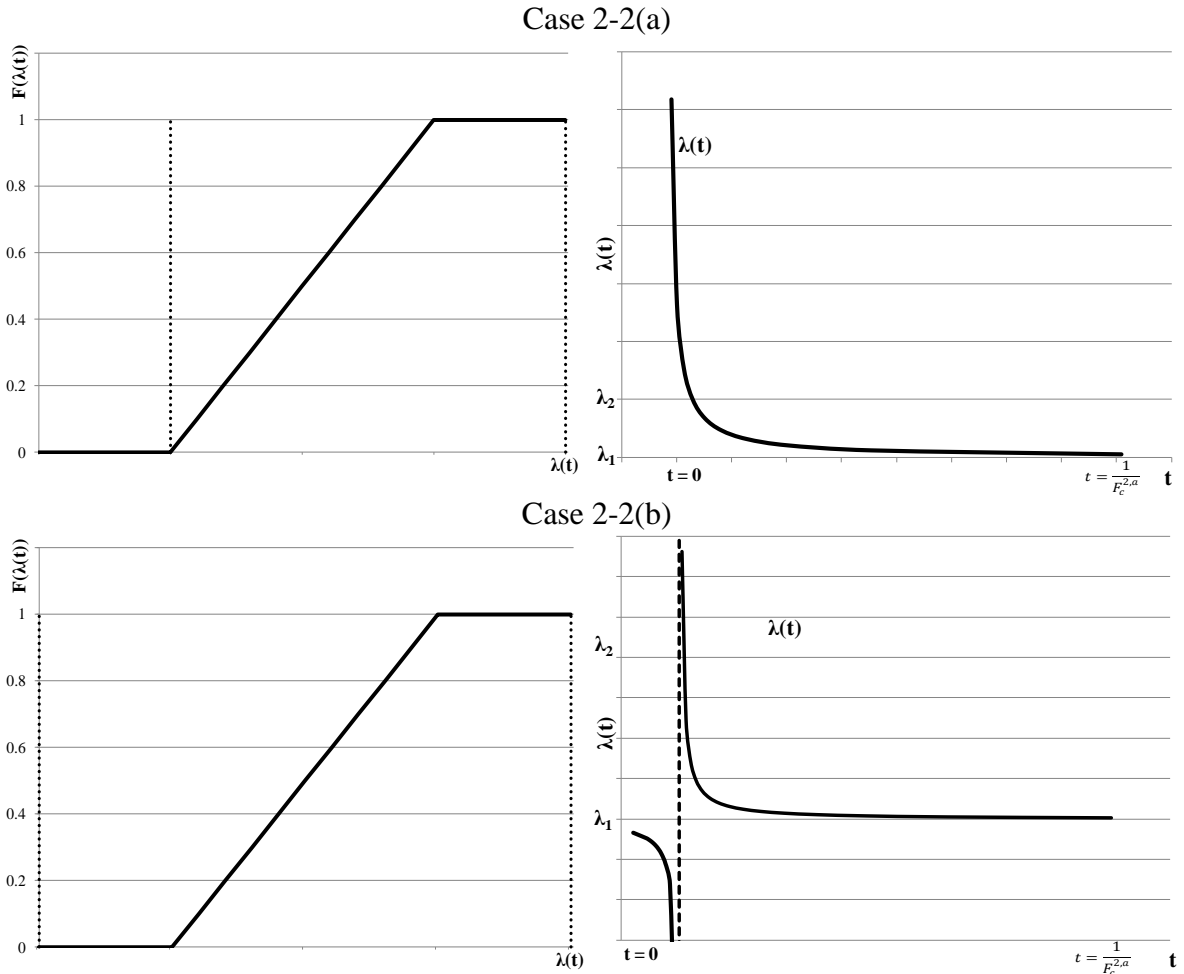


Figure 4.10 CDF and indifference value of time, Case 2-2.

We have two “regimes” in case 2-2 separated by a time t^{2-2} , $0 \leq t^{2-2} \leq \frac{1}{F_c}$. This is the time for which $\lambda(t) = \lambda_2$ and the instant for which $F(\lambda(t)) = 1$:

$$t^{2-2} = \frac{\beta_j - \beta_k}{2\lambda_2} + \frac{1}{2F_c^{2-2}} + \frac{m_j - m_k}{2} \quad (4.47)$$

All passengers who arrive on the interval $0 \leq t \leq t^{2-2}$ are assigned to vehicle type k , while passengers who arrive on the interval $t^{2-2} \leq t \leq \frac{1}{F_c^{2-2}}$ are divided between vehicles. Following the notation established in the base case, the sum of the variable cost component of the supplier cost and the passenger cost of the total logistics cost functions for these two regimes is termed G^{2-2} . The sum of G^{2-2} and the fixed cost $\frac{F_c^{2-2} \sum_{i \in c} \alpha_i}{2Q}$ is the total logistics cost:

$$\begin{aligned}
z_c^{2-2} = & \frac{F_c^{2-2} \sum_{i \in c} \alpha_i}{2Q} + F_c^{2-2} t^{2-2} \beta_k \\
& + \int_0^{t^{2-2}} F_c^{2-2} \frac{\lambda_2}{2} (t + m_k) dt \\
& + \int_{t^{2-2}}^{\frac{1}{F_c^{2-2}}} F_c^{2-2} \left((1 - F(\lambda(t))) \left(\beta_j \right. \right. \\
& + \left. \left. \left(\frac{1}{F_c^{2-2}} - t + m_j \right) E(\lambda | \lambda > \lambda(t)) \right) \right. \\
& + F(\lambda(t)) (\beta_k \\
& \left. \left. + (t + m_k) E(\lambda | \lambda < \lambda(t)) \right) \right) dt
\end{aligned} \tag{4.48}$$

The full function and the truncated function are presented in Appendix A2.1. Again, we have two functions, the full model (4.48) and the truncated model without the log term, as we had in the base case. For all possible combinations of $(\beta_j - \beta_k)$, $(m_k - m_j)$, F_c^{2-2} , and λ_2 , we calculate z_c^{2-2} and $\widetilde{z_c^{2-2}}$, and find an overall average percent difference (-3.92%), maximum percent difference (-6.83%), and 90th percentile percent difference (-5.28%). As was found in the base case, these values are relatively small. For the truncated model, we find the frequency that minimizes total logistics cost by minimizing the total logistics cost function $\widetilde{z_c^{2-2}}$ over the decision variable $\widetilde{F_c^{2-2}}$.

$$\begin{aligned}
\widetilde{F_c^{2-2}}^* = & (Q\lambda_2)^{\frac{1}{2}} \left(4 \sum_{i \in c} \alpha_i \right. \\
& - \frac{Q}{\lambda_2} \left(3 \left(\sum_i \beta_i^2 \right) + \beta_j (-6\beta_k + 4\lambda_2(m_j - m_k)) \right. \\
& \left. \left. + \lambda_2 (\lambda_2(m_j - m_k)^2 + 4\beta_k(m_k - m_j)) \right) \right)^{-\frac{1}{2}}
\end{aligned} \tag{4.49}$$

Upon determining $\widetilde{F_c^{2-2}}^*$ it is possible that another case could become valid. However, it will not be possible for the base case to become valid if $\widetilde{F_c^{2-b}}^* > \widetilde{F_c^{2-2}}^*$. Holding all other components of $\lambda(t)$ constant, if $\frac{1}{F_c}$ increases, the denominator of $\lambda(t)$ will decrease and $\lambda(t)$ will increase. Therefore, if $\widetilde{F_c^{2-b}}^* > \widetilde{F_c^{2-2}}^*$, the only possible case alternative to case

2-2 is 2-1(b) where $\lambda(t) \geq \lambda_2 \forall t$, such that all passengers are assigned to vehicle type k . We investigate numerically and find that $\widetilde{F}_c^{2-2^*}$ is strictly smaller than $\widetilde{F}_c^{2-b^*}$ for all plausible ranges of β_i, m_i, λ_2 and $\alpha_i \forall i$, which implies that the only possible case alternative is 2-1(b). The resulting value for $\widetilde{z}_c^{2-2^*}$ is determined with $\widetilde{F}_c^{2-2^*}$. While an analytic solution for $\widetilde{z}_c^{2-2^*}$ can be determined, it is a complicated function from which it is difficult to gain insights and not presented.

Upon determining the value of $\widetilde{F}_c^{2-2^*}$, we re-calculate the value of $\lambda(t)$. If we find that the initial conditions for case 2-2(a) or 2-2(b) hold, then case 2-2 is the optimal solution. However, it is possible that, upon solving for $\widetilde{F}_c^{2-2^*}$, that the recalculation of $\lambda(t)$ finds that the initial conditions for case 2-2(a) or 2-2(b) are violated. Because $\widetilde{F}_c^{2-b^*} > \widetilde{F}_c^{2-2^*}$, the only possible case is that $\lambda(t) \geq \lambda_2 \forall t$, case 2-1(b) such that all passengers are assigned to vehicle type k . As case 2-1(b) is a terminal case, solving for either case 2-1(b) or determining that 2-2 is the appropriate case would be the final step.

Now that the single vehicle case, the mixed vehicle base case, and the three valid alternative mixed vehicle cases are solved, we present the solution algorithm:

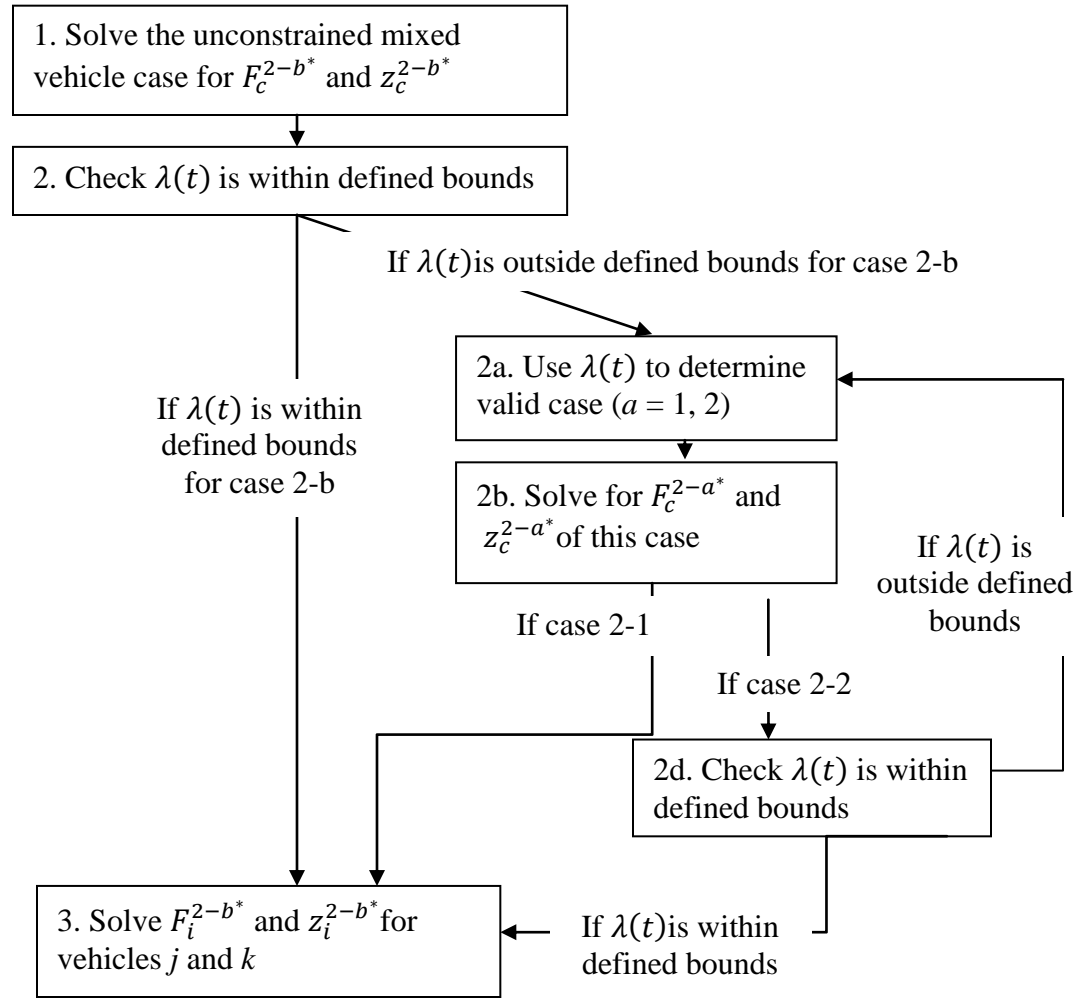


Figure 4.11 Passenger scenario 2 solution algorithm.

Upon solving for the single vehicle case, $z_i^{2-b*} \forall i$, and z_c^{2-a*} through the solution algorithm, we find the minimum total logistics cost combination (either single or mixed) by enumeration. In solving this function we are looking for the technology mix of both technology size and type, that minimizes cost across all potential mixes.

4.4 Total Logistics Cost Models for Passenger Scenario Three

In this section, we relax the assumption that passengers must be assigned to a vehicle bounding the headway in which they desire to depart. It therefore is no longer the case that headways must be constant and that vehicles be scheduled in an alternating sequence of vehicle types. To keep the discussion general, we will again consider two vehicle types: k and j ; the index i will represent either vehicle. We present a list of parameters and decision variables below.

Parameters:

- α_i Vehicle fixed cost, \$/Operation
- β_i Vehicle variable cost, \$/Passenger
- m_i In-vehicle travel time, Time/Passenger
- Q Total flow of passengers, Passenger/Time
- t Time
- $\lambda(t)$ Indifference value of passenger time, \$/Passenger – Time
- λ_1, λ_2 Minimum and maximum values in the distribution of value of time
- $F(\lambda(t))$ Probability a passenger has a value of time below $\lambda(t)$

Decision Variables:

- H_{jj} The length of a headway when bound only by vehicles of type j , Time/Operation
- H_{kj} The length of a headway when bound by vehicles of type j and of type k
Time/Operation; $H_{kj} = H_{jk}$

Recall $m_k > m_j$ and $\beta_j > \beta_k$, such that j is the faster, more expensive vehicle and k is the slower, less expensive vehicle. We limit our scope to the consideration of vehicle type k scheduled between two vehicles of type j . Additional changes could be made to broaden the scope to include a scenario with a vehicle of type k scheduled between more than two vehicles of type j . With minor changes, the case of vehicle type j schedule between two vehicles of type k could also be solved. In this model there are two types of headways: those bounded by a vehicle of type j only (H_{jj}), and those bound by the mixed vehicle types of k and j (H_{kj}). Again, we consider an infinite timeline of an intercity corridor with vehicles scheduled to serve a single origin destination pair with unconstrained vehicle availability. Shown in Figure 4.12, one cycle is equal to $H_{kj} + \frac{H_{jj}}{2}$. All passengers who desire to depart in one cycle will be assigned to one vehicle scheduled in that cycle, as a passenger could never minimize their cost by crossing cycles. Therefore a single cycle can be evaluated alone and can be generalized to the entire corridor. Figure 4.13 shows the time region detail for one cycle.

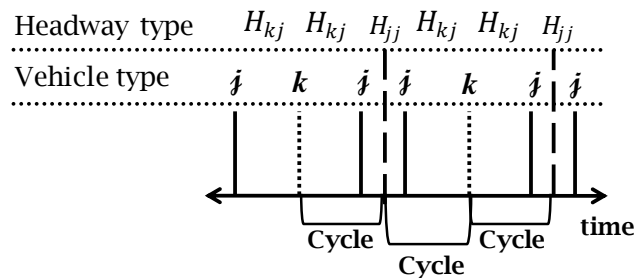


Figure 4.12 Headway and cycle representation in passenger scenario 3.

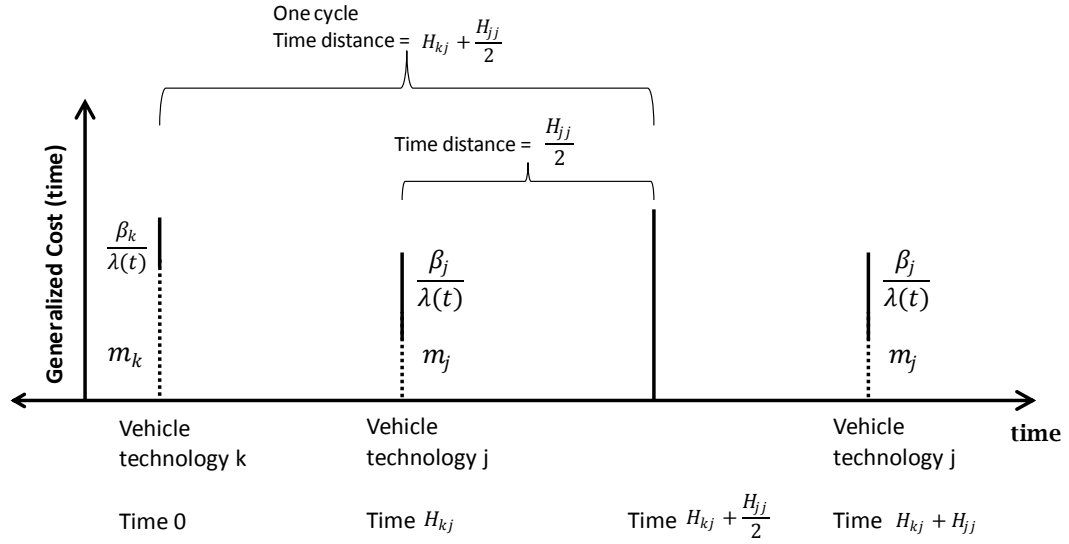


Figure 4.13 Generalized cost (time), time regions, and related quantities for passenger scenario 3.

We again consider fleets consisting of two vehicle types. There are four passengers categories 1 – 4, defined by the headway in which they desire to depart and the vehicle type to which they are assigned. These are depicted below. The first entry specifies the headway and the second the assigned vehicle.

Passenger Group	Headway	Vehicle Type
1	H_{jj}	j
2	H_{kj}	j
3	H_{kj}	k
4	H_{jj}	k

Continuing from the previous section, we consider the value of time to have a uniform distribution and employ the concept of indifference value of time. Under the assumptions of passenger scenario 3 there are two ranges for this indifference value of time: one for $t \in [0, H_{kj}]$ and one for $t \in [H_{kj}, \frac{H_{jj}}{2}]$. For passengers of type 2 and 3 that desire to depart in H_{kj} , the indifference value of time is the same as determined in the previous section, $\lambda(t) = \frac{\beta_j - \beta_k}{m_k - m_j + 2t - H_{kj}}$. For passengers type 4 and 1 that desire to depart in H_{jj} , we must derive the value. We do this by considering a headway interval $0 \leq t \leq \frac{H_{jj}}{2}$ and setting the generalized costs of passenger type 4 to that of the generalized cost of passenger type 1.

$$m_k + \frac{\beta_k}{\lambda(t)} + t + H_{kj} = m_j + \frac{\beta_j}{\lambda(t)} + t; \quad 0 \leq t \leq \frac{H_{jj}}{2} \quad (4.50)$$

$$\lambda(t) = \frac{\beta_j - \beta_k}{H_{kj} + m_k - m_j}; \quad 0 \leq t \leq \frac{H_{jj}}{2} \quad (4.51)$$

Note that the indifference value of time does not depend on the desired departure time t . Both passenger types would incur a time cost of t , while only passenger group 4 would incur the additional cost of H_{kj} .

The indifference value of time $\lambda(t)$ is:

$$\lambda(t) = \begin{cases} \frac{\beta_j - \beta_k}{m_k - m_j + 2t - H_{kj}} & 0 \leq t \leq H_{kj} \\ \frac{\beta_j - \beta_k}{H_{kj} + m_k - m_j} & H_{kj} < t \leq \frac{H_{jj}}{2} \end{cases} \quad (4.52)$$

In the following sections we will build the passenger cost and variable supplier cost functions for the two groups of passengers that arrive in the same headway: 2 and 3, and 1 and 4. The fixed operating cost is discussed in the next section. It will be again be convenient to superscript the decision variables and the total logistics cost with the case designation $3-a$, and refer to the sum of the passenger cost and variable supplier cost as $G^{3-a}(H_{ij})$. We begin with the base case for passenger scenario 3 and present additional cases in the following section.

Passenger cost function, type 2 and 3

Passengers of type 2 and 3 arrive in a headway of type H_{kj} bound by vehicles of type k and j . Passengers of type 2 are assigned to vehicle of type j and passengers of type 3 are assigned to vehicle of type k . Passengers served in a headway of type H_{kj} desire to depart at a time $t \in [0, H_{kj}]$. These passengers and their related costs are identical to those explored previously in section 4.3.2. A passenger of type 2 who desires to depart at time t will incur a schedule delay cost of $H_{kj} - t$ and a travel time cost of m_j , while a passenger of type 3 who desires to depart at a time t would incur a schedule delay cost of t and a travel time of m_k . The passenger and variable cost derived in (4.48) are shown again below in (4.53) and (4.54):

$$G^{3-b}(H_{kj}) = \int_0^{H_{kj}^{3-b}} \frac{1}{H_{kj}^{3-b}} \left((1 - F(\lambda(t))) (\beta_j + (H_{kj}^{3-b} - t + m_j)E(\lambda|\lambda > \lambda(t))) + F(\lambda(t))(\beta_k + (t + m_k)E(\lambda|\lambda < \lambda(t))) \right) dt \quad (4.53)$$

$$\begin{aligned}
G^{3-b}(H_{kj}) &= \beta_j + \frac{\lambda_2}{4} (H_{kj}^{3-b} + 2m_j) \\
&+ \frac{(\beta_j - \beta_p)^2}{4H_{kj}^{3-b}\lambda_2} \ln \left(\frac{-H_{kj}^{3-b} + (m_k - m_j)}{H_{kj}^{3-b} + (m_k - m_j)} \right)
\end{aligned} \tag{4.54}$$

Following the discussion in the previous section regarding bounds, (4.54) holds when $0 < \lambda(t) < \lambda_2$. Violation of this bound is discussed in the previous section.

Passenger cost function, type 1 and 4

Passengers of type 1 and 4 arrive in a headway of type H_{jj} bound by two vehicles of type j . By definition passengers of type 1 are assigned to vehicle of type j and passengers of type 4 are assigned to vehicle of type k . If we consider the first vehicle in this headway to depart at time 0 (rather than H_{kj}), passengers who desire to depart in a headway of type H_{jj} can do so over the time interval $t \in \left[0, \frac{H_{jj}}{2}\right]$. A passenger of type 1 who arrives at time t will incur a schedule delay cost of t and a travel time cost of m_j ; a passenger of type 4 would incur a schedule delay cost of $H_{kj} + t$ and a travel time of m_k .

Expressions for the expected passenger value of time and the cumulative percent of passengers with value of time $\lambda(t)$ in (4.37) and (4.38) hold. The passenger cost and the variable operating cost for a passenger that desires to depart over time interval $t \in \left[0, \frac{H_{jj}}{2}\right]$ is therefore:

$$\begin{aligned}
G^{3-b}(H_{jj}) &= \int_0^{\frac{H_{jj}^{3-b}}{2}} \frac{2}{H_{jj}^{3-b}} \left((1 - F(\lambda(t))) \left(\beta_j \right. \right. \\
&+ (t + m_j)E(\lambda|\lambda > \lambda(t)) \Big) \\
&+ F(\lambda(t)) \left(\beta_k \right. \\
&+ \left. \left. (H_{kj}^{3-b} + t + m_k)E(\lambda|\lambda < \lambda(t)) \right) \right) dt
\end{aligned} \tag{4.55}$$

We multiply this equation by $\frac{2}{H_j}$ to calculate the weighted average considering the number of passengers that arrive in each time slice $t, 0 \leq t \leq \frac{H_{jj}}{2}$. We solve the integral and achieve:

$$G^{3-b}(H_{jj}) = \beta_j + \frac{\lambda_2}{2} \left(\frac{H_{jj}^{3-b}}{4} + m_j \right) - \frac{(\beta_j - \beta_k)^2}{2\lambda_2(H_{kj}^{3-b} - m_j + m_k)} \tag{4.56}$$

With substitution of function (4.52), we see that this function is:

$$G^{3-b}(H_{jj}) = \beta_j + \frac{\lambda_2}{2} \left(\frac{H_{jj}^{3-b}}{4} + m_j \right) + \frac{\lambda(t)}{\lambda_2} \left(\frac{\beta_k - \beta_j}{2} \right) \tag{4.57}$$

The first two terms of the function capture the passenger cost for a passenger of type 1 assigned to vehicle type j . The third term captures the difference in variable costs and the percent of passengers who are assigned to vehicle type k . This term will be negative by definition, such that the overall contribution of the variable cost will be less than β_j , reflecting that some passengers incur β_k for which $\beta_k < \beta_j$.

Equation (4.56) considers that the indifference value of time $\lambda(t)$ falls on the interval $(0, \lambda_2)$. As $\lambda(t)$ is independent of t over the interval $t \in [H_{kj}, \frac{H_{jj}}{2}]$, there are only two ways $\lambda(t)$ can fall outside the interval $(0, \lambda_2)$: $\lambda(t) < 0$ or $\lambda(t) > \lambda_2$; these two scenarios yield mathematically identical results. For convenience, we will continue the numbering scheme from the previous section, and call this case 2-3.

In case 2-3, $\lambda(t) \geq \lambda_2$ or $\lambda(t) > 0$ such that all passengers are assigned to a vehicle of type k . The expected schedule delay is the sum of the expected schedule delay endured in the headway in which they desire to depart ($\frac{H_{jj}}{4}$), and the full headway of H_{kj} . The function is:

$$G^{2-3}(H_{jj}) = \beta_k + \frac{\lambda_2}{2} \left(m_k + \frac{H_{jj}}{4} + H_{kj} \right) \quad (4.58)$$

Total logistics cost function

In defining the total logistics cost function for the base case, we must consider the fixed cost. For every cycle, there are $Q \left(H_{kj} + \frac{H_{jj}}{2} \right)$ passengers that desire to depart. The operating cost per passenger is then:

$$\frac{\sum_{i \in c} \alpha_i}{Q(2H_{kj} + H_{jj})} \quad (4.59)$$

The total logistics cost function can be presented in a generic form. If we consider the passenger and variable cost components $G^{3-a}(H_{kj})$ and $G^{3-a}(H_{jj})$, then:

$$\begin{aligned} z_c^{3-a} = & \frac{\sum_{i \in c} \alpha_i}{Q(H_{jj} + 2H_{kj})} + \left(\frac{H_{jj}}{2H_{kj} + H_{jj}} \right) G^{3-a}(H_{jj}) \\ & + \frac{1}{2} \left(\frac{H_{kj}}{2H_{kj} + H_{jj}} \right) G^{3-a}(H_{kj}) \end{aligned} \quad (4.60)$$

where $\left(\frac{H_{jj}}{2H_{kj} + H_{jj}} \right)$ is the proportion passengers that incur a cost of $G^{3-a}(H_{kj})$ and $\frac{1}{2} \left(\frac{H_{kj}}{2H_{kj} + H_{jj}} \right)$ is the proportion passengers that incur a passenger cost of $G^{3-a}(H_{kj})$.

For the base case 3-b, the total logistics cost function is:

$$\begin{aligned}
z_c^{3-b} &= \frac{\sum_{i \in c} \alpha_i}{Q(2H_{kj} + H_{jj})} \\
&+ \frac{H_{jj}(\beta_j + \frac{\lambda_2}{8}(H_{jj} + 4m_j) - \frac{(\beta_j - \beta_k)^2}{2\lambda_2(H_{kj} - m_j + m_k)})}{2H_{kj} + H_{jj}} \\
&+ \frac{H_{kj}\lambda_2(4\beta_j + \lambda_2(H_{jj} + 2m_j)) + (\beta_j - \beta_k)^2 \ln\left(\frac{-H_{kj} + (m_k - m_j)}{H_{kj} + (m_k - m_j)}\right)}{8(2H_{kj} + H_{jj})\lambda_2}
\end{aligned} \tag{4.61}$$

Equation (4.61) is the objective function to be minimized over H_{jj} and H_{kj} . An analytic expression for the optimum does not exist in either full or truncated form.

Equation (4.61) is the objective function when $0 < \lambda(t) < \lambda_2 \forall t$. Upon determining this condition is violated for any value of t , the appropriate case can be determined using the indifference value of time. The total logistics cost function for passenger scenario 3 includes costs incurred over two headway types: H_{kj} and H_{jj} . If the condition on $\lambda(t)$ is violated over $t \in [0, H_{kj}]$, the alternative cases are $a = \{1, 2\}$, as presented in passenger scenario 2. If this condition is violated over $t \in [H_{kj}, \frac{H_{jj}}{2}]$, the alternative cases is $a = 3$. The new cases are 3-1 and 3-2:

Case 3-1: Combination of case 2-1 ($t \in [0, H_{kj}]$) and case 2-3 ($t \in [H_{kj}, \frac{H_{jj}}{2}]$), all passengers are assigned to vehicle type k

Case 3-2: Combination of case 2-2 ($t \in [0, H_{kj}]$), where some passengers are assigned to k and others divided, and the base case 3-b ($t \in [H_{kj}, \frac{H_{jj}}{2}]$), with all passengers divided

A new total logistics cost function is developed for each case. As analytic solutions for optimal frequency cannot be determined, each function is described conceptually.

Case 3-1

If $\lambda(t) < 0 \forall t$ or $\lambda(t) \geq \lambda_2 \forall t$, all passengers are assigned to a vehicle of type k . Either range holds over $t \in [0, H_{kj}]$; because for $t \geq H_{kj}$, $\lambda(t)$ takes on a constant value as the function for $\lambda(t)$ is independent of t over this region, the range also holds for $t \geq H_{kj}$. The graph of the indifference value of time over t for the two possible ranges of $\lambda(t)$ which yield case 3-1 are illustrated in Figure 4.14.

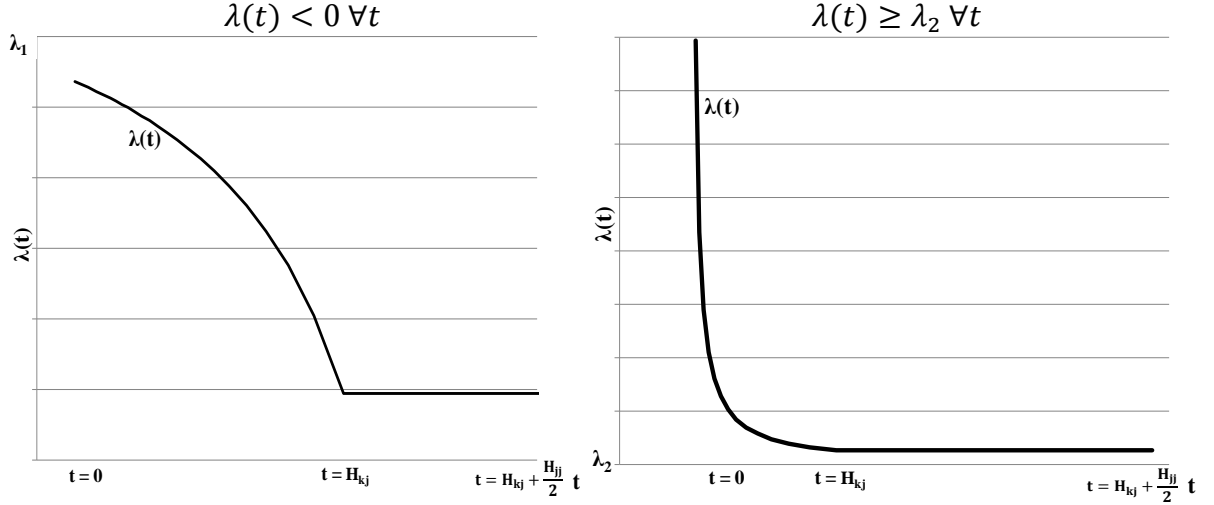


Figure 4.14 Indifference value of time, Case 3-1.

The expected value of time is again $\frac{\lambda_2}{2}$. The total logistics cost function is then a function of the supplier and passenger cost in both cases:

$$z_c^{3-1} = \left(\frac{H_{jj}}{H_{jj} + 2H_{kj}} \right) G^{2-3}(H_{jj}) + \frac{1}{2} \left(\frac{H_{kj}}{2H_{kj} + H_{jj}} \right) G^{2-1}(H_{kj}) + \frac{\sum_{i \in c} \alpha_i}{Q(H_{jj} + 2H_{kj})} \quad (4.62)$$

$$z_c^{3-1} = \left(\frac{H_{jj}}{2H_{kj} + H_{jj}} \right) \left(\beta_k + \frac{\lambda_2}{2} \left(m_k + \frac{H_{j,2}}{4} + H_k \right) \right) + \frac{1}{2} \left(\frac{H_{kj}}{2H_{kj} + H_{jj}} \right) \left(\beta_k + \frac{\lambda_2}{2} \left(m_k + \frac{H_{kj}}{2} \right) \right) + \frac{\sum_{i \in c} \alpha_i}{Q(H_{jj} + 2H_{kj})} \quad (4.63)$$

The concept of assignment region is not relevant in these cases, as passengers are directly assigned to either vehicle type. Therefore, there is no possibility that, up on solving case 3-1 or 3-2 that passengers could minimize cost by being assigned in a different way. Therefore, case 3-1 is a terminal case.

Case 3-2

In case 3-2, all passengers desiring to depart in a headway of type H_{jj} are divided between vehicles such that $\lambda(t) \in (0, \lambda_2)$ (the base case, 3-b). Some passengers desiring to depart in a headway of type H_{kj} are assigned to a vehicle of type k and the remaining are divided (case 2-2). The graphs of the indifference value of time over t for case 3-2 is illustrated in Figure 4.15.

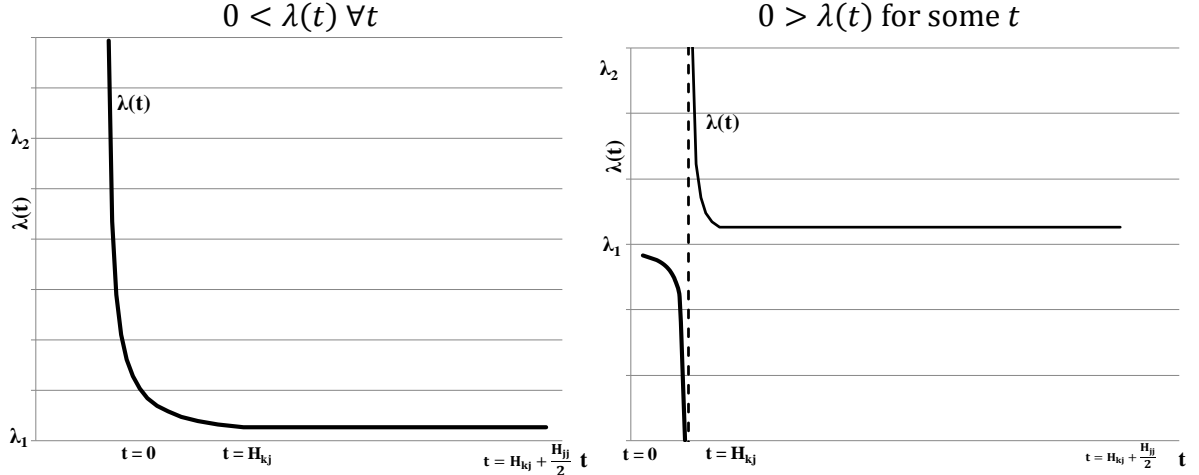


Figure 4.15 Indifference value of time, Case 3-2.

The total logistics cost function for case 3-2 is therefore:

$$z_c^{3-2} = \left(\frac{H_{jj}}{2H_{kj} + H_{jj}} \right) G^{3-b}(H_{jj}) + \frac{1}{2} \left(\frac{H_{kj}}{2H_{kj} + H_{jj}} \right) G^{2-2}(H_{kj}) + \frac{\sum_{i \in C} \alpha_i}{Q(H_{jj} + 2H_{kj})} \quad (4.64)$$

Where:

$$G^{2-2}(H_{kj}) = \left(\frac{t^{2-2}}{H_{kj}} \right) \beta_k + \int_0^{t^{2-2}} \frac{\lambda_2}{2H_{kj}} (t + m_k) dt + \int_{t^{2-2}}^{H_{kj}} \frac{1}{H_{kj}} \left((1 - F(\lambda(t))) (\beta_j + (H_{kj} - t + m_j) E(\lambda | \lambda > \lambda(t))) + F(\lambda(t)) (\beta_k + (t + m_k) E(\lambda | \lambda < \lambda(t))) \right) dt \quad (4.65)$$

$$\text{and } t^{2-2} = \frac{\beta_j - \beta_k}{2\lambda_2} + \frac{H_{kj}}{2} + \frac{m_j - m_k}{2}.$$

From the discussion related to case 2-2, it is possible that upon solving for the optimal frequency that $F_c^{3-2*} > F_c^{3-1*}$. If this is the result, case 3-1 should be solved for as the solution; and as it is a terminal case, should be the final solution.

Now that the single vehicle case, the mixed vehicle base case, and the alternative mixed vehicle cases are solved, we present the solution algorithm.

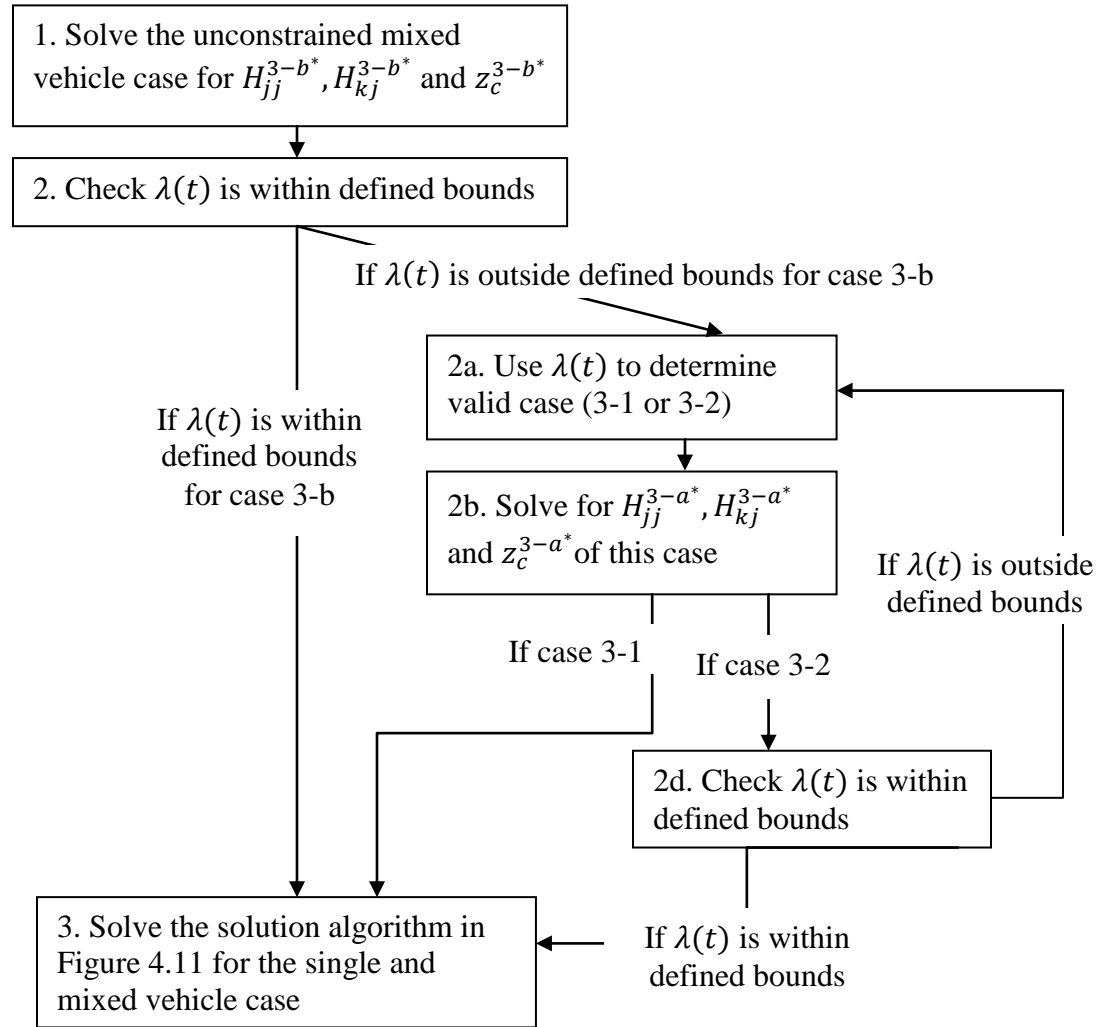


Figure 4.16 Passenger scenario 3 solution algorithm.

Upon solving for $z_c^{2-a^*}$, $z_c^{3-a^*}$ and $z_i^{2-b^*} \forall i$ through the solution algorithm, we find the minimum total logistics cost combination (either single or mixed) by enumeration. In solving this function we are looking for the technology mix of both technology size and type, that minimizes cost across all potential mixes.

In developing the model for passenger scenario 3 in this way, we capture a central planner organizing vehicle departures of different types jointly. It is possible to approach the concept of unequal headways from a different perspective. Consider uncoordinated vehicle departures of two vehicle types, j and k , and the two decision variables: the frequency of vehicle type j , F_j and the frequency of vehicle type k , F_k . Using the ratio of the decision variables, we can determine the headway lengths and the passenger assignment in each headway type. Such a model approaches capturing unequal headways in a more general way, yet is less consistent with the system optimal perspective of a central planner organizing vehicle departures of all types.

4.5 Conclusions

In this chapter, we develop analytic models characterizing the intercity transportation system to conceptually evaluate the relationship between optimum service characteristics and fuel price. The models represent the total logistics cost of an intercity transportation system in that they include both vehicle operating costs and costs incurred by the passenger. In summing operating and passenger costs, we exploit the cost-reducing potential of alternative vehicles with different cost structures and service attributes. The models are developed for both single and mixed vehicle services and determine the vehicle size, technology mix, and frequency to serve a corridor at minimum total logistics cost.

In chapter 3 we established that supplier-to-supplier input substitution is minimal, such that operating costs can be modeled with a simple mathematic function. Defining vehicles generically and characterizing them simply with a fixed cost, a variable cost per seat, and a passenger cost in the form of travel time, enables the consideration of many intercity transportation vehicles. Furthermore, we consider aircraft vehicle size to be endogenous and continuous. This is the benefit of employing continuum approximation models and capturing all pertinent costs – those incurred from operating vehicles and traveling in them – in one function. While we found in chapter 3 that the interaction term between fuel price and aircraft size was positive, the resulting aircraft size that minimized operating cost per seat-mile was larger than technically feasible. Therefore, representing operating cost as the sum of a fixed cost and a cost that varies with seats, hence implying infinite aircraft size to minimize operating cost per seat-mile, is appropriate given current aircraft technology bounds.

The total logistics cost models are formulated to be sensitive to fuel price, which may change significantly in the future as a result of market conditions or environmental policies. We find that increasing fuel price impacts vehicle frequency due to two components of the intercity transportation system. The first is the fixed cost – as fuel price increases, fixed vehicle operation cost increases, and frequency decreases. The second is from the vehicle variable cost per seat. As fuel price increases, the absolute difference between vehicle variable costs increases in a mixed vehicle service, and the vehicles are more differentiated. In this research we find that as vehicles become more differentiated, the optimal vehicle frequency increases. This is because passengers are increasingly unwilling to wait for a particular vehicle as the vehicles are more differentiated. A change in fuel price therefore forces frequency to decrease, with the rate of decrease diminishing with fuel price.

In analyzing an intercity passenger transportation corridor, we allow for passengers with heterogeneous values of time. Passenger scenario 1 considers discrete passenger groups, each defined by a demand rate and a value of time. Passenger scenario 2 and 3 allow value of time to follow a continuous (uniform) distribution. Considering a distributed value of time captures a more realistic picture of passenger preferences. Finally, by not pre-defining the value of time we consider a wide range of future scenarios. It is well known that a single passenger experiences a value of time that varies over time and

situation. Furthermore, the value of time for a population will also change over time due to socioeconomic forces. Therefore, considering value of time a variable enables both parametric analysis for short and long run value of time variations.

For the three passenger scenarios, we present a solution algorithm for the mixed vehicle total logistics cost function. As no passenger scenario has a single total logistics cost function that describes all mixed vehicle cases, the solution algorithm is based around a key value that determines the valid case. For passenger scenario 1, this is the optimal value of frequency. As the base case for passenger scenario 1 requires that all passengers be served in the headway in which they desire to depart, there is a well defined range in which the optimal frequency may fall. If it falls outside this range, we present five alternative solutions, or cases. For passenger scenarios 2 and 3, we simply find the range of the indifference value of time to determine the valid case. The range to which the indifference value of time is compared is the upper and lower bound of the value of time distribution; the case which is valid follows from if and how these bounds are broken. In presenting multiple cases for the mixed vehicle function for each passenger scenario, we preserve the transparency of the total logistics cost models, such that we are able to gain insights between fuel costs and optimal service despite the host of cases possible for each passenger scenario.

The solution algorithms also provide us with a path to total logistics cost minimization. We find the minimum total logistics cost combination (either single or mixed) by enumeration. We first identify the vehicles under consideration and a set of input parameters for each vehicle. For passenger scenarios 1 and 2, we solve for the minimum total logistics cost in the single vehicle case for all vehicles in consideration; for passenger scenario 3, we solve the single vehicle case defined in passenger scenario 2. For passenger scenarios 1 and 2, we then solve for the mixed vehicle total logistics cost for all possible vehicle mixes. For passenger scenario 3, we would also solve for the vehicle arrangement with two vehicles of type j for each vehicle of type k . For each passenger scenario, we would then compare the total logistics costs of all possible vehicle combinations and identify the minimum total logistics cost vehicle combination.

5.

Numerical Case Study

In this chapter we seek to illustrate the analytic model of intercity transportation to gain insights into the impact of fuel price on optimal service mix in representative corridors. Using the total logistics cost function for passenger scenario 1 (discrete passenger groups), we explore an intercity passenger transportation corridor served by jet aircraft technology, turboprop aircraft technology, or High Speed Rail (HSR) technology. Through numerical examples, we explore how the minimum cost vehicle technology changes with fuel price. We also explore comparative relationships across vehicle combinations with numerical examples, including the difference in total logistics cost across vehicle combinations.

In chapter 3, we develop a linear operating cost model for jet aircraft; the estimated coefficients become parameters in the total logistics cost function. In this chapter, we begin by estimating a similar function on a related dataset for turboprop aircraft; additionally for both jet and turboprop aircraft we estimate travel time functions. As HSR does not exist in the United States yet, we rely on projected cost and operating statistics from the California High Speed Rail Business plan, published in December 2009. Because the figures in the business plan are projected, we validate the projections with cost and operating statistics reported by existing HSR systems across the world, summarized and presented in a report by de Rus et al. (2009).

In identifying additional parameters such as demand and value of time, we collect operating statistics and published values from the literature and publically available sources. While we keep the discussion general rather than pick a specific intercity corridor to analyze, we base the constants on the California Corridor, specifically from San Francisco to Los Angeles. We choose this corridor as the distance between airports and between HSR stations (377 and 418 miles respectively) is similar; the passenger demand is mostly generated at the ends of the corridor as it is defined; and there is an existing high level of passenger traffic service that, by 2020, may be served by air or rail.

5.1 Additional Model Development

In this section we develop the necessary operating cost and travel time models, and identify additional necessary parameters to serve as inputs to the analytic total logistics cost model. The jet operating cost model is presented in chapter 3. In this section we develop and present the turboprop and HSR operating cost model. Next, we develop travel time relationships with distance for the three vehicle types. Finally, we establish

parameter values for the other key quantities based on the literature and operating statistics of the California Corridor.

5.1.1 Turboprop Operating Cost

In this section, we develop a linear turboprop operating cost model. We estimate this model using data from the same US Department of Transportation (DOT) Form 41 database used in chapter 3. We collect 494 observations from 9 airlines and 7 aircraft types on a per airline (c), per aircraft type (n), and per year-quarter (q) basis for the date range 2003-2009. We again have the key variables of seats per departure ($seat$), average stage length traveled (asl), and airline fixed effects (c). To be consistent with the jet aircraft linear operating cost model, we develop a separate fuel consumption model (3.10) and an operating cost model without fuel costs (3.9). We add these two models together (with the fuel model multiplied by a fuel price) to achieve operating cost, shown in (3.8). Like the linear operating cost model for jet aircraft, we deflate the cost values to be in constant 2006 dollars. The dataset is an unbalanced panel and the same estimation technique, ordinary least squares and panel specific standard errors and assumed autocorrelation within panels, is used. The following equations show the linear jet aircraft technology operating cost model (5.1) and the turboprop technology operating cost model (5.2) (full estimation results are in Appendix A3.1 and A3.2).

$$\begin{aligned}
 O_{cnq}(\text{jets}) & \\
 &= fuel * (3.49seat_{cnq} + 2.39asl_{cnq}) \\
 &+ (11.15seat_{cnq} + 3.02asl_{cnq})
 \end{aligned} \tag{5.1}$$

$$\begin{aligned}
 O_{cnq}(\text{turboprop}) & \\
 &= fuel * (2.03seat_{cnq} + 0.50asl_{cnq}) \\
 &+ (13.81seat_{cnq} + 0.32asl_{cnq})
 \end{aligned} \tag{5.2}$$

We see the turboprop operating costs are less sensitive to fuel price, an expected result based on conclusions from chapter 2. Turboprops burn less fuel per seat and per mile compared with jet aircraft. For the non-fuel operating cost, we see that the turboprop has a slightly higher cost related to seats and a significantly lower cost related to distance.

5.1.2 Jet and Turboprop Ownership Cost

In this section, we consider the cost of aircraft ownership, data for which is published in the US DOT Form 41, Schedule P-5.2. We collect data on aircraft depreciation and rentals for turboprops and jets separately for each airline (c), aircraft type (n), and year-quarter (q). To be consistent with the linear operating cost models, the data spans the years 2003-2009 inclusive and we deflate the cost values to be in constant 2006 dollars. We estimate separate vehicle ownership costs models following the equation in (5.3) for turboprop and jet aircraft, using ordinary least squares and panel specific standard errors and assumed autocorrelation within panels.

$$OWN_{cnq} = \alpha + \sum_c \phi_c + \omega seat_{cnq} + \varepsilon_{cnq} \quad (5.3)$$

Where

$seat_{cnq}$ is the seat capacity

ϕ_c and ω are coefficients to be estimated

The results are presented in Appendix A3.3 and A3.4. The constant terms were insignificant in both the jet and the turboprop operating cost models, so that the preferred model for ownership cost is simply a function of seat capacity and the airline fixed effects. Comparing the preferred model for turboprops and jets, we see that the value of ω reflects the lower ownership costs of turboprops.

5.1.3 High Speed Rail Cost

Defining a HSR cost model presents a unique set of challenges compared with the aircraft cost model development. There are currently no HSR systems in the United States from which to collect cost and operating statistics. While there are many HSR systems across the world, publicly available data is limited and not available in a consistent format. For example, many HSR operators present their operating statistics in annual reports, yet these statistics may be aggregated with conventional rail operations. De Rus et al. (2009), in a comprehensive study of HSR system costs and HSR modeling techniques, notes the challenge of comparing (and therefore modeling) costs across HSR systems. Because HSR projects are built over various topographical landscapes, different technical solutions and levels of investment are needed. Therefore, instead of employing a statistical model to capture HSR costs, we will build an engineering model for HSR operating cost in which we sum the key drivers of cost.

The data source chosen for the development of such a model is the California High Speed Rail Authority 2009 Business Plan Report to the Legislature. As discussed in chapter 1, the CA HSR system is one of the designated corridors to receive federal funding; it is also under a state-wide mandate for the development of the system. Furthermore, as we are interested in short-haul travel, the 520 mile distance of the Phase 1 development from San Francisco to Anaheim and the 490 distance from San Francisco to Los Angeles is a good fit for the scope of the numerical example (the individual segments are presented in Table 5.1).

Phase 1 development is expected to be complete in 2020, the year when operations begin. The CA HSR Business Plan reports projected operating statistics starting in 2020 from which we can estimate the number of operations a trainset makes in one year. The CA HSR Business Plan reports the number of train operations per day and the number of trainsets required to make this number of train operations per day (Table 5.2). It is also noted that trains can be made of one or two trainsets. Assuming that half of all train operations include a single trainset, we estimate the average operations per trainset-day to be 4.03, which we scale to 1470.4 operations per year.

Table 5.1 California High Speed Rail segments.

Segment Start	Segment End	Distance (miles)
San Francisco Bay Area	San Jose	50
San Jose	Merced	120
Merced	Fresno	60
Fresno	Bakersfield	115
Bakersfield	Palmdale	85
Palmdale	Los Angeles Basin	60
Los Angeles Basin	Anaheim	30

Table 5.2 Trainset operating statistics for CA HSR, 2020-2035.

Year	Train operations per day (Reported)	Trainset operations per day (Estimated)	Trainsets required (Reported)	Operations per trainset-day (Estimated)
2020	121	181.5	45	4.03
2021	174	261.0	65	4.02
2022	219	328.5	82	4.01
2023	245	367.5	91	4.04
2024	247	370.5	92	4.03
2025	249	373.5	93	4.02
2026	251	376.5	93	4.05
2027	253	379.5	94	4.04
2028	255	382.5	95	4.03
2029	257	385.5	96	4.02
2030	259	388.5	96	4.05
2031	261	391.5	97	4.04
2032	263	394.5	98	4.03
2033	265	397.5	99	4.02
2034	268	402.0	100	4.02
2035	270	405.0	100	4.05

In the following sections, we develop separate HSR cost models for ownership and operating costs such that the cost definitions are consistent with the aircraft cost models; in the final section of the chapter, we will consider the infrastructure development cost of HSR. One challenge related to these cost and operational estimates are that they are projected, not experienced. To this end, we put the cost projections into context by reviewing costs experienced for HSR systems across the world presented in de Rus et al. (2009). All values presented in this HSR section are in 2006 dollars.

5.1.3.1 Ownership Cost

The CA HSR Business Plan reports that the cost of one HSR trainset, with an expected 500 seats, is \$32.17 million, or \$64,340/seat. De Rus et al. (2009) reports three categories of HSR vehicle acquisition costs: a low cost scenario of \$33,700/seat; a medium cost scenario of \$56,167/seat; and a high cost scenario of \$73,017/seat. The CA HSR Business Plan estimates are between the medium and high scenarios.

To achieve a value of vehicle ownership cost per operation, we estimate the value of vehicle ownership for an increment of time and then scale this cost by the number of operations. We will do this by using the capital recovery formula presented by de Neufville (1990) shown in (5.4). This function converts the total purchase price into a present value of yearly payments (R) by capturing amortization of the present value of the trainset cost ($P = \$32.17$ million) over $N = 40$ years at an interest rate of $r = 3.5\%$. The interest rate is the published rate in the CA HSR Business Plan, and de Rus et al. (2009) reports that the expected useable life of a HSR train is 40 years. We achieve a value of \$1.51 million in vehicle ownership costs per year. We divide this total over the 1470.4 trainset operations per year (Table 5.2), and achieve a fixed vehicle cost per operation of \$1026.93.

$$R = \frac{P[r(1+r)^N]}{[(1+r)^N - 1]} \quad (5.4)$$

The fixed cost is for a single trainset with 500 seats. However, more than 500 passengers may be assigned to a HSR vehicle per operation. Therefore, we consider a variable cost related to a vehicle cost as well. As each trainset has 500 seats, we calculate a per seat cost of \$2.06. This will be added to the variable cost, further explored in the following section.

5.1.3.2 Operating Cost

Direct and indirect operating costs are estimated and reported in the CA HSR Business Plan for the first 15 years of planned operation, 2020-2035 (Table 5.3). To be consistent with the operating costs considered for aircraft, we consider direct operating costs only: labor, power/energy, and direct maintenance of trainsets. The operating costs are reported for the year 2035 (presented in 2006 dollars).

From the data in Table 5.2 we estimate there are 147,825 trainset operations per year in 2035; with 500 seats per trainset, there are 73.9 million seat operations in the year 2035. The CA HSR business plan also reports in 2035, 43.1 million trainset-miles will be covered. Using the direct operating cost (DOC) figures in Table 5.3 along with the operating statistics, we estimate a DOC per seat-mile of \$0.0386. We compare this DOC figure to the results presented in de Rus et al. (2009) for operating costs and direct maintenance costs of HSR systems in Europe (Table 5.4).

Table 5.3 Operating cost categories for High Speed Rail.

	Category	Cost (\$ millions)
Direct Operating Costs (DOC)	Train Driving and Staffing	108.96
	Power/Energy with Green surcharge	344.47
	Maintenance of Trainsets and Vehicles	377.28
	Total DOC	830.71
Indirect Operating Costs (IOC)	MOW Materials and Contracts	68.64
	Maintenance of Way (MOW) Labor	41.61
	Program Contingency	54.69
	Station Services and Security	61.56
	Sales, Marketing and Reservations	68.85
	Control Center Operations	4.40
	General/Admin Support	17.91
	Total IOC	317.66

We see that the value estimated from the CA HSR plan is less than those presented across the world. An explanation could be the significantly lower expected cost of energy. Comparing industrial energy prices by end-use sector from the United States and Europe, we find that in some instances the energy prices in Europe are almost double those experienced in the United States (European Union, 2010; Energy Information Agency, 2010). A related issue that could be responsible for the operating cost discrepancy is the leverage a HSR operator has over the energy supplier; this is cited as a source of energy cost discrepancy across European HSR systems (de Rus et al., 2009). A final explanation could be labor and staffing rates. The CA HSR expects to use higher levels of automation seen in the systems listed below (California High Speed Rail Authority, 2008).

Table 5.4 Operating cost for European High Speed Rail systems.

Country	Type of Train	Seats	Operating Cost per Seat-Mile (\$)
France	TGV Reseau	377	0.182
	TGV Duplex	510	0.150
	Thalys	377	0.288
Germany	ICE-1	627	0.241
	ICE-2	368	0.336
	ICE-3	415	0.202
	ICE 3 Polyc.	404	0.238
	ICE-T	357	0.244
Italy	ETR 500	590	0.323
	ETR 480	480	0.318
Spain	AVE	329	0.310

Including variable vehicle operating cost, the final variable cost coefficient is $\beta_h = 2.06 + .03855 * seat * distance$.

5.1.4 Travel Time

We estimate travel time functions, with travel time as a function of distance, for the three vehicle types. For the aircraft, we use the operating statistics from the DOT Form 41 dataset. For turboprop and jet aircraft, the travel time function is as follows:

$$tt_{cnq} = \alpha + \delta asl_{cnq} + \varepsilon_{cnq} \quad (5.5)$$

Where tt is the travel time and asl is the average stage length traveled by an airline-aircraft pair in a year-quarter. Again, the dataset is an unbalanced panel, and we estimate using ordinary least squares and panel specific standard errors and assumed autocorrelation within panels. The results are shown in Appendix 4.

For the travel time function for HSR, the data is simply for one system, for one year, and for one vehicle type. We collect 44 observations of travel time (tt) and distance (which we will refer to as stage length, sl , as it is not an average) from the California High Speed Rail Authority (2010). The function is a simpler representation of travel time, and we use ordinary least squares for the estimation.

$$tt = \alpha + \delta * sl + \varepsilon \quad (5.6)$$

We find that the jet aircraft has the highest fixed travel time and the lowest variable travel time, while the HSR vehicle has the lowest fixed travel time and the highest variable travel time. Jet aircraft operations involve gate push-back, taxi, take-off; then they reach a cruising altitude at which they travel at very high speeds. While the HSR operation involves less of this fixed travel time, the speeds achieved by the system are significantly slower than jet travel. The turboprop aircraft experiences fixed and variable travel times between those of the jet and HSR. As an aircraft, it has a fixed travel time involving push-back, taxi and take-off, but compared with the jet achieves a lower cruising altitude. When it reaches that altitude, it travels slower than the jet aircraft, yet still faster than the HSR.

It should be noted that all travel times estimated are vehicle travel times and not passenger travel times. Passenger travel times on a corridor could be defined more broadly, to include port (airport or HSR station) access time and a port processing (security) time. The inclusion of such additional times would likely affect the numerical examples to be presented below, yet the direction of influence is unclear. Related to a processing time, the CA HSR Business Plan notes that HSR travelers are not expected to face security screening, consistent with the current North East Corridor rail system; the processing time of air will therefore certainly be longer. Related to port access time, the HSR systems will have stations with high accessibility, located in the downtown areas with business and some residential density. However, the aircraft modes benefit from more dispersed origin and destination airports, which match the land patterns in the United States closely (Clever, 2006). The incorporation of additional travel time for

terminal access and egress is discussed in the following chapter and left as a direction for future research.

5.1.5 Additional Inputs

The additional inputs required for our model include the travel distance, passenger flows, the distribution of passengers across value-of-time groups, and the value of time for each group.

Both Berry et al. (1996) and Adler et al. (2005) distinguish two passenger groups, business and leisure, using discrete choice models with data collected from aviation passengers. Adler et al. (2005) estimates that passengers are 43 percent business and 57 percent leisure. In the same study, it was found that the dollar values of in-flight time and schedule delay for the two groups are statistically different. The value of in-flight time is \$69.70/hour for business passengers and \$31.20/hour for leisure passengers while the value of schedule delay is \$30.30/hour for business passengers and \$4.80/hour for leisure passengers. Beyond the estimation, the use of different values of time for travel time and schedule delay is also represented in the literature. In a recent report by Ball et al. (2010), in-flight delay and schedule delay are valued at different rates, with the in-flight value of time being a weighted average across business and leisure travelers, \$37.6/hour in 2007 dollars, and the schedule delay being the weighted average of schedule delay from the Adler et al. (2005) study.

The analytic total logistics cost function as currently written does not allow for different values of travel time and schedule delay. In the function, we consider that the value of the time spent in schedule delay to be equal to the value of travel time. In the following numerical example, we will consider the business passenger value of time to be \$69.70/hour and that of leisure passengers to be \$31.20/hour.

To determine passenger flow, we collect data from the US DOT Form 41 Schedule T100 database. T100 contains data on passenger traffic in the US at the segment level, from which we determine the number of aviation passengers traveling from San Francisco International Airport (SFO) and Los Angeles International Airport (LAX). The corridor flow one year, October 2007-September 2008, equates to 387 passengers per hour in each direction (when we consider there are 365 days in one year and 16 typical hours of vehicle operations per day).

In considering the California Corridor from San Francisco to Los Angeles, we use the Form 41 reported 377 miles between SFO and LAX. While the HSR distance is longer (SFO-Los Angeles is 418 miles, while San Francisco to Los Angeles is 490 miles), for illustration purposes will set the constant distance to be 377 miles.

While we will consider the total logistics cost variation over fuel price, also it will become convenient to explore the sensitivity of the results to parameters beyond fuel price. Therefore, we will need to choose a value of fuel price to hold constant. Using Form 41 data, we estimate that across all jet and turboprop observations, the average fuel price paid in 2008 (converted to 2006 dollars) is \$3.21/gallon.

Table 5.5 presents a summary of the additional inputs presented in this section.

Table 5.5 Literature summary on traveler inputs.

Parameter	Parameter Value	Description	References
Business traveler value of time (λ_h)	\$69.70/hour	In-flight time	Adler et al. (2005)
	\$30.30/hour	Schedule delay	
Leisure traveler value of time (λ_l)	\$31.20/hour	In-flight time	Adler et al. (2005)
	\$4.80/hour	Schedule delay	
Average traveler value of time ($\bar{\lambda}$)	\$37.6/hour	In-flight time	Ball et al. (2010)
	\$15.77/hour	Schedule delay	
Percent			
Business travelers (% Q_h)	43		Adler et al. (2005)
Leisure Travelers (% Q_l)	57		
Total passenger demand per hour (Q_t)	387		US DOT
Distance traveled (miles)	377		
Fuel price (\$/gallon)	\$3.21/gallon		

Values in **bold** are used in the numerical examples.

5.2 Numerical Examples

5.2.1 Sensitivity of Total Logistics Cost to Fuel Price

When we plot the total logistics cost (TLC) per passenger against fuel price for all six vehicle combinations (Figure 5.1), we first see that the curves cross between \$4.00/gallon and \$6.25/gallon. This “transition region” is contained, such that for fuel prices below \$4.00/gallon there is a consistent cost ordering while for fuel prices above \$6.25/gallon there is a different, but also consistent, cost ordering. Thus the minimum cost vehicle combination is only impacted by fuel price in a small transition area; and the fuel prices that bound the transition area are fuel prices we expect to experience in the next 25 years. In 2010, the Energy Information Administration (EIA) (2010) reports that jet fuel prices are \$2.06. In 2020, the predicted fuel price is \$3.58; this prediction rises to \$6.00/gallon in 2035 (all EIA predictions are reported in 2006 dollars). This transition area is therefore particularly important to analyze for the California Corridor. In this transition area, the minimum cost designation changes from jets alone to turboprops alone to turboprops and HSR.

HSR TLC is not impacted by fuel price (as we assumed the HSR energy price is independent of fuel price) while the TLC for a corridor served by jets alone or turboprops alone increases almost linearly with fuel price. For the mixed vehicle cases with HSR as one of the vehicles, the rate of increase with fuel price decreases with fuel price. This is because, as fuel price increases, more and more passengers are assigned to the HSR, a vehicle unaffected by increasing fuel price.

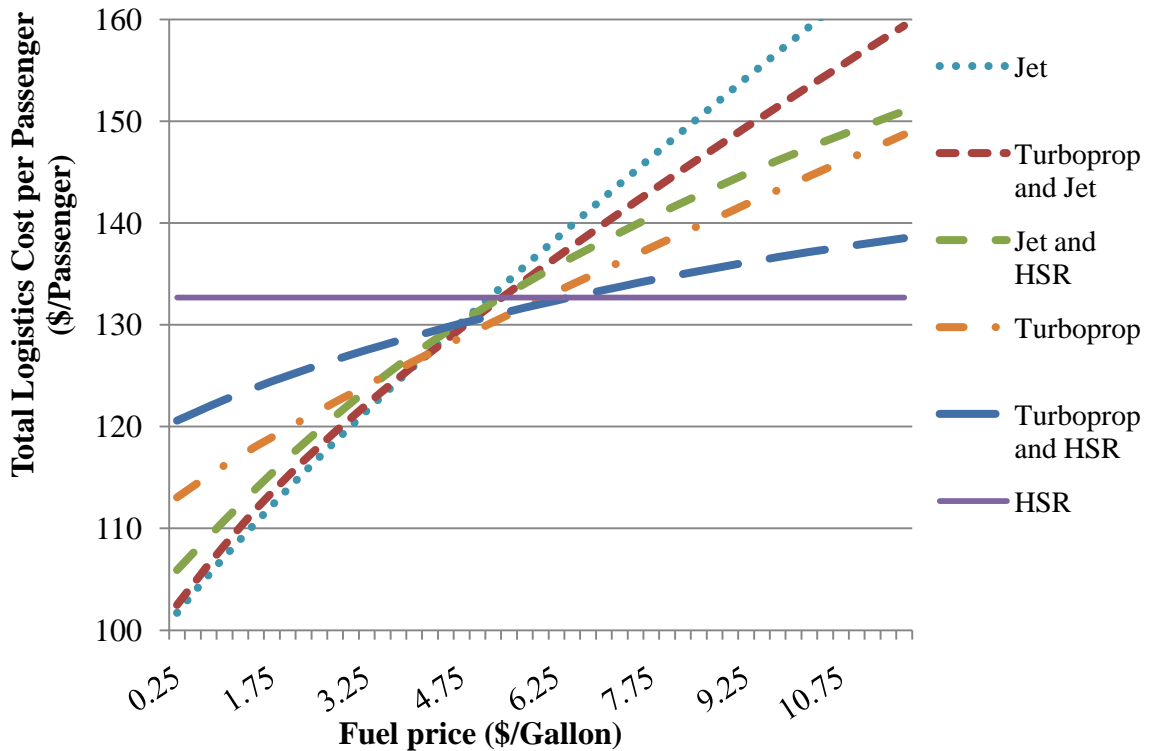


Figure 5.1 Total logistics cost vs. fuel price.

We next evaluate how the vehicle frequency that minimizes total logistics cost changes over fuel price for each vehicle combination (Figure 5.2). As we expect, each plot of frequency vs. fuel price is monotonically decreasing. The curves decrease more slowly as fuel price increases because total logistics cost is concave in frequency. The minimum TLC cost technology does not necessarily have the highest frequency, as passengers also value travel time in addition to schedule delay.

The results show that it is possible to increase the vehicle frequency that serves a corridor by switching modes, for example, from jet to HSR. The possibility of increasing frequency at the expense of increasing travel depends on the relationship between the unit costs of travel time and schedule delay, which, as discussed above, are assumed equal in this analysis. It is possible that with onboard amenities (such as wireless internet) and with uninterrupted “laptop open” time, the value of schedule delay may become more heavily weighted compared with the value of in-vehicle time (Neels and Barczi, 2010).

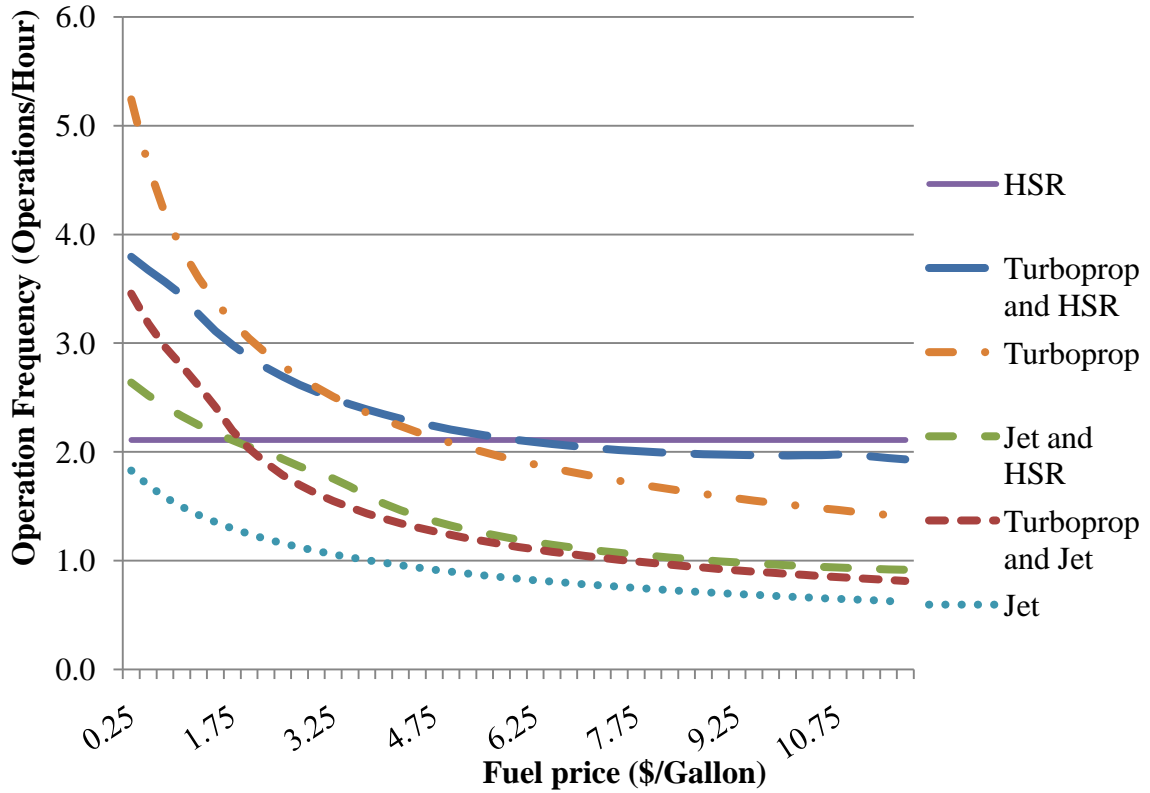


Figure 5.2 Frequency vs. fuel price.

5.2.2 Sensitivity of Total Logistics Cost to Distance

To consider the sensitivity of these results to distance, we vary distance while holding fuel price and the other parameters constant (Figure 5.3). We find that, for the current set of parameters, there is a distance transition point between 300 and 375 miles. For corridors of distances below 300 miles, there is a clear order from highest to lowest cost vehicle combinations; a different but equally well-defined order exists for corridors of distances great than 375 miles. As the fuel price increases, the transition point occurs at a longer stage length. Longer stage lengths favor the faster jet technology, but higher fuel prices favor the HSR technology that is insensitive to fuel price. As fuel price increases, the transition from HSR to jet (along with the mixed technologies) therefore occurs at a longer stage length. Therefore, we find that for a given fuel price, there is a well-defined transition point, before and after which the order of minimum cost combinations are not impacted by distance.

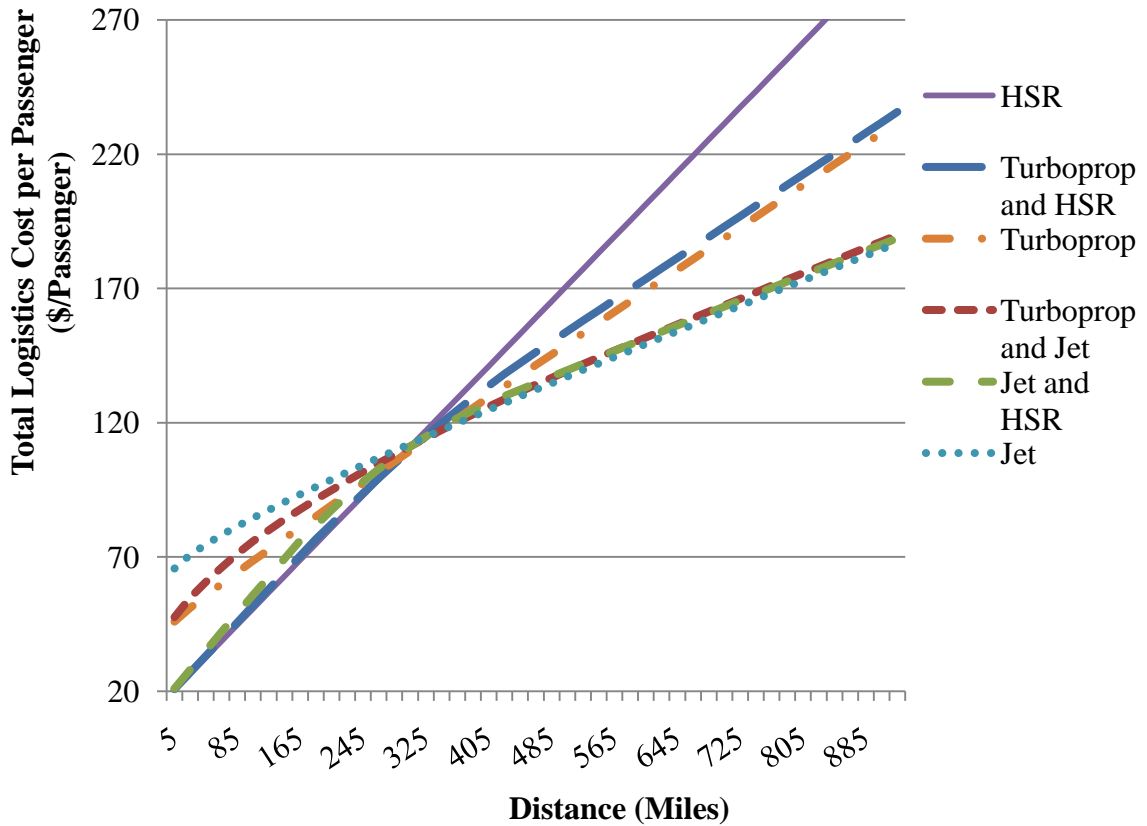


Figure 5.3 Total logistics cost vs. distance.

5.2.3 Sensitivity of Total Logistics Cost to Passenger Demand and Value of Time

To consider the sensitivity of these results to passenger demand, we vary the total demand while keeping the 43/57 percent ratio of business/leisure passengers constant. We find for the set of parameters in Table 5.5, for passenger demands about 325 passengers/hour and greater, there is an order of minimum-cost vehicle combinations that does not change. However for passenger demands lower than 325/hour, there is significant switching of minimum-cost designations across vehicle combinations. Therefore, we find that for more extreme demands (for example, higher demands than the California Corridor) jet aircraft alone minimize costs at the given level of parameters. This seems to conflict with the widespread belief that HSR becomes more competitive as corridor density increases. However, at the level of inputs explained by Table 5.5, the turboprop has a lower fixed cost and therefore, for low levels of passenger demands, has the minimum cost. At higher demand levels, the HSR certainly has higher frequencies compared with the jet, but the jet is able to achieve minimum cost due to the other cost incurred by the passengers, the travel time.

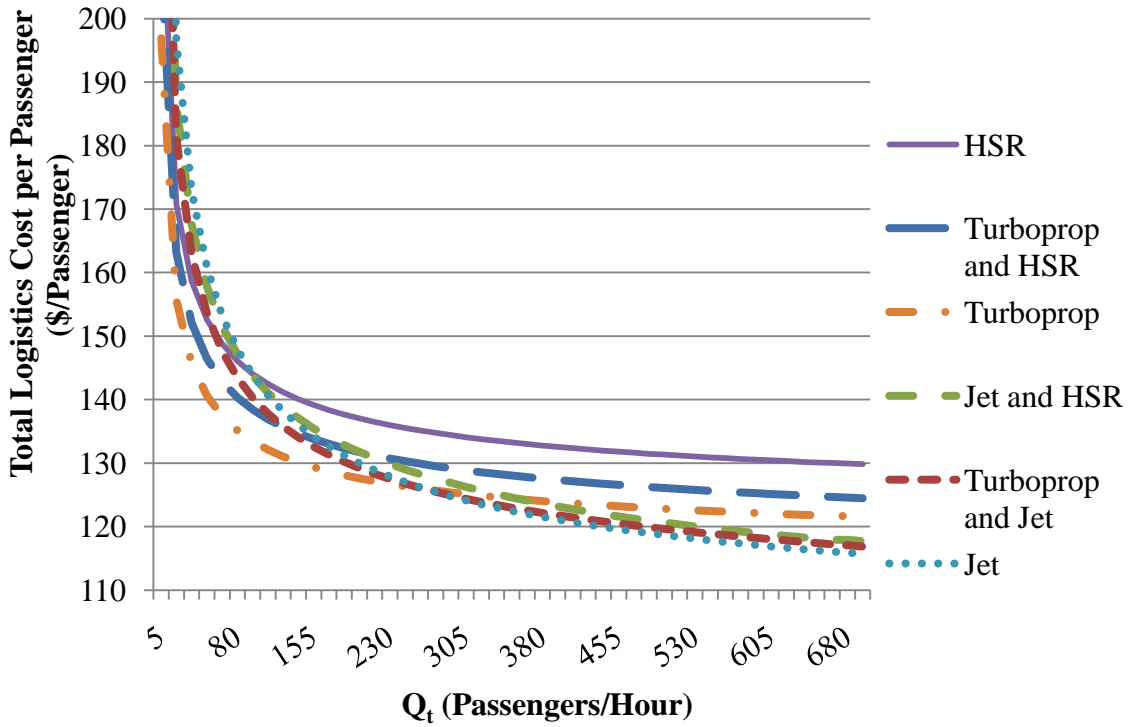


Figure 5.4 Total logistics cost vs. total passenger flow.

In Figure 5.5, we find when we vary the ratio of business/leisure passengers that the order of minimum-cost vehicle combinations is fairly stable, except at very low percentages of business passengers.

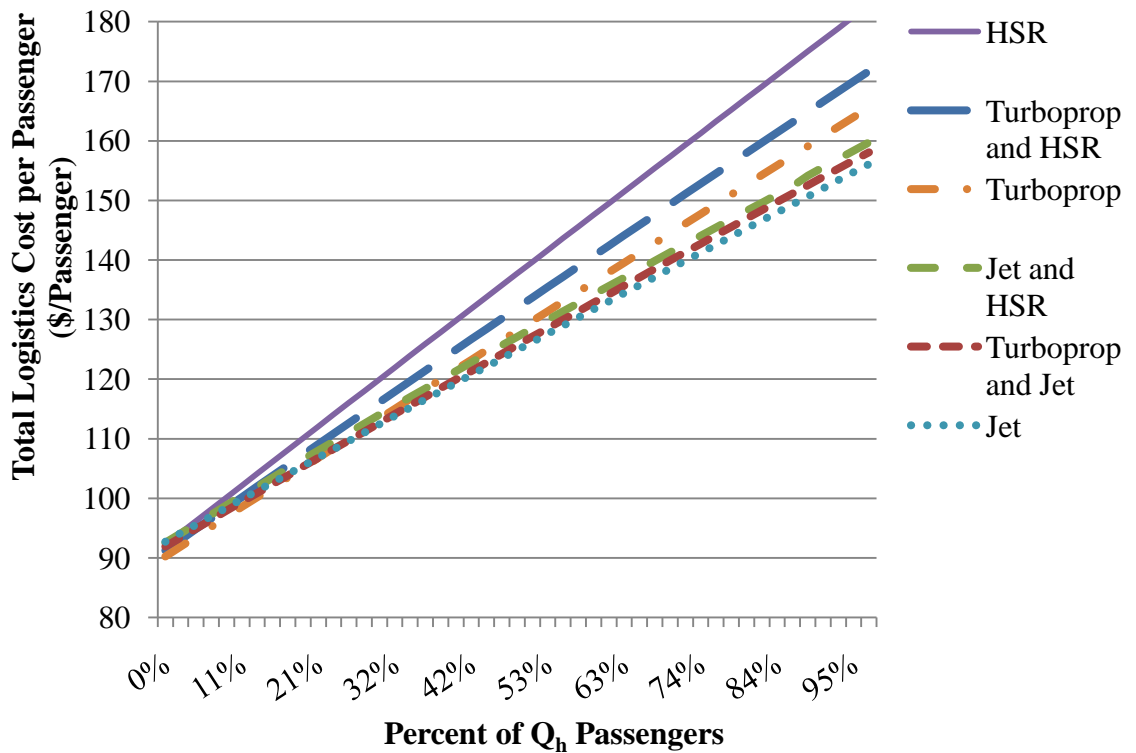


Figure 5.5 Total logistics cost vs. percent of business passengers.

When we fix the ratio of business to leisure value of time to $\frac{\lambda_h}{\lambda_l} = 2.23$ and vary the business (and leisure) passenger value of time, we find a specific transition point. Figure 5.6 shows how the TLC varies with business passenger value of time. Again, we find a very specific transition point at $\lambda_h = \$30\text{-}58/\text{hour}$, which is close to the estimates presented in the literature (Table 5.5).

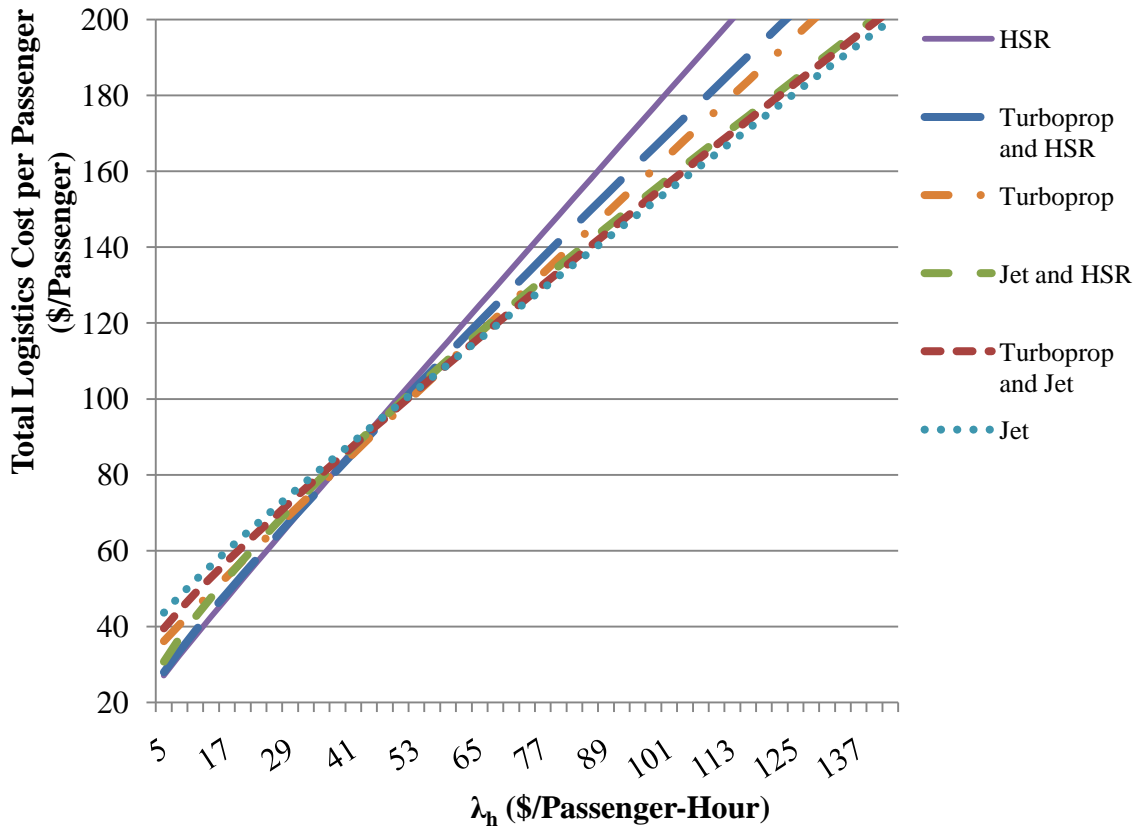


Figure 5.6 Total logistics cost vs. business passenger value of time.

5.3 High Speed Rail Infrastructure Costs

An additional consideration related to HSR is the cost to construct the system. Infrastructure is presented as a consideration for HSR as HSR systems in the United States are either in the planning or early stages of development. While the air transportation system certainly incurred an infrastructure-related cost at one time and continues to incur costs a related to maintenance and possible expansion, the HSR system must be developed and then additionally maintained.

The infrastructure costs of the CA HSR system are presented in the CA HSR Business Plan. Costs are presented in four broad categories. The first category is installing the necessary communication and electrification systems. The second is testing and commissioning of the system. The third is program implementation, which includes pre-construction activities including environmental reviews, preliminary engineering, and pre-construction activities. The fourth considered is all other infrastructure costs, which are reported as specific to the corridors shown in Table 5.1. These include final design;

right-of-way; environmental mitigation; rail and utility relocation; earthworks items; structures, tunnels, and walls; grade separations; building items; and track items. All costs are presented in the CA HSR Business Plan as year of expenditure costs over all or a subset of the years 2009 and 2020 inclusive. We convert these values into the 2006 present value of the total cost for each category using the following function:

$$P = \sum_N \frac{R}{(1+i)^N} \quad (5.7)$$

where R is the value of a future payout in one year, N is the number of years over which the expenditure is incurred, i is the interest rate (set to 3.5% as reported in the CA HSR Business Plan), and P is the present value of all the infrastructure related expenditures. While the costs are not all incurred over the full 12 years, we can consider that the infrastructure charges can be allocated in this way because operations do not begin until 2020. To convert the present value of the total infrastructure related cost, we use the capital recovery equation (5.4). For the capital recovery equation we define N , the number of years for which the payments can be amortized, to be 47. De Rus et al. (2009), in discussing a methodology for which to develop HSR cost functions, discusses that the operating life should be considered to be 35 years in addition to the construction time (which is 12 years noted in the CA HSR Business Plan). The totals presented in Table 5.6 (in 2006 dollars) represent the infrastructure costs for the entire corridor of length 520 miles.

Table 5.6 Infrastructure and related costs for CA HSR.

Category	Present Value (\$ millions)	Present Value per Mile (\$ millions)	Present Value per Year (\$ millions)
Infrastructure	28051.20	53.95	1224.97
Systems and Electrification	3712.70	7.14	162.13
Testing and Commissioning	87.75	0.17	3.83
Program Implementation	3048.92	5.86	133.14
Total	30560.48	67.12	1524.080

For comparison we again consider the work of de Rus et al. (2009), which reports infrastructure and systems and electrification costs per mile (in 2006 million \$/mile) for a variety of systems (Table 5.7). We see that the CA HSR estimate is on the higher end, similar to lines under construction in Italy and the Netherlands. De Rus et al. (2009) state that the differences in infrastructure and related costs vary widely with topography and geography, as well as the number and density of urban areas the system serves. There are many geography and density related challenges to building the CA HSR that could explain the cost discrepancy.

Table 5.7 Global infrastructure costs for HSR projects.

Country	Lines in Service		Lines Under Construction	
	Lower	Upper	Lower	Upper
Austria			20.78	44.48
Belgium	18.09		16.85	
France	5.28	21.12	11.23	25.84
Germany	16.85	32.35	23.59	37.07
Italy	28.65		15.73	73.92
Japan	22.47	34.71	28.08	44.93
Korea	38.42			
Netherlands			49.09	
Spain	8.76	22.47	10.00	19.66

In the consideration of infrastructure related costs, we evaluate if the HSR system savings are larger than the infrastructure costs on a per seat basis. Considering the number of trainset operations per year from Table 5.2 we find that the infrastructure cost per trainset-operation is \$9,028/operation or \$18.06/seat. We plot the total logistics cost per passenger against fuel price for two distances, 100 miles and 377 miles, shown in Figure 5.7, and evaluate if the savings from HSR is greater than \$18.06/seat. The figures include a black dotted line representing the sum of the HSR total logistics cost per passenger with an added \$18.06/seat to represent the infrastructure cost per seat. For a short distance of 100 miles, compared with a single vehicle fleet of jets alone, the HSR system savings are larger than the infrastructure costs for all fuel prices. When compared with a system of turboprop aircraft alone, the HSR system savings are larger than the infrastructure costs for jet fuel prices greater than \$3.25/gallon. For a distance of 377 miles, when compared with a system jet aircraft alone, the HSR system savings are larger than the infrastructure costs for jet fuel prices greater than \$8.25/gallon, a fuel price not anticipated to be experienced through the timeframe 2035 (Energy Information Administration, 2010).

5.4 Conclusions

The numerical example presented in this section shows that the minimum cost vehicle combination is sensitive to key parameters. For several parameters, including fuel price, there is a small transition zone within which the cost ordering changes significantly, and outside of which the orderings are stable. In the case of fuel price, we find this transition area to be in the \$4.00/gallon to \$6.25/gallon range, which is the range of fuel prices expected by the EIA between the years 2010-2035. We obtain similar results for several other parameters, but not all of them. This allows for more detailed, targeted studies of corridors with these models. The numerical example provides insight into HSR and aircraft operations over the California Corridor. We find that for shorter distances the HSR system has a lower cost than the aircraft modes over a wide range of fuel prices; this cost advantage erodes with distance. This points to the possibility of focusing on the role of rail in providing shorter distance service, for example, between San Diego and Los Angeles, a-167 mile corridor.

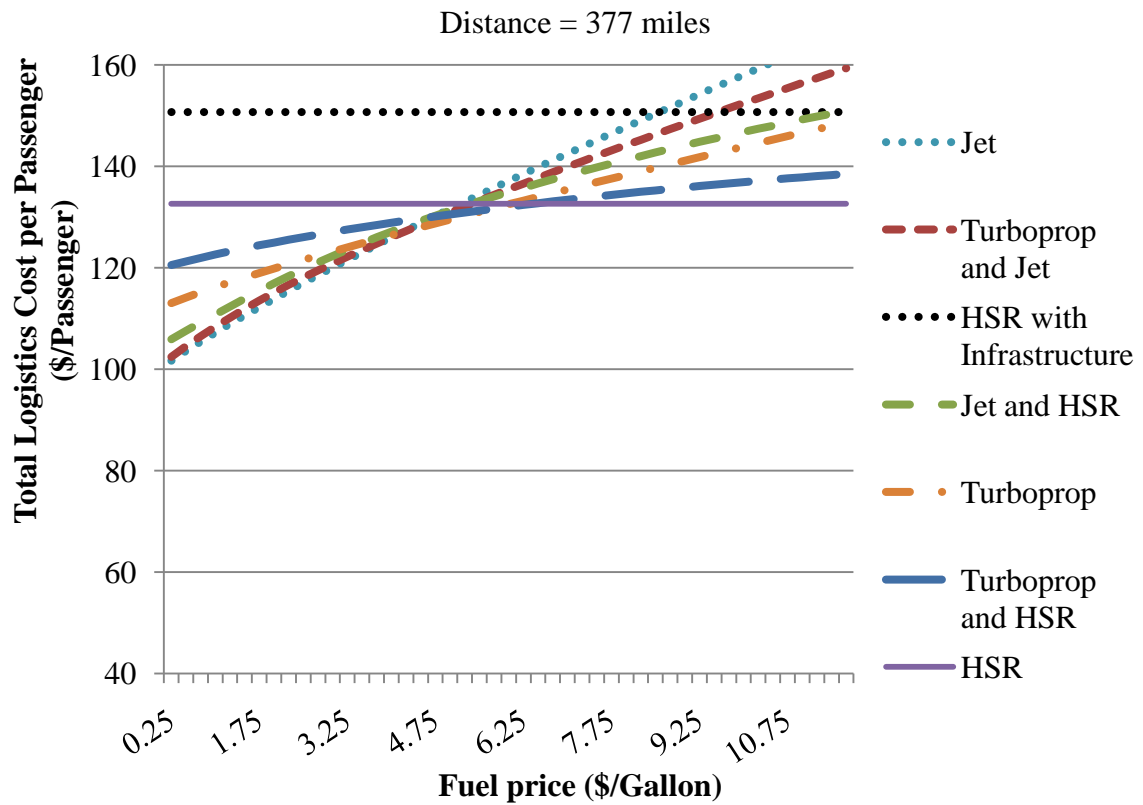
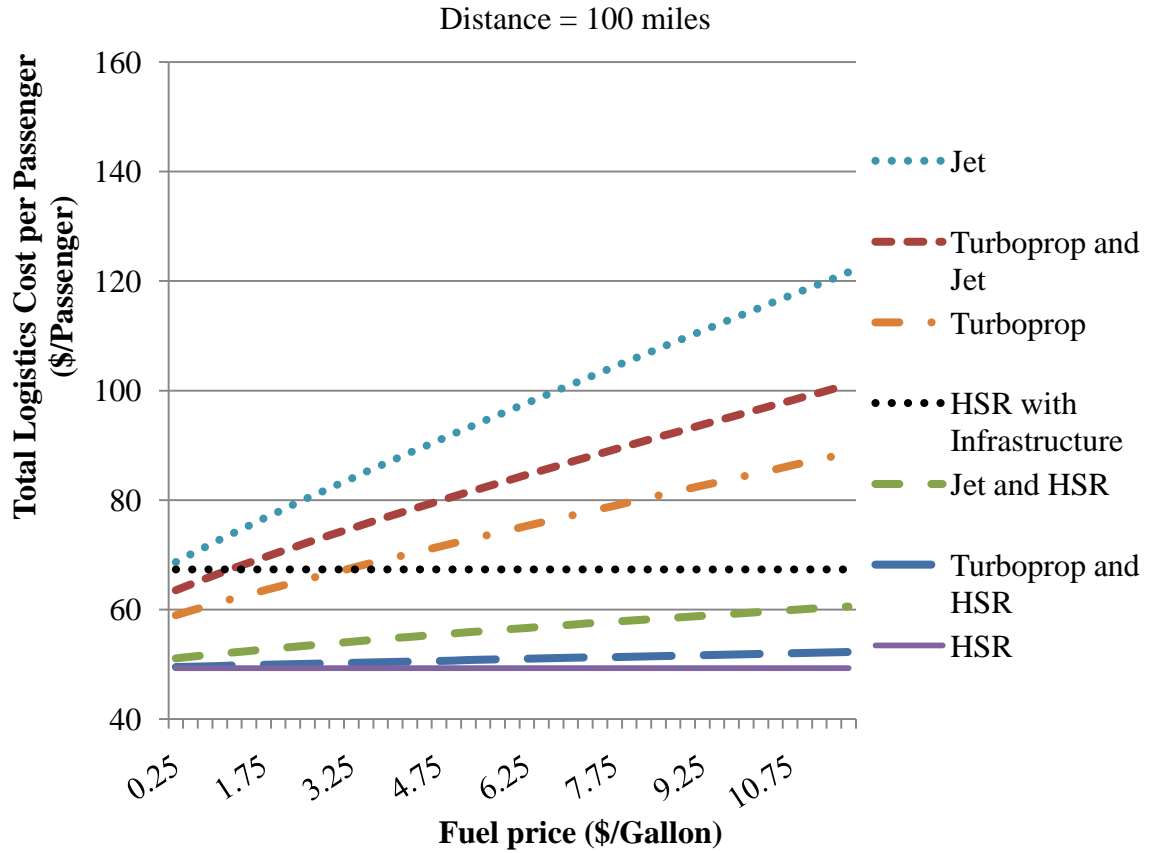


Figure 5.7 Total logistics cost vs. fuel price with infrastructure cost curve.

6.

Conclusions

6.1 Contributions

This research presents a methodology to determine the vehicle size, technology mix, and frequency to serve an intercity transportation corridor at minimum total logistics cost. Total logistics cost include both vehicle operating costs and costs incurred by the passenger. These costs are summed and compared for single and mixed vehicle scheduled services. The total logistics cost function captures the cost-reducing potential of alternative vehicles with different cost structures and service attributes. The models are formulated to be sensitive to fuel price, which may change significantly in the future as a result of market conditions or environmental policies.

In this research we develop two categories of models: empirical models and analytic models. Empirical vehicle operating cost models provide direct insights into the relationship between operating cost and fuel price and guide development of the analytic models. The analytic models provide a characterization of the intercity transportation system through which we can conceptually evaluate the relationship between optimum service characteristics and fuel price, among other factors.

The empirical models examine the roles of input substitution and induced technological change in managing fuel-related costs. Using Leontief cost models, which assume that the mix of inputs required to operate a given air vehicle is insensitive to factor prices, we find the minimum cost vehicle mix is highly sensitive to fuel price over the range of fuel prices experienced through 2010. We evaluate supplier-to-supplier input substitution by developing and comparing predictions from a Leontief model and a translog cost model estimated from the same data, at fixed values of seat capacity over a variety of distances and fuel prices. By building the two models and comparing their predictions, we illustrate a method to determine the prediction potential of a Leontief technology model and assess the importance of input substitution at the vehicle level. Also, in developing the translog model, we establish a comprehensive picture of the variables that influence operating cost. We find relationships between seat capacity, fuel price, and other key variables that have yet to be documented in the literature.

The empirical operating and passenger cost models together form a total logistics cost function through which the minimum cost vehicle technology and operational frequency can be determined. However, the scenarios for which empirical model predictions can be used are limited. The data used to generate such models reflect current vehicle technology, such as materials, propulsion systems, and the type of fuel. These models cannot, therefore, predict the impact of changes in such technologies. With the analytic

models, in contrast, we draw relationships between variables based on our underlying understanding of the nature of transport system production. To support the development of analytic models, we use the empirical models to identify induced technological change and input substitution as the qualitative changes in response to a fuel price increase or environmental policy.

In this thesis, we demonstrate the capability of analytic total logistics cost models to explore the impact of fuel price on the intercity transportation system. The analytic models consider aircraft vehicle size to be endogenous and continuous. By defining vehicles generically and characterizing them simply – by a fixed cost, a variable cost per seat, and a passenger cost in the form of travel time – this study enables the consideration of a multiplicity of intercity transportation vehicles. This is the benefit of employing continuum approximation models and capturing all pertinent costs incurred from operating and traveling in vehicles in one function.

Finally, in analyzing an intercity transportation corridor, this research allows for passengers with heterogeneous values of time. We begin by considering discrete passenger groups, each defined by a demand rate and a value of time. We then allow value of time to follow a continuous (uniform) distribution, such that the necessary parameters are a minimum and a maximum value of time. Considering a distributed value of time captures a more realistic picture of passenger preferences. By not pre-defining the value of time, we consider it a variable for parametric analysis. As values of time change with socioeconomic changes, this further generalizes the models presented.

In this research, we take a systems-level view to investigate the effects of climate change policy on aviation and develop a methodology to capture the system optimal response. This system optimal view presents the best achievable, or lowest total logistics cost, organization of intercity transportation. However, as we originally relaxed the constraint of existing institutions, we will want to compare this unconstrained model to a competitive model that captures the actions of existing intercity transportation institutions, such as the carriers. Comparing the system optimal and competitive models will shed light on the gap between ideal and realized. Furthermore, by quantifying the difference in fuel consumption and cost between the two models, we capture the monetary and GHG emissions cost of existing institutional constraints. It is recommended that these two models be components in a broader framework to support the formation and analysis of climate policy.

A proposed framework for intercity transportation system environmental impact assessment includes environmental impact models and environmental *policy* impact models. Environmental impact models characterize the level of emissions and resulting ecological and welfare impact from a given transportation system, while environmental policy impact models estimate what the system would look like – what and how vehicles will be operated over what network – after an environmental policy is instituted. The environmental impact models, generally computer-based models that take intercity transportation system characteristics as inputs, create a baseline picture of system pollutants and their effects. These inputs may inform the environmental policy scenarios

which become the inputs for the environmental *policy* impact models. This is a group of models that capture how an environmental policy scenario impacts system characteristics, such as vehicles in the system, operational levels and network structures. The output of the environmental policy impact models becomes an input for a second run of the environmental impact models to calculate a level of pollutants after an environmental policy. This framework, depicted in Figure 6.1, shows the relationship between environmental impact models and environmental policy impact models and that environmental considerations can be incorporated as both model inputs (as a policy) and outputs (as resulting pollutant profiles).

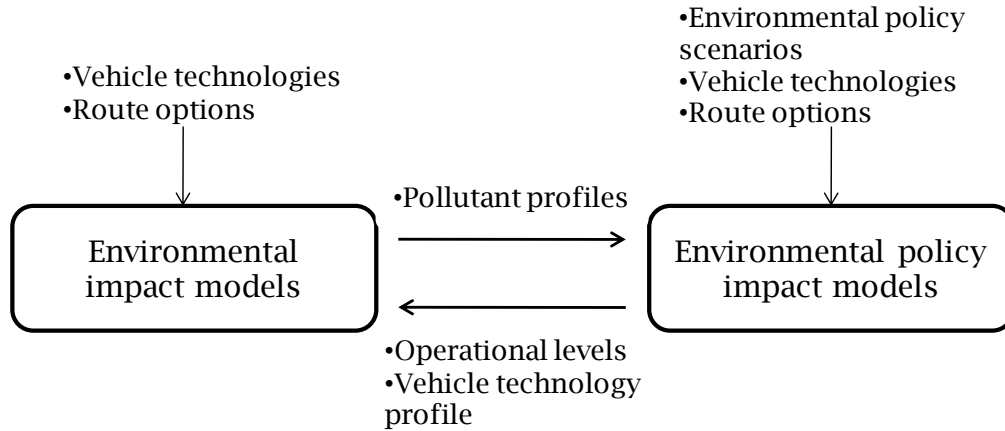


Figure 6.1 Intercity transportation environmental impact assessment framework.

Environmental impact models represent computer-based environmental models that simulate system inputs and capture the profiles of pollutants. These models are well developed and it can be expected that future models will continue the decades long trend toward increased modeling capability using more accessible, powerful and less expensive computer resources. However, while substantial efforts to improve the fidelity, usability, and level of integration of environmental impact models are underway, the need for environmental policy impact models has received less attention. This group of models can capture the long and short term impact of an environmental policy along with the system optimal and competitive responses. The outputs of these models then become inputs in the environmental impact models, such that the policy impact models show the operational profile of the system and the impact models estimate the environmental impact of such an operational profile.

In the proposed future work, we focus on the environmental policy impact models component, and suggest model refinements and developments.

6.2 Future Work

The research presented in this thesis can be built upon in many directions. The model can be refined, such that additional modes or details are captured; it can be expanded upon, such that additional system components are added; and additional models can be built for comparative purposes.

The modes considered could include other intercity modes, such as bus, auto, and conventional rail. While the addition of multi-passenger modes could be done with little change to the existing models, the addition of personal auto transportation would require additional variables. These variables would be necessary to capture an individual passenger's potential to not be assigned to the multi-passenger modes and rather be assigned to personal transportation. Additional refinements come in the addition of stochastic delay attributed to a mode related to weather, mechanical failures, and congestion in the total logistics cost function. A passenger would internalize these costs along with a central planner, as they generate excess time in the system along with excess operating cost.

The total logistics cost model developed in this dissertation could be extended to an intercity transportation network. The extension could come in the form of considering the local access and egress system as part of the intercity corridor or in considering a line-haul network, with the former illustrated here. The corridor could be extended into three phases of transport: access, line-haul, and egress. In the model developed in this thesis, the cost faced by the passenger is the time spent in the system, in terms of schedule delay and travel time in vehicle. As trips do not begin or end at the terminal (the airport or the high speed rail terminal), passengers internalize an expanded definition of time in the system: time spent in access and egress from the terminal. Furthermore, a central planner may internalize the operating cost of different access modes. Considering true-origin and true-destination enables an expanded definition of intercity vehicles. A mode with no access time, egress time, or schedule delay, such as auto, will be able to differentiate itself from a mode with access time. A mode with a port in the center of a highly dense city may find it has a lower relative cost when access cost is considered.

An additional model to develop is one that captures the competitive relationship between intercity transportation carriers. The “ideal,” or system optimal, arrangement could be compared with a competitive cost-based model that evaluates how operations will change when the intercity modes compete over a corridor. A competitive model of intercity travel using a game theoretic framework could include players such as a high speed rail or other surface intercity transportation operator, a single airline with a mixed technology fleet, or multiple airlines with single vehicle technology fleets. In the competitive models, demand must be elastic such that passengers switch between players, or modes, or choose auto or a no-travel option. Two categories of models, one that assumes the players set their schedules and vehicle technology independently (simultaneous), and one that assumes a dominant player (leader-follower game) could be developed; it is natural that in the context of intercity transportation the dominant player be an airline with jet aircraft especially for medium-haul distances. As system optimal models are used for policy planning and represent the best possible achievable outcome, they are a baseline against which the models of actual outcomes, the competitive models, can be compared.

Bibliography

Abrahams, M. (1983). A service quality model of air travel demand: an empirical study. *Transportation Research Part A: Policy and Practice*, 17, 385–393.

Adler, T., Falzarano, C. S., & Spitz, G. (2005). Modeling service trade-offs in air itinerary choices. *Transportation Research Record: Journal of the Transportation Research Board*, 1915, 20-26.

Air Transport Association. (2010). *Quarterly Cost Index: US Passenger Airlines*. Retrieved from <http://www.airlines.org/economics/finance/Cost+Index.htm>

Airbus. (2010). *A330/A340 Family*. Retrieved July 20, 2010, from www.airbus.com/en/aircraftfamilies/a330a340

Airbus. (2007). *A380 Navigator*. Retrieved December 19, 2007, from <http://events.airbus.com/A380/default1.aspx>

Albers, S., Böhne, J., & Peters, H. (2009). Will the EU-ETS instigate airline network reconfigurations? *Journal of Air Transport Management*, 15 (1), 1-6.

Anger, A. (2010). Including aviation in the European emissions trading scheme: Impacts on the industry, CO2 emissions and macroeconomic activity in the EU. *Journal of Air Transport Management*, 100-105.

ATR. (2008). *Products: ATR 72-500*. Retrieved from <http://www.atr.fr/public/atr/html/products/products.php?aid=506>

Ball, M., Barnhart, C., Dresner, M., Hansen, M., Neels, K., Odoni, A., et al. (2010). *Total delay impact study: a comprehensive assessment of the costs and impacts of flight delay in the United States*. Washington, D.C.: Federal Aviation Administration.

Berry, S., Carnall, M., & Spiller, P. T. (1996). *Airline Hubs: Costs, Markups and the Implications of Customer Heterogeneity*. NBER Working Papers, No. 5561.

Boeing Company. (2010). *787 Dreamliner*. Retrieved July 20, 2010, from <http://www.boeing.com/commercial/787family/background.html>

Boeing Company. (2008). *Commercial Airplanes: 737 Family*. Retrieved from <http://www.boeing.com/commercial/dc-9/index.html>

Bonnefoy, P. A., & Hansman, R. J. (2007). Investigation of the Potential Impacts of the Entry of Very Light Jets in the National Airspace System. *Journal of Aircraft, American Institute of Aeronautics and Astronautics*, 44 (4), 1318-1326.

Bureau of Transportation Statistics. (2008). *Direct Maintenance-Flight Equipment*. Retrieved from http://www.bts.gov/programs/airline_information/item_list_guide/html/schedule_p_5_2/direct_maintenance.html

Bureau of Transportation Statistics. (2007). *September 2007 Airline Traffic Data: Nine-Month 2007 System Traffic Up 3.6 Percent from 2006*. Retrieved from http://www.bts.gov/press_releases/2007/bts057_07/html/bts057_07.html

California High Speed Rail Authority. (2009). *Business Plan: December 2009 Business Plan Report to the Legislature*. Retrieved from http://www.cahighspeedrail.ca.gov/Business_Plan_reports.aspx

California High Speed Rail Authority. (2010). *Explore the Route: Interactive Map*. Retrieved from <http://www.cahighspeedrail.ca.gov/>

California High Speed Rail Authority. (2008, November 7). *High Speed Train Systems*. Retrieved from http://www.cahighspeedrail.ca.gov/Business_Plan_reports.aspx

Carter, D. A., Rodgers, D. A., & Simkins, B. J. (2004, July). *Fuel Hedging in the Airline Industry: The Case of Southwest Airlines*. Retrieved from <http://ssrn.com/abstract=578663>

Caves, D. W., Christensen, L. R., & Tretheway, M. W. (1984). Economies of Density Versus Economies of Scale: Why Trunk and Local Service Airlines Differ. *Rand Journal of Economics*, 15, 471-489.

Chester, M. V. (2008). *Life-cycle Environmental Inventory of Passenger Transportation in the United States*. Ph.D. thesis, University of California, Berkeley.

Chester, M., & Horvath, A. (2010). Life-cycle assessment of high-speed rail: the case of California. *Environmental Research Letters*, 5.

Chua, C. L., Kew, H., & Yong, J. (2005). Airline Code-share Alliances and Costs: Imposing Concavity on Translog Cost Function Estimation. *Review of Industrial Organization*, 26 (4), 461-487.

Clarke, J. P., Ho, N. T., Liling, R., Brown, J. A., Elmer, K. R., Tong, K., et al. (2004). Continuous Descent Approach: Design and Flight Test for Louisville International Airport. *Journal of Aircraft*, 41 (5), 1054-1066.

Clever, R. (2006). *Airport and Station Accessibility as a Determinant of Mode Choice*. Ph.D. thesis, University of California, Berkeley.

Coogan, M., RSG, Hansen, M., Kiernan, L., Last, J., Marchi, R., et al. (2009). *Innovative Approaches to Addressing Aviation Capacity in Coastal Mega-Regions*. Airport Cooperative Research Program .

Daganzo, C. F., & Garcia, R. C. (2000). A Pareto Improving Strategy for the Time-Dependent Morning Commute Problem. *Transportation Science*, 34 (3), 303-311.

Daganzo, C. F., & Newell, G. F. (1993). Handling Operations and The Lot Size Trade-Off. *Transportation Research Part B: Methodological*, 27 (3), 167-183.

Daganzo, C. (1999). *Logistics Systems Analysis* (Third Edition ed.). Berlin: Springer.

de Neufville, R. (1990). *Applied Systems Analysis, Engineering Planning and Technology Management*. New York: McGraw-Hill, Inc.

de Rus Mendoza, G., Méndez, F. J., Gagnepai, P., Nash, C. A., Segui, A. U., Vickermann, R., et al. (2009). *Economic Analysis of High Speed Rail in Europe*. Fundación BBVA Report.

Diewert, W. E., & Wales, T. J. (1987). Flexible Functional Forms and Global Curvature Conditions. *Econometrica*, 55 (1), 43-68.

Douglas, G. W., & Miller, J. C. (1974). *Economic Regulation of Domestic Air Transport: Theory and Policy*. Washington, DC: The Brookings Institution.

Embraer. (2008). *ERJ 145 Family*. Retrieved from http://www.embraercommercialjets.com/english/content/home_erj/

Energy Information Administration. (2010). *Average Retail Price of Electricity to Ultimate Customers: Total by End-Use Sector*. Retrieved from Independent Statistics and Analysis: Forecasts & Analysis: http://www.eia.doe.gov/cneaf/electricity/epm/table5_3.html

Environmental Protection Agency. (2010). *Greenhouse Gas Emissions*. Retrieved June 1, 2010, from Environmental Protection Agency: <http://epa.gov/climatechange/emissions/index.html>

Environmental Protection Agency. (2007). *Inventory of US Greenhouse Gas Emissions and Sinks: 1990-2005*. Washington DC.

Eriksen, S. E. (1978). *Demand Models for US Domestic Air Passenger Markets*. Cambridge, Massachusetts: Department of Aeronautics and Astronautics, MIT.

Espinoza, D., Garcia, R., Goycoolea, M., Nemhauser, G., & Savelsbergh, M. W. (2008). Per-Seat, On-Demand Air Transportation, Part I: Problem Description and an Integer Multi-Commodity Flow Model. *Transportation Science*, 42 (3), 263-278.

Eurocontrol. (2007). *SESAR: Objectives and Scope*. Retrieved August 12, 2007, from http://www.eurocontrol.int/sesar/public/standard_page/overview.html

European Environment Agency. (2006). *EMEP/CORINAIR Emission Inventory Guidebook –2007: Group 8: Other Mobile Sources and Machinery*. Retrieved from <http://reports.eea.europa.eu/EMEPCORINAIR4/en/page017.html>

European Union. (2010). Retrieved from Europe's Energy Portal: <http://www.energy.eu/#Domestic>

Federal Aviation Administration. (2007). *Capacity Needs in the National Airspace System: An Analysis of Airports and Metropolitan Area Demand and Operational Capacity in the Future*. MITRE Corporation.

Federal Aviation Administration. (Thursday, January 17, 2008, Notices). *Policy Regarding Airport Rates and Charges, Vol. 73, No. 12*. Federal Register.

Federal Railroad Administration. (2008, June 26). *Analysis of the benefits of high-speed rail on the Northeast corridor, Federal Railroad Administration Number: CC-2008-091*. Retrieved from Federal Railroad Administration: http://www.oig.dot.gov/sites/dot/files/pdfdocs/HSR_Final

Federal Railroad Administration. (2010). *High-Speed Rail Corridor Descriptions*. Retrieved September 15, 2010, from <http://www.fra.dot.gov/Pages/203.shtml>

Gittell, J. H. (2002). *The Southwest Airlines Way: Using the Power of Relationships to Achieve High Performance*. New York: McGraw-Hill.

Hansen, M. (1991). Assessing Tiltrotor Technology: A Total Logistics Cost Approach. *Transportation Research Record: Journal of the Transportation Research Board*, 1296, 31-44.

Hansen, M. M., Gillen, D., & Djafarian-Tehrani, R. (2001). Aviation Infrastructure Performance and Airline Cost: a Statistical Cost Estimation Approach. *Transportation Research Part E: Logistics & Transportation*, 37, 1-23.

Huber, M. (2008, October 7). New Turboprops: OEMs Flight Testing New Turboprops, Just as Fuel Costs Renew Interest in the Sector. *Aviation International News, Aircraft Section*, pp. <http://www.ainonline.com/news/single-news-page>.

Johnston, D. (1995, August 19). Relief for the Turboprop Blues; Small Is Suddenly Beautiful for Short-Hop Travelers. *New York Times, Business*.

Keeler, T. E., Merewitz, L. A., & Fisher, P. (1975). *Full Costs of Urban Transport*. Berkeley: University of California, Berkeley: Institute of Urban and Regional Development.

Kim, B., Waitz, I. A., Vigilante, M., & Bassarab, R. (2009). *Guidebook on Preparing Airport Greenhouse Gas Emissions Inventories*. Airport Cooperative Research Program Report 11.

Meyer, M. D., & Miller, E. J. (1984). *Urban Transportation Planning: A Decision-Oriented Approach*. McGraw-Hill.

Morrell, P., & Swan, W. (2006). Airline Jet Fuel Hedging: Theory and Practice. *Transport Reviews*, 26 (6), 713–730.

Mozdzanowska, A., & Hansman, R. J. (2004). *Evaluation of Regional Jet Operating Patterns in the Continental United States*. International Center for Air Transportation Report ICAT- 2004-1.

Neels, K., & Barczy, N. (2010). The Effects of Schedule Unreliability on Departure Time Choice. *NEXTOR Research Symposium, Federal Aviation Administration Headquarters*. Washington D.C.

Neuman, C., & Smilowitz, K. (2002). Strategies for Coordinated Drayage Movements. In R. Hall, & P. Mirchandani (Ed.), *Proceedings of NSF Real Time Logistics Workshop*. Long Beach, CA.

Odoni, A., & de Neufville, R. (2003). *Airport Systems: Planning, Design and Management*. New York: McGraw-Hill Professional.

Oster Jr, C. O., & McKey, A. (1984). Cost Structure and Short-Haul Air Service. In J. R. Meyer, & C. O. Oster Jr, *In Deregulation and the New Airline Entrepreneurs*.

Pew Center on Global Climate Change. (2004). *Global Warming Facts and Figures*. Retrieved June 2008, from http://www.pewclimate.org/global-warming-basics/facts_and_figures

Plaut, P. O. (1998). The Comparison and ranking of policies for abating mobile-source emissions. *Transportation Research Part D: Transport and Environment*, 3 (4), 193–205.

Reimer, D. S., & Putnam, J. E. (2007). The law of aviation-related climate change: The airport proprietor's role in reducing greenhouse gas emissions. *Journal of Airport Management*, 2 (1), 82–95.

Ryerson, M. S., & Hansen, M. (2009). Assessing the Role of Operating, Passenger, and Infrastructure Costs in Fleet Planning under Fuel Price Uncertainty. *Proceedings of the Eighth Annual FAA/EUROCONTROL Air Traffic Management Research and Development Seminar*. Napa, CA.

San Francisco International Airport. (2007). *Summary of Airport Charges Fiscal Year 2007/2008*. Retrieved from www.flysfo.com/web/export/sites/default/download/about/reports/pdf/SummaryofChargesFY0708.pdf

Scheelhaase, J. D., & Grimme, W. G. (2007). Emissions Trading for international aviation-an estimation of the economic impact on selected European airlines. *Journal of Air Transport Management*, 13, 253-263.

Smilowitz, K., & Daganzo, C. (2007). Continuum approximation techniques for the design of integrated package distribution systems. *Networks*, 50 (3), 183 – 196.

Smilowitz, K., Atamtürk, A., & Daganzo, C. (2003). Deferred Item and Vehicle Routing within Integrated Networks. *Transportation Research E: Logistics & Transportation*, 39, 305-323.

Smirti, M., & Hansen, M. (2007). Achieving a Higher Capacity National Airspace System: An Analysis of the Virtual Airspace Modeling and Simulation Project. *AIAA Modeling and Simulation Technologies Conference*. Hilton Head, SC, USA.

Steer Davies Gleeve. (2006). *Air and Rail Competition and Complementarity*. European Commission.

Swan, W. M., & Adler, N. (2006). Aircraft Trip Cost Parameters: A Function of Stage Length and Seat Capacity. *Transportation Research Part E: Logistics & Transportation*, 42, 105–115.

Viton, P. (1986). Air Deregulation Revisited: Choice of Aircraft Load Factors, and Marginal-Cost Fares for Domestic Air Travel. *Transportation Research Part A: Policy and Practice*, 2 (5), 361-371.

Waitz, I., Townsend, J., Cutcher-Gershenfeld, J., Greitzer, E., & Kerrebrock, J. (2004). *Aviation and the Environment: A National Vision Statement, Framework for Goals and Recommended Actions*. Retrieved October 3, 2007, from http://web.mit.edu/aeroastro/partner/reports/congrept_aviation_envirn.pdf

Wei, W., & Hansen, M. (2003). Cost Economics of Aircraft Size. *Journal of Transport Economics and Policy*, 37 (2), 279–296.

Wei, W., & Hansen, M. (2005). Impact of aircraft size and seat availability on airlines' demand and market share in duopoly markets. *Transportation Research Part E: Logistics & Transportation*, 41 (4), 315–327.

Williams, V. (2007). The Engineering Options for Mitigating the Climate Impacts of Aviation. *Philosophical Transactions of the Royal Society A*, 365, 3047–3059.

Zou, B., & Hansen, M. (2010). Impact of operational performance on air carrier cost structure-evidence from US airlines. *Presented at the 12th World Conference on Transportation Research*. Lisbon, Portugal.

Appendix 1: Jet Aircraft Operating Cost Model Estimates

A1.1 Aircraft Models and Airlines in Operating Cost Analysis

Year of Intro.	Aircraft Model	Seats	Airlines
1992	Canadair RJ-200/ER/-440	49	Air Wisconsin
2001	Canadair RJ-700	68	AirTran
2002	Embraer EMB-170	72	Alaska
1982	BAE-146-200	88	Aloha
1988	BAE-146-300	91	America West
2004	Embraer EMB-190	100	American
1997	Boeing B-777-300ER	111	ATA
1990	Boeing B-737-500	113	Atlantic Southeast
2003	Airbus A318	114	Comair
1996	Airbus A319	123	Continental
1998	Boeing B-737-700/700LR	128	Delta
1988	Boeing B-737-400	143	Frontier
1988	Airbus A320-100/200	148	Hawaiian
1998	Boeing B-737-800	150	Horizon
2001	Boeing 737-900	169	Independence Air
1996	Airbus A321	170	JetBlue
1982	Boeing B-767-200/ER	178	Midwest
1983	Boeing B-757-200	184	National
1998	Boeing B-757-300	222	Northwest
1986	Boeing B-767-300/ER	231	Pinnacle
1995	Boeing 777-200/20LR/233LR	282	Skywest
1997	Boeing B-767-400	286	Southwest
1989	Boeing B-747-400	360	Spirit
			Trans World
			United
			USAir

A1.2 Jet Aircraft Translog Operating Cost Model Results

	Model 1		Model 2	
Variable	Parameter Estimate	Standard Error	Parameter Estimate	Standard Error
t	-0.002***	0.001	-0.002***	0.001
First Order Terms				
Seats	0.400***	0.083	0.447***	0.029
Average stage length	0.803***	0.054	0.737***	0.019
Labor price	0.296***	0.038	0.329***	0.013
Fuel price	0.408***	0.037	0.417***	0.014
Utilization	-0.124***	0.036	-0.090***	0.014
Materials price	0.302	0.210	0.375***	0.084
Average age	0.037***	0.007	0.033***	0.005
Technology age	0.004**	0.002	0.003**	0.002
Second Order Terms				
Seats	0.206***	0.062	0.200***	0.050
Average stage length	0.126***	0.033	0.145***	0.030
Labor price	0.038***	0.012	0.043***	0.010
Fuel price	0.155***	0.034	0.134***	0.028
Utilization	-0.011	0.007	-0.009*	0.005
Materials price	0.717	0.632		
Average age	-0.001***	4.44*10 ⁻⁴	0.200	0.050
Technology age	-1.28*10 ⁻⁴	0.0003		
Interaction Terms				
Seats – Average stage length	-0.162**	0.079	-0.146***	0.065
Seats – Labor price	-0.123***	0.044	-0.125***	0.032
Seats – Utilization	0.015	0.033		
Seats – Materials price	0.123	0.273		
Seats – Fuel price	0.123***	0.048	0.127***	0.028
Seats - Average age	-0.021**	0.010	-0.016***	0.005
Seats – Technology age	0.003	0.007		
Fuel price – Average stage length	9.88*10 ⁻⁵	0.030		
Fuel price – Labor price	-0.114***	0.037	-0.097***	0.025
Fuel price – Average Age	-0.014***	0.005	-0.016***	0.004
Fuel price – Materials price	-0.582***	0.245	-0.316**	0.143
Fuel price – Utilization	-0.008	0.026		
Fuel price – Technology age	0.001	0.003		
Average stage length – Labor price	0.012	0.027		
Average stage length – Utilization	-0.040**	0.020	-0.042***	0.014
Average stage length –	0.085	0.171		

	Model 1		Model 2	
Variable	Parameter Estimate	Standard Error	Parameter Estimate	Standard Error
Materials price				
Average stage length – Average Age	-0.001	0.005		
Average stage length – Technology age	-0.006	0.004		
Labor price – Utilization	-0.007	0.021		
Labor price – Materials price	0.026	0.152		
Labor price – Average Age	0.015***	0.005	0.012***	0.003
Labor price – Technology age	0.003	0.003		
Technology age – Utilization	0.002	0.003		
Technology age – Materials price	0.010	0.019		
Technology age – Average age	-0.001*	0.001	-0.001**	0.000
Materials price – Average Age	0.043*	0.025	0.044***	0.018
Materials price – Utilization	0.096	0.101		
Utilization – Average age	-0.003	.005		
Airline Effects				
American	-0.002	0.020	0.004	0.020
Alaska	-0.125***	0.020	-0.126***	0.020
JetBlue	0.035	0.035	0.035	0.031
Continental	-0.014	0.021	-0.014	0.020
Independence	-0.045	0.059	-0.065	0.058
AirTran	0.035	0.029	0.033	0.029
Frontier	0.088**	0.041	0.088**	0.041
Hawaiian	-0.089	0.127	-0.139	0.110
America West	-0.017	0.023	-0.023	0.022
Spirit	-0.002	0.047	-0.005	0.046
Northwest	-0.029	0.020	-0.030	0.020
United	0.110***	0.017	0.106***	0.017
USAir	0.027	0.021	0.021	0.022
Southwest	-0.306***	0.027	-0.309***	-0.027
Midwest	-0.032	0.032	-0.033	0.032
Air Wisconsin	0.189***	0.057	0.162***	0.053
Comair	0.008	0.044	-0.008	0.041
SkyWest	-0.070	0.051	-0.090*	0.048
Horizon	-0.031	0.075	-0.049	0.072
Trans World	-0.095*	0.053	-0.095*	0.049

	Model 1		Model 2	
Variable	Parameter Estimate	Standard Error	Parameter Estimate	Standard Error
ATA	0.070**	0.034	0.071**	0.034
Atlantic Southeast	-0.005	0.046	-0.019	0.044
Pan Am Clipper Connection	-0.083	0.062	-0.103**	0.052

***Variables are significant at the 1% level

**Variables are significant at the 5% level

*Variables are significant at the 10% level

A1.3 Jet Aircraft Pilot Cost per Block Hour Model Results

Variable	Parameter Estimate	Standard Error
Constant	314.438***	39.920
Seats	0.828***	0.176
Airline Effects		
American	-25.110	25.299
Alaska	-20.503	28.213
JetBlue	-180.870***	31.739
Continental	-49.119**	24.533
Independence	-188.609***	37.497
AirTran	-164.132***	30.843
Frontier	-132.280***	30.638
Hawaiian	8.420	61.310
America West	-173.594***	24.456
Spirit	-221.711***	48.908
Northwest	-70.711***	24.013
United	-41.738	26.556
USAir	-82.430**	35.450
Southwest	-108.392***	26.724
Midwest	-86.371***	36.884
Air Wisconsin	-215.511***	33.358
Comair	-185.863***	33.426
SkyWest	-176.738***	34.009
Horizon	-147.673***	39.278
Trans World	-204.455***	40.344
ATA	-153.566***	53.292
Atlantic Southeast	-189.164***	41.761
Pan Am Clipper Connection	-244.283***	32.920

***Variables are significant at the 1% level

**Variables are significant at the 5% level

*Variables are significant at the 10% level

A1.4 Jet Aircraft Fuel Consumption Linear Model

Variable	Full Model		Preferred Model	
	Parameter Estimate	Standard Error	Parameter Estimate	Standard Error
Constant	497.638**	224.433		
Average stage length	-0.388	0.237	2.392***	0.175
Seats	-4.021**	1.984	3.488***	0.970
Average stage length – Seats	0.0175***	0.00191		
Airline Effects				
Air Wisconsin	88.345	95.192	-490.506***	49.100
AirTran	126.303**	62.524	-727.460***	91.610
America West	122.482**	56.713	-611.329***	118.635
American	558.048**	268.120	92.937	334.827
American Eagle	42.622	107.023	-675.819***	-57.589
Alaska	-250.841***	61.314	-1033.857***	121.057
Aloha	-55.811	149.729	-1562.045***	249.149
Atlantic Southeast	423.453	104.047	-174.969	124.797
JetBlue	-35.199	81.920	-848.261***	145.828
Comair	124.432	102.512	-861.667***	-574.414
Continental	291.747**	130.065	-470.137***	155.185
Express Jet	81.152	115.5483	-700.754***	72.030
Frontier	-34.323	69.112	-927.286***	110.398
Hawaiian	187.373***	68.88476	-315.227***	100.775
Mesa	29.107	102.048	-750.054***	77.500
Northwest	-378.042**	164.086	-825.624***	-407.044
SkyWest	-59.377	129.569	-1076.967***	141.734
Southwest	121.120***	51.124	-774.777***	-486.948
Spirit	-378.042**	164.086	-970.158***	166.591
Trans States	-2.061	110.386	-649.159***	74.051
United	260.616***	77.146	-488.175***	133.609
USAir	145.843**	65.886	-487.559***	103.647

***Variables are significant at the 1% level

**Variables are significant at the 5% level

*Variables are significant at the 10% level

A1.5 Jet Aircraft Operating Cost (without Fuel) Linear Model

Variable	Full Model		Preferred Model	
	Parameter Estimate	Standard Error	Parameter Estimate	Standard Error
Constant	2927.21***	723.6904		
Average stage length	-1.848***	0.796	3.022***	0.357
Seats	-9.203*	5.390	11.146***	2.628
Average stage length – Seats	0.030***	0.005		
Airline Effects				
Air Wisconsin	-446.699	604.698	141.159	429.931
AirTran	-245.594	297.746	-587.831***	230.240
America West	506.852	458.520	121.076	423.029
American	4627.376***	1202.379	4525.655***	1261.702
American Eagle	-1407.432***	414.309	-987.274***	107.471
Alaska	-468.584	367.820	-898.286***	347.322
Aloha	3103.488***	1006.948	1497.725	1050.043
Atlantic Southeast	-243.910	348.087	-244.009	238.408
JetBlue	-609.477	408.240	-1000.499**	442.607
Comair	-778.532*	404.847	-649.411***	187.607
Continental	721.357***	308.258	304.969	275.767
Express Jet	-806.462*	433.808	-463.443***	131.434
Frontier	-566.650	371.387	-1086.396***	323.638
Hawaiian	-218.149	330.912	70.612	292.730
Mesa	-290.692	425.052	-52.242	314.233
Northwest	126.960	359.862	-217.446	346.508
SkyWest	-744.739*	430.347	-898.368***	223.527
Southwest	-912.741***	294.320	-1152.409***	246.138
Spirit	-175.452	523.030	-422.205	530.884
Trans States	-1000.567***	424.393	-456.385***	109.281
United	64.194	384.052	-317.343	337.320
USAir	1593.440***	650.395	1429.206***	595.325

***Variables are significant at the 1% level

**Variables are significant at the 5% level

*Variables are significant at the 10% level

Appendix 2: Total Logistics Cost Model, Case 2-2

A2.1 Full Total Logistics Cost Function, Case 2-2

$$\begin{aligned}
& z_c^{2-2} \\
&= \frac{\sum_{i \in c} \alpha_i F_c^{2-2}}{2Q_t} + \frac{\beta_k F_c^{2-2}}{2} \left(\frac{1}{F_c^{2-2}} + \frac{\beta_j - \beta_k}{\lambda_2} + m_j - m_k \right) \\
&\quad + \frac{(\lambda_2 + F_c^{2-2}(\beta_j - \beta_k + \lambda_2 m_j - \lambda_2 m_k))(\lambda_2 + F_c^{2-2}(\beta_j - \beta_k + \lambda_2(m_j + 3m_k)))}{16F_c^{2-2}\lambda_2} \\
&\quad + \frac{(\lambda_2 + F_c^{2-2}(\beta_k - \beta_j - \lambda_2 m_j + \lambda_2 m_k))(\lambda_2 + F_c^{2-2}(7\beta_j + \beta_k + \lambda_2(3m_j + m_k)))}{16F_c^{2-2}\lambda_2} \\
&\quad + \frac{(\beta_j - \beta_k)^2 F_c^{2-2}}{4\lambda_2} \ln \left[\frac{(\beta_j - \beta_k) F_c^{2-2}}{\lambda_2 (1 + F_c^{2-2}(m_k - m_j))} \right]
\end{aligned}$$

A2.1 Truncated Total Logistics Cost Function, Case 2-2

$$\begin{aligned}
& \widetilde{z_c^{2-2}} \\
&= \frac{\sum_{i \in c} \alpha_i F_c^{2-2}}{2Q_t} + \frac{\beta_k F_c^{2-2}}{2} \left(\frac{1}{F_c^{2-2}} + \frac{\beta_j - \beta_k}{\lambda_2} + m_j - m_k \right) \\
&\quad + \frac{(\lambda_2 - F_c^{2-2}(\beta_j - \beta_k + \lambda_2(m_j - m_k)))(\lambda_2 + F_c^{2-2}(7\beta_j + \beta_k + \lambda_2(3m_j + m_k)))}{16F_c^{2-2}\lambda_2} \\
&\quad + \frac{(\lambda_2 + F_c^{2-2}(\beta_j - \beta_k + \lambda_2(m_j - m_k)))(\lambda_2 + F_c^{2-2}(\beta_j - \beta_k + \lambda_2(m_j + 3m_k)))}{16F_c^{2-2}\lambda_2}
\end{aligned}$$

Appendix 3: Linear Operating Cost Model Results

A3.1 Turboprop Aircraft Fuel Consumption Linear Model

Variable	Full Model		Preferred Model	
	Parameter Estimate	Standard Error	Parameter Estimate	Standard Error
Constant	85.799*	46.468		
Average stage length	0.076	0.201	0.495***	0.026
Seats	0.049	0.954	2.030***	0.112
Average stage length – Seats	0.010**	0.004		
Airline Effects				
American Eagle	3.936	5.515	8.231**	4.066
SkyWest	-17.152***	6.978	-12.202***	3.154
Mesaba	-9.853**	4.670	-8.314***	3.183
ExpressJet	15.155***	6.193	18.402***	5.855
Trans States	4.184	4.071	6.937**	3.497
Horizon	-5.541	7.111	-1.638	4.150
Mesa	2.481	8.377	-1.285	9.275
Air Wisconsin	4.320	4.447	2.307	4.523
Executive	-22.688*	13.305	-37.882***	10.142

***Variables are significant at the 1% level

**Variables are significant at the 5% level

*Variables are significant at the 10% level

A3.2 Turboprop Aircraft Operating Cost (without Fuel) Linear Model

Variable	Full Model		Preferred Model	
	Parameter Estimate	Standard Error	Parameter Estimate	Standard Error
Constant	-57.971	703.828		
Average stage length	1.820	3.085	0.317	0.792
Seats	21.032*	12.157	13.807***	3.237
Average stage length – Seats	-0.052	0.056		
Airline Effects				
American Eagle	115.015	148.158	197.847	140.509
SkyWest	-133.427	135.675	15.338	80.909
Mesaba	12.184	104.755	146.718	100.250
ExpressJet	-99.556	104.793	-24.064	110.598
Trans States	299.596*	181.281	388.846***	164.932
Horizon	0.169	143.073	143.562*	84.490
Mesa	11.342	261.496	135.219	277.789
Air Wisconsin	432.041***	172.019	571.315***	189.281
Executive	-199.379	251.152	36.562	192.452

***Variables are significant at the 1% level

**Variables are significant at the 5% level

*Variables are significant at the 10% level

A3.3 Jet Aircraft Ownership Linear Model

Variable	Full Model		Preferred Model	
	Parameter Estimate	Standard Error	Parameter Estimate	Standard Error
Constant	929.227	749.464		
Seats	6.627***	1.767	10.675***	1.990
Airline Effects				
Air Wisconsin	-820.899	657.698	-148.654	140.264
AirTran	-662.324	576.432	-224.038	245.522
America West	-91.468	556.152	243.152	312.189
American	-692.662	543.391	-452.212	382.900
American Eagle	-945.615	674.277	-221.108	101.784
Alaska	-532.760	544.226	-196.468	297.515
Aloha	1934.179**	877.941	2338.229	742.130
Atlantic Southeast	-887.830	579.415	-443.828	248.454
JetBlue	-340.663	584.889	70.272	307.717
Comair	-712.101	659.335	-32.215	132.071
Continental	46.384	549.637	371.439	326.912
Express Jet	-684.819	687.377	64.563	114.790
Frontier	-492.157	576.523	-73.631	270.369
Hawaiian	-1131.029*	578.753	-685.388	240.440
Mesa	-334.695	667.085	343.143*	192.052
Northwest	-689.539	541.733	-378.398	315.643
SkyWest	-428.038	684.211	248.813	219.491
Southwest	-1181.760**	572.253	-753.621	247.601
Spirit	-15.036	640.095	254.543	501.295
Trans States	-678.567	675.641	48.163	104.821
United	-924.575*	548.385	-578.680	292.511
USAir	-23.517	602.395	302.223	386.246

***Variables are significant at the 1% level

**Variables are significant at the 5% level

*Variables are significant at the 10% level

A3.4 Turboprop Aircraft Ownership Linear Model

Variable	Full Model		Preferred Model	
	Parameter Estimate	Standard Error	Parameter Estimate	Standard Error
Constant	-21.190	63.213		
Seats	7.353***	1.235	7.070***	0.594
Airline Effects				
American Eagle	145.569***	41.481	137.770***	39.436
SkyWest	135.540***	37.078	122.934***	23.745
Mesaba	63.849*	35.911	52.287**	26.875
ExpressJet	91.060***	39.366	83.169**	37.633
Trans States	131.923***	43.224	124.070***	34.507
Horizon	7.489	31.067	-3.151	24.251
Mesa	9.649	103.882	-1.742	102.211
Air Wisconsin	199.885*	118.259	187.855	115.550
Executive	70.858	84.738	66.571	87.746

***Variables are significant at the 1% level

**Variables are significant at the 5% level

*Variables are significant at the 10% level

Appendix 4: Travel Time Model Results

A4.1 Jet Aircraft

Variable	Parameter Estimate	Standard Error
Constant	0.628***	0.0175
Distance	.00205***	2.5×10^{-5}

A4.2 Turboprop Aircraft

Variable	Parameter Estimate	Standard Error
Constant	0.350***	0.0162
Distance	3.97×10^{-3} ***	9.06×10^{-5}

A4.3 High Speed Rail

Variable	Parameter Estimate	Standard Error
Constant	0.125**	0.0434
Distance	5.57×10^{-3} ***	1.33×10^{-4}
